Matrix Methods to Analyze Long-Range Transport of Air Pollutants

January 1981

U.S. DEPARTMENT OF ENERGY
Assistant Secretary for Environment
Office of Environmental Assessments
Regional Impacts Division

DISCLAIMER

Printed in the United States of America

Available from

National Technical Information Service
U.S. Department of Commerce
5285 Port Royal Road
Springfield, VA 22161

NTIS price codes

Printed Copy:	$ 9.00
Microfiche Copy:	$ 3.50

DOE/EV-0127
UC-2, 11, 13, 34b-61,
90i, 90j, 91, 97

Matrix Methods to Analyze Long-Range Transport of Air Pollutants

January 1981

U.S. DEPARTMENT OF ENERGY
Assistant Secretary for Environment
Office of Environmental Assessments
Regional Impacts Division
Washington, D.C. 20585

THIS PAGE

WAS INTENTIONALLY

LEFT BLANK

ACKNOWLEDGMENTS

As the principal author, I would like to acknowledge the substantial contributions to this report by several co-authors. Mr. Jay Arnold and Mr. A. Bruce Crane of The Aerospace Corporation participated in analyses of results, preparation of tables and figures, and writing of the text. Mr. Ronald E. Meyers was principal investigator at Brookhaven National Laboratory and, along with Dr. Lawrence Kleinman and Mr. Thomas Carney, developed and applied the BNL modeling and matrix generation procedure and wrote sections of the report describing them. Dr. William J. Eadie and Mr. William E. Davis of Battelle Pacific Northwest Laboratory developed and applied PNL modeling and matrix procedures and wrote sections of the report describing them.

The present report represents results from several years of work sponsored and directed through the Regional Impacts Division (RID) of the Office of Environmental Assessments (OEA) and predecessor organizations, Assistant Secretary for Environment, Department of Energy. Dr. Peter House, Director of OEA, and Dr. Roger Shull, Director of RID, have supported and encouraged the work since its inception. Dr. Ronald Matheny has provided valuable suggestions and assistance.

Other researchers also participated in development of transport models and matrix methods. At Brookhaven, Mr. Richard T. Cederwall was involved in methods development, and Dr. Paul Michael, Head of the Atmospheric Sciences Division, supervised Brookhaven efforts. At Battelle, Mr. William Sandusky was involved in methods development and Dr. Ronald Drake, Manager of the Atmospheric Dynamics and Aerosol Research Section, supervised modeling work.

The Aerospace Corporation supported the Department of Energy in the analysis and application of matrices and preparation of this report. Ms. Josephine Peck and Ms. Laurana McCants performed most of the computer programming and, along with Mr. William Swartwood, prepared computer-generated graphic figures and tables.

The authors also express their appreciation for reviewing and commenting on an earlier draft to Dr. Fred Lipfert of Brookhaven, Dr. David Ballantine of the Office of Health and Ecological Research, DOE, and Mr. Douglas Carter and Mr. Robert Kane of OEA, DOE.

Dr. Richard H. Ball
Regional Impacts Division

THIS PAGE

WAS INTENTIONALLY

LEFT BLANK

CONTENTS

CONTENTS (Continued)

LIST OF TABLES

LIST OF FIGURES

LIST OF FIGURES

THIS PAGE

WAS INTENTIONALLY

LEFT BLANK

EXECUTIVE SUMMARY

Need for Methods

In the environmental assessment of national energy policies, the Office of Environmental Assessments (OEA) must determine the impact of possible future energy scenarios on the Nation's air quality. Each scenario yields a unique set of pollutant emissions from the particular combination and geographical distribution of energy activities, as well as from all other emission sources (e.g., industry). Predictions of these future emission patterns are provided by large-scale scenario models, such as the Strategic Environmental Assessment System (SEAS).

The assessment process must take into account the environmental impacts of emission patterns resulting from energy activities. Regulatory constraints imposed by government generally specify limits on ambient concentrations rather than on emissions directly; therefore, it is necessary to determine the concentrations that would result in each geographic area from proposed emission patterns. Environmental impacts that are currently unregulated (e.g., acid rain) may be restricted in the future, and current regulations may be modified as the need becomes apparent. These constraints need to be anticipated for long-term energy planning.

Determining concentrations and deposition caused by given emissions -- the "air transport" problem -- is not an easy matter. The wind intermingles pollutants from many sources and transports and disperses them, often over great distances. The pollutants are removed sooner or later by precipitation or interaction with surface features. In addition, with some pollutants (such as sulfur dioxide), chemical transformations take place along the way producing secondary pollutants.

A number of pollutants emitted by energy-related activities tend to persist in the atmosphere for several days or more in some form. Such substances can be transported in substantial quantities up to several thousand kilometers. Important pollutants include particulate matter, sulfur oxides, oxides of nitrogen, and hydrocarbons and/or their reaction products. The average distance each pollutant is transported may vary greatly with meteorological conditions, release height, and background pollution. There is considerable uncertainty about ranges for oxides of nitrogen and many hydrocarbons.

For conditions where long-range transport may be substantial, environmental analyses must consider the potential impacts of emissions on areas far removed from the source. Transport across the boundaries of air quality planning regions, states, and even nations can be important. Deposition of sulfur compounds and nitrates in the form of acid precipitation, for example, is considered an important international problem. Various pollutants need to be examined to see whether long distance transport is a significant problem. The question is whether there might be geographic areas in which transport from many distant sources, perhaps in combination with local sources, could produce adverse levels of suspended concentrations or deposition of pollutants.

To assess air quality constraints and impacts of energy activities, models that account for long-range transport processes, as well as for local effects of meteorological dispersion, are required. At the present state of the art of modeling, separate models are used to estimate the detailed, rapidly varying effects of local sources and the long-term average effects of distant sources. OEA uses both types in its assessments to study different effects and constraints. Local models can treat the short-term peak values due to specific nearby sources; however, their usefulness in national scenarios often is limited by a lack of knowledge of exact site locations and their meteorological conditions. Long-range transport models account for the combined effects of many sources and for the presence of secondary pollutants due to transformations; however, most current models can only estimate long-term average values on the order of several weeks to a year.

OEA has used long-range transport models developed at Brookhaven National Laboratory (BNL) and at Battelle Pacific Northwest Laboratory (PNL) to estimate long-term impacts of sulfur oxide emissions and fine particulate emissions for future energy scenarios. These models are based on the principle of tracking the trajectories of emitted pollutants as they are carried across the United States by large-scale wind motions. A "puff" of pollutant emitted at a particular time is tracked for several days, taking account of its vertical dispersion, chemical transformations, and removal by precipitation and interaction with surface features. Succeeding puffs at intervals of about 6 hours are similarly tracked until 1 month of emissions has been counted, using actual meteorological data for a particular month. Many sources are treated at different locations (as many as a thousand for some studies). The method accounts for significant detail about the emission scenario, but requires substantial resources and time for data preparation and computer processing.

Introduction of Matrices

In some types of analyses, it is inconvenient or infeasible to calculate air quality and impacts by use of large trajectory models. Development of the air transport matrix method was undertaken to provide a simpler, faster method of analysis. The method represents results of comprehensive long-range transport models in a simple, easy to use form.

The transport matrix concept is based on the assumption that the average concentration of a pollutant in one geographic region (the "receptor") is a sum of contributions received from emissions in every other region (the "sources"). The constants of proportionality connecting each source region with each receptor region form a two-dimensional array or matrix. For example, at the Air Quality Control Region (AQCR) level, a 238 x 238 matrix represents the expected transport of pollutants from each AQCR to every other AQCR. Each of the constants of proportionality multiplied by the emission from its corresponding source region yields a partial value for the expected concentration in the receptor region. To determine the total concentrations, the components attributable to each source region must be summed up.

OEA asked BNL, and later PNL, to develop matrix representations based on their respective long-range transport models. The present report is a description of the concept and methodologies used in developing those matrices, a preliminary analysis of those matrices and their properties, and a guide to the types of applications they can serve. Matrices have been generated by BNL for transport of sulfur oxide emissions among the 238 Air Quality Control Regions in the conterminous United States, using their AIRSOX model. PNL has used their long-range transport model and a streamlined calculation method to generate matrices for sulfur oxides and for emitted fine particulates. Matrices have been completed for 4 months of meteorological data (one in each season) from 1974. BNL further separates matrices according to three categories of sources: utility, industrial, and area sources. They differ in terms of effective stack heights and detailed distribution of source locations within each AQCR. Matrices have also been calculated at the more aggregated levels of state and Federal region boundaries.

Uses for Matrices

Matrices provide a number of useful properties and can be used in several types of applications. In comprehensive assessments of national scope, they permit rapid and economical calculation of air impacts for multiple scenarios of emissions. In more limited analyses, they permit quick calculation of the incremental impacts of an incremental change in emission patterns. The choice of three geographic levels (AQCR, state, and Federal region) permits one to examine imports and exports among any of these geographic units. It also provides the analyst with simple methods for making broad regional estimates using a microcomputer or hand calculator.

As an example of current capabilities, Figure 3-1 is a contour map of incremental sulfate concentrations (a secondary pollutant) that could be expected if additional electrical utilities were placed in AQCR #183 and which emitted 1 million metric tons per year of sulfur dioxide. (This much emission is not presently emitted or planned in that AQCR.) Although indicative of the type of problems handled and the graphic display capability, this map does not represent a specific Department of Energy scenario analysis.

Applications

The matrix method has been used in several Department of Energy comprehensive assessment studies and for in-house, fast-response analyses of policy issues. In the Regional Issue Identification and Assessment (RIIA) II, national matrices for sulfur dioxide and sulfate were used to project future levels of those pollutants at the AQCR level of detail. In the Technology Assessment of Solar Energy (TASE), matrices were used to project primary fine particulate levels as well as sulfur dioxides. State level matrices are currently being used to project sulfur oxide levels for the National Energy Impact Projection (NEIP) III report.

In each of those studies, the matrix method made it possible to analyze air quality impacts of several scenarios quickly and to easily modify

the analyses when scenarios were altered. Additional sensitivity analyses were made to identify the effects of particular source classes or regions. Similar studies carried out in the past with large transport models required substantially more time and effort to process each scenario and variation.

Several fast response analyses were carried out by Department of Energy staff to develop insight about fast moving policy issues. Two examples are described in Section 4. One example, the "oil-to-coal conversion" issue, pertained to legislation for converting oil- and gas-fired powerplants to coal. In this case, a matrix analysis indicated the general levels of ambient concentration impacts to be expected in different regions of the United States from the conversions. Incremental levels of concentrations for monthly averages were relatively small, but exposures were greatest in populated regions such as the New York City metropolitan area.

Another example of applied analysis was an examination of interregional sulfur transport in the upper Ohio Valley region. A matrix analysis indicated that monthly ambient concentration levels of SO_2 and SO_4 are substantially due to inter-AQCR transport, even in AQCRs with large local emissions. Violations of annual standards and high levels of SO_2 and TSP appear to be an inter-AQCR and interstate problem.

Limitations

Important questions remain about the validity of the transport matrix method in general and about the accuracy of matrices derived with current models and methods. Chemical and physical processes that transform and remove air pollutants, such as sulfur oxides, from the air often are not linear in terms of the amount of pollutant present. However, most large-scale, long-range transport models in current use are based on linear approximations. This is due to the difficulties in simulating nonlinear processes and lack of knowledge about the processes. Hence, the matrix method is at least a reasonable way to represent the results of those models in a convenient form. There are also theoretical reasons to suggest that a linear representation should be reasonable for longer term, regional average concentrations.

Current matrices derived with the BNL and PNL models appear to give reasonable correspondence with observed concentration values of sulfur dioxide and sulfates in the mid-1974 period. However, the detailed cause-effect relationships among regions are difficult to verify. Hence, these matrix relationships must be regarded as experimental until more comprehensive validation work can be completed. The accuracy of projections of incremental impact of one region's emissions on another and the range of varlation with meteorological period are not well established.

Future Directions

Further development and testing of long-range transport models and of matrix representations is required. Modeling methods need to be extended to cover other important pollutants, such as oxides of nitrogen, nitrates, and ozone, and to treat shorter time intervals. Models need to be applied and

matrices generated for more periods of meteorological data to establish climatological averages and fluctuations therefrom. Models need to be validated against observed data to refine parameters and establish limits of accuracy.

A particular need is to improve the representation of deposition phenomena. Wet deposition of acidic sulfate and nitrate compounds is familiar as the "acid rain" issue. The few current models that treat long-range transport and deposition of sulfur show widely different results for the amount of sulfur deposited by several different mechanisms. Furthermore, the sporadic nature of rain indicates that many months of meteorological data should be taken into account when estimating the climatology of deposition.

THIS PAGE

WAS INTENTIONALLY

LEFT BLANK

1. INTRODUCTION

1.1 NEED FOR MATRIX METHOD

The Office of Environmental Assessments (OEA), Assistant Secretary for Environment, analyzes the impacts of energy-related environmental policies, laws, and regulations; assesses impacts on the environment; identifies environmental research requirements for the energy technologies being developed by the Department of Energy (DOE); and delineates the national and regional environmental, health, and safety impacts of DOE policies and programs.

Environmental assessments of national policies and trends must consider the implications of changing patterns of air pollutant emissions. In some cases, only an indicator of the general trend in air quality might be needed. In other cases, it is important to estimate the potential for violation of ambient air quality standards. In the absence of applicable standards, there is a need to estimate the impact of changes in emissions on human health and ecological systems.

When assessments are conducted for general, long-term policies or comprehensive national programs, a large number of individual emission sources may be affected and their locations may be problematical. Detailed modeling of the air impacts of each source usually is impractical even if the locations were well known and is of debatable significance when the locations are undefined or highly speculative. Partly for this reason, national assessments often resort to simplifications in their air quality analyses, such as consideration of generic site impacts, simple roll-back models of air quality, or analysis of emission trends. (Another problem is that models for dealing with many sources and multiple regions have not been available.)

Estimation of changes in air pollutant emissions, while useful in itself, is not always a reliable measure of air quality impacts. Emissions have different significance in each area because of differences in existing air quality, local atmospheric dispersion characteristics and transport from one region to another, in addition to any differences in the susceptibility of receptors and in air quality objectives. Hence, there is a need to translate emission estimates into measures of air quality impact that are more closely related to the environmental impacts and standards that are at issue.

Studies of typical single source conditions are useful in illustrating local effects and identifying the difficulties of complying with single source, peak value limitations, but they do not capture the aggregate problems experienced by regions. Roll-back models capture, in a crude fashion, aggregate local effects, but they, like single-source models, do not deal with the effect of pollutants transported across regional boundaries.

The Office of Environmental Assessment has responded to some of those shortcomings for regional impacts projection by employing several techniques in its assessments. In particular, two different long-range

transport models have been used to estimate the long-term average interactive effects of interregional transport of sulfur compounds and particulates. These are the AIRSOX model of Brookhaven National Laboratory (BNL) and the long-range transport model of Pacific Northwest National Laboratory (PNL). In early assessments, the PNL model was used to calculate transport in the western half of the United States and the BNL model in the eastern half. Those applications included the National Coal Utilization Assessment (DOE, 1979a) and the Regional Impact Identification and Assessment (DOE, 1979b).

Utilization of the BNL and PNL long-range transport models provides long-term average concentration estimates that take interregional atmospheric transport into account. However, preparation of an emission source scenario and computation of concentrations for each new emission pattern is expensive and time-consuming. Recalculation of new trajectories is not a practical approach for use in quick-turnaround impact studies, processing numerous emission scenarios, or analytic exploration of certain characteristic properties of transport. Furthermore, there was a need to extend the scope of long-range transport analyses in assessments to include more months of meteorological data (only 1 month of data was feasible in earlier studies) and to cover the whole conterminous United States with one continuous set of computations.

In addition to use in comprehensive assessments of regional scenarios, rapid methods are required to provide indicators of air quality impacts in national level assessments. Because information on locations of new plants is usually unavailable in such studies, a model that deals with aggregate regional emissions may be preferable. In the case of pollutants that undergo substantial interregional transport and alteration, the method should reflect these effects. For convenience, a method that yields reasonable indicators of air quality and impacts directly from emissions estimates is desired.

The matrix method described in this report is intended to support several of the needs described above. It provides simple analytic relationships between aggregate regional emissions of sulfur dioxide or fine particulates and several measures of their environmental impacts. These environmental impact measures include long-term, regionwide averages of suspended concentrations of sulfur dioxide, sulfates, and emitted fine particulates and exposure of humans to these concentrations. New matrices in preparation will also describe deposition of sulfur compounds in several forms. Other measures of environmental impact or ambient quality, such as visibility impairment, exposures to selected receptors, and concentrations of other pollutants, are being studied for possible future implementation. However, the matrix method is not appropriate for all types of air impacts and should be considered as only one component of assessment techniques. In particular, the current form of matrices do not predict short-term (daily or less) averages or local values such as individual monitoring station trends. Hence, many air quality regulatory questions cannot be addressed.

1.2 STATUS OF TECHNIQUES FOR ASSESSING LONG-RANGE TRANSPORT

A number of pollutants emitted by energy-related activities tend to persist in the atmosphere for several days or longer in some form. Such substances will be transported in substantial quantities for several thousand kilometers or more. There is a general need to analyze their transport to determine whether the levels of atmospheric concentrations or deposition are sufficient to violate environmental standards or otherwise cause adverse effects. Depending on the pollutant form and the receptor, the mechanisms for effects may involve short-term peak values, longer term averages or cumulative measures of concentrations, deposition fluxes, or volume effects. Hence, the precise form of prediction or measure of impact required of a model can only be identified after the nature of potential adverse effects has been clarified or standards have been established.

Methods for describing and predicting the transport of pollutants over long distances are still in an early stage of development and validation. Models for predicting local behavior of plumes from point and other sources to distances of 10 km or so have been extensively developed over the last two decades (Turner, 1979). In addition, characterization of long-term global scale transport has been carried out for a number of long-lived pollutants. However, models for dealing with regional-scale pollution in the range of 100 to several thousand km have been developed only recently (Meyers et al., 1979b; Bass, 1980). Available models are limited in the pollutants treated, the temporal and spatial resolution, and the proven accuracy of prediction. No regional-scale models have been tested and evaluated sufficiently to satisfy regulatory requirements.

Although regional models have not yet been approved for detailed regulatory decisions, a number of models are operational or being developed. Table 1-1, adapted from Bass (1980), summarizes many of the major models. Several of these models are operational and considered to be useful for assessment and general strategic analysis purposes. These can be divided according to their applicability to short-term air quality measures, usually with limited space and time coverage, or to broader geographic coverage and longer term averages.

Regional transport of any suspended matter that is nonreactive or subject to known decay and removal rates can be modeled reasonably well with sufficient data on atmospheric motions. Among important pollutants, many radioactive species, carbon monoxide, and emitted fine particulates should be predictable, although comprehensive observations needed to confirm fine particulate predictions are not yet available. Transport of sulfur oxides has received considerable attention and several operational models appear to give a reasonable representation of available observations of suspended concentrations. However, uncertainties in knowledge of deposition and transformation processes have led to wide differences in predictions of individual deposition pathways for sulfur. Models for highly reactive organic compounds, oxides of nitrogen, and photochemical oxidants are not yet operational for very large regions, although several models have been developed for urban and somewhat larger areas.

Table 1-1. Current Long-Range Transport Models (USA)

Type	Name	Sponsoring Group
Short-Term Models		
Puff	Atmospheric Transport and Diffusion Model (ARL-ATAD)	NOAA Air Resources Lab
Puff	EURMAP-2	SRI
Puff	MESOPUFF	ERT
Plume Segment	Source-Transport Receptor Analysis Model (STRAM)	Battelle Pacific Northwest Lab
Plume Segment	MESOPLUME	ERT
Grid	Northern Great Plains Regional Model	SAI
Grid	MESOGRID	ERT
Long-Term Models		
Statistical Trajectory	Advanced Statistical Trajectory Regional Air Pollution Control Model (ASTRAP)	Argonne National Lab
"Square" Puff	PNL Regional Pollutant Transport Model	Battelle Pacific Northwest Lab
Puff	ARL-ATAD	NOAA Air Resources Lab
Puff	EURMAP-1/ENAMAP	SRI
Puff/Vertical Finite Difference	AIRSOX	Brookhaven National Lab
Representative Research and Development Models		
Puff/Vertical Finite Difference	Mesoscale Trajectory and Diffusion Model	NOAA Air Resources Lab
Puff	PNL Regional Model	Battelle Pacific Northwest Lab
Plume Segment	Segmented Plume Model	Savannah River Lab
Particle-in-Cell	ADPIC-MATHEW	Lawrence Livermore Lab
Grid	SULFA3D	EPRI/ERT
Grid	SURAD	EPRI/ERT
Grid	Regional Transport Model	Teknekron
Grid	"Regional Supermodel"	EPA Meteorology Lab
Trajectory	Limited Area Mesoscale Prediction System (LAMPS)	Drexel-NCAR-BNL

For pollutants suspected of having impacts at very long distances, such as fine particulates and sulfur, it is important to have broad geographic coverage. Comprehensive assessment of their impacts requires analysis of a major portion of the intensive source areas of North America, preferably all of the United States and Southern Canada. Because of the computer and data requirements associated with such large areas, long-range transport models for sulfur and particulates have had to simplify their description of chemical processes and restrict their spatial resolution.

Among current regional-scale models for sulfur compounds, there appear to be five major long-term models (or groups of related models) that have been implemented for grids covering a major part of the Eastern United States and Canada. Two of these, the BNL and PNL models described in this report, have been operated for a comprehensive set of sources over the entire contiguous United States simultaneously. Three others have been operated for various geographic regions and sets of sources. These are the ASTRAP model developed at Argonne National Laboratory (Shannon, 1979), the ENAMAP model developed by SRI International (Bhumralker et al., 1980), and several versions of the ARL-ATAD model developed by the National Oceanic and Atmospheric Administration (Heffter, 1980; Draxler, 1980). Other models have been developed or are under development but have not been operated (or results published) on comprehensive data at this same large geographic coverage.

1.3 THE TRANSPORT MATRIX CONCEPT

The methodology described in this report is based on a simple concept: a large geographical area (the conterminous United States in this case) is subdivided into a number (n) of smaller regions. The objective is to relate levels of air pollution in each region to the emissions of precursor pollutants from each of the regions. The key assumption is made that the average concentration of a particular pollutant in any region is a linear combination of emissions of its precursor pollutant in every region. For example, concentration in region 1 is given by

$$C_1 = T_{11}E_1 + T_{12}E_2 + T_{13}E_3 + \ldots + T_{1n}E_n$$

where E_j is the emission rate in region j, and T_{1j} are a set of transport coefficients. Thus, each region is assumed to contribute to concentrations in its own and all other regions in proportion to its emissions, and these contributions are additive. A similar formula for concentration holds in each other region (i), except that a different set of values of the coefficients, T_{ij}, will apply. Thus, a two-dimensional array of coefficients, or a matrix, is required to determine the concentrations values in all regions in terms of a set of emissions from all regions. Matrices can also be defined for other measures of air quality, such as mass deposition and light scattering.

The essence of a matrix representation is the assumption that the coefficients themselves do not depend on the emission values, E_j. They will, in general, depend on the geographic boundaries chosen, the pollutant properties, and the meteorological transport properties of the atmosphere.

Because of differences in meteorological conditions at various times, one expects that the coefficients applicable for one period of time will differ to a greater or lesser extent from those applicable for another period. To be useful as a predictive tool, it is essential that the matrices are based on a statistically sound estimate of future meteorology.

Ordinarily, one expects that the emissions with the greatest proportional impact on a region will be those emitted within the region. Hence, the coefficients with $i = j$ in the matrix -- the so-called "diagonal" elements or intraregional coefficients -- should be among the largest in value. The interregional coefficients or "off-diagonal" matrix elements ($i \neq j$) account for transport from one region to another. The relative magnitude of the interregional transport coefficients in comparison with the intraregional depends on the properties of the pollutant and the size of the geographic regions chosen for the matrix representation.

Transport matrices might, in principle, be estimated by several empirical and theoretical methods. The primary method discussed in this report uses two existing computer models of long-range atmospheric transport. These models are in turn based on observed meteorological data for several monthly periods of time. A model used for calculating interregional transport matrices must be capable of identifying the individual contributions to ambient concentrations from emissions in each region. Other methods, including short-range models, could be used for the diagonal elements.

Using a model, matrices are generated by first tracking the computer-simulated movement of pollutants emitted from a sample set of sources in each emitter region as they are transported by large-scale air motions across the United States. Ground level concentrations, deposition, and other measures of interest are then tabulated for the receptor regions. Pollutants are released at regular intervals and the resulting impacts are averaged over a period of time (1 month in the present case) and over the area of the receptor region. Then the matrix element T_{ij} is obtained by separating out the concentration (or other impact measure) produced in each region i (ΔC_{ij}) by emissions in region j and dividing by the magnitude of those emissions, i.e.,

$$T_{ij} = \Delta C_{ij}/E_j$$

This procedure is repeated for each source region until an entire matrix of coefficients is obtained for each impact measure. The procedure used for generating matrices with the BNL and PNL models is described in more detail in Section 5.

The table of values of the ΔC_{ij} are just the calculated contributions of incremental concentrations in each region due to other regions, for a particular emission scenario. The matrix T_{ij} may be interpreted as a table of incremental concentrations associated with unit emissions from each source region. (Examples of T_{ij} and $\Delta C_{ij} = T_{ij} \cdot E_j$ are shown in Tables 2-1 and 2-2, respectively.)

The matrix becomes a model (in effect, a linear model of the parent model used to generate it) through the assumption that the concentration increments will change in direct proportion to E_j.

1.4 AIR ASSESSMENT METHODS PROGRAM

To improve the efficiency and scope of long-range transport analysis in comprehensive assessments and also to provide quick-turnaround assessment tools, a program of applied methodology development is being carried out at BNL and PNL for the Regional Impacts Division.* This program has focused on applications of existing models and development of methods to improve their utility in assessments. Several types of computational improvements have been incorporated to increase the efficiency and scope of air quality assessments, including:

- Development of transport matrices at the Air Quality Control Region (AQCR) and state and Federal region levels for use in quick-turnaround applications.
- Extension of the computation grid for each model to cover the entire conterminous United States, parts of Canada, and adjacent oceanic areas (to capture trajectories that circle back onto the continent).
- Development and testing at PNL of streamlined procedures for computing new source locations.
- Application of the PNL model to treat fine particulate transport and development of matrices for this pollutant.
- Development and testing of time-averaged representation of precipitation in wet removal processes for the PNL model.
- Testing of the sensitivity of the PNL model to different chemical conversion rates and incorporation of improvements into the model.
- Incorporation of rainfall data in the wet removal process in the BNL model.
- Extension of the scope of sources in the BNL model to cover distributed or "area" sources as well as industrial and utility sources of emissions.

Other related air quality assessment methods are being developed and applied at Argonne National Laboratory (ANL) and Los Alamos Scientific Laboratory (LASL). ANL has developed and applied methods for local air

* Support for some of the development and computations was also received from the Technology Assessment Division of OEA and from the Multistate Atmospheric Power Production Pollution Study (MAP3S) program of DOE and the Environmental Protection Agency.

quality analysis. They have assisted the matrix development by analyzing local air quality data and potential methods for calibrating matrices to observed data. LASL has developed and applied methods for predicting visibility impacts from both long-range and short-range transport, prediction of NO_2 formation in plumes, and incorporation of air quality factors into Western U.S. siting issues. Methods being developed by LASL may permit prediction of regional haze visibility impairment conditions in conjunction with BNL and PNL long-range transport matrices.

The matrix methodology has been developed and implemented to create several hundred matrices to date. These include sulfur compounds and respirable particulates as pollutants, AQCR, state and Federal region-level matrices, three source types, two types of averaging, and 4 months of meteorological data. Matrices are being utilized in comprehensive assessments such as the Technology Assessment of Solar Energy, the National Environmental Impact Projection, and other applications. Testing to establish the properties and validity of the matrices continues. (Some preliminary results of this testing work are described in Section 5.)

2. CHARACTERISTICS AND ADVANTAGES OF MATRIX METHOD

2.1 GENERAL

In this section, the characteristics and advantages of the long-range transport matrix method, as currently implemented by OEA, are briefly described. Some limitations of the method are expected, however, based on the general theoretical considerations discussed in Section 5.1. Fundamental limitations on accuracy are associated with the validity of the assumption of a linear relationship. These must be considered when choosing pollutants and measures of impact to be represented in matrix form. Practical limitations pertain to any given matrix in terms of the spatial and temporal resolution of the representation, accuracy of the underlying model and data used to generate the matrix, and realism of the source distribution assumed.

2.2 ECONOMY OF EFFORT

Transport matrices summarize the results of many computations generated by the parent models. The parent models generate different trajectories for puffs originating at each source point and for each time step in the simulation. Each puff trajectory is computed based on 1 month of wind speed data. Precipitation and stability conditions encountered in these trajectories are used to compute pollutant transformation and deposition rates. This amounts to a very large number of computations for even 1 month of weather data. However, with current (linear) models, the computations are independent of the quantity of the pollutant emissions. Thus, for a given kind of pollutant, the same transport characteristics can be used for any quantity of emission desired. Pollution control policy studies require investigation of many hypothetical emission vectors. Because the transport matrices summarize the transport information generated by the parent models, the effects of many hypothetical emission vectors can be explored simply by multiplying each by the appropriate matrix. The parent models are too complex to be used repeatedly in this manner. The economy of effort produced by the matrices allows policy analysts to investigate a large number of scenarios easily, greatly enhancing the usefulness of the information generated by the parent models.

2.3 PRACTICALITY OF AQCR LEVEL

AQCR-level transport matrices are very practical because they correspond well to the regulatory jurisdictions used for air quality planning and for collection of emission data. They provide a computational mesh fine enough for most long-range transport studies, at least in the Eastern United States, and coarse enough to keep the computations manageable. The parent models themselves are capable of even finer detail than AQCRs. Fine detail can be important for studies of single-point sources but is too cumbersome for national-level studies. However, the large size of western AQCRs may necessitate some refinement in the future.

2.4 AVERAGE CONCENTRATIONS

Implementation of the matrix method is currently limited to relatively long-term time averages and broad regional spatial averages of suspended concentrations. Better spatial and temporal resolution is possible in principle, but peak short-term values for 1 day or less are not considered feasible with the current parent models nor are they likely to be linear in terms of regional emission totals. Monthly and annual average values provide an indicator of air quality trends. They also are expected, on theoretical grounds, to correlate with many types of health and ecological effects. Annual averages can be used in analyzing broad regional attainment of annual air quality standards, but will not necessarily correspond well with violation of short-term standards or peaks reached at isolated monitoring points.

Figure 2-1 shows a map of concentrations of SO_4 computed from a matrix generated by the BNL AIRSOX model.

2.5 MATRIX TYPES

The matrices represent rather compact summaries of the information generated by repeated parent model runs. This compactness facilitates a variety of comparisons if the appropriate matrices have been generated. Matrices have been generated for transport from three different stack heights: 20 m, 100 m, and 200 m, corresponding roughly to area, industrial, and utility sources. Matrices have also been generated for both population-weighted averages (appropriate for health effects) and for area-weighted averages (more appropriate for acid rain and crop damage). Aggregated matrices have been produced at the state and Federal region levels.

2.6 STATE AND FEDERAL REGION MATRICES

Policy issue studies that require long-range transport analyses are frequently at the state or Federal regional level. Transport matrices have been developed by BNL and PNL at the state level and have been aggregated to the Federal regional level using the following formula:

$$T^k_{\alpha\beta} = \sum_{i\varepsilon\alpha} \sum_{j\varepsilon\beta} \frac{X_i}{X_\alpha} T^k_{ij} \frac{E^k_j}{E^k_\beta}$$

where: α = receptor region (Federal region)

β = source region (Federal region)

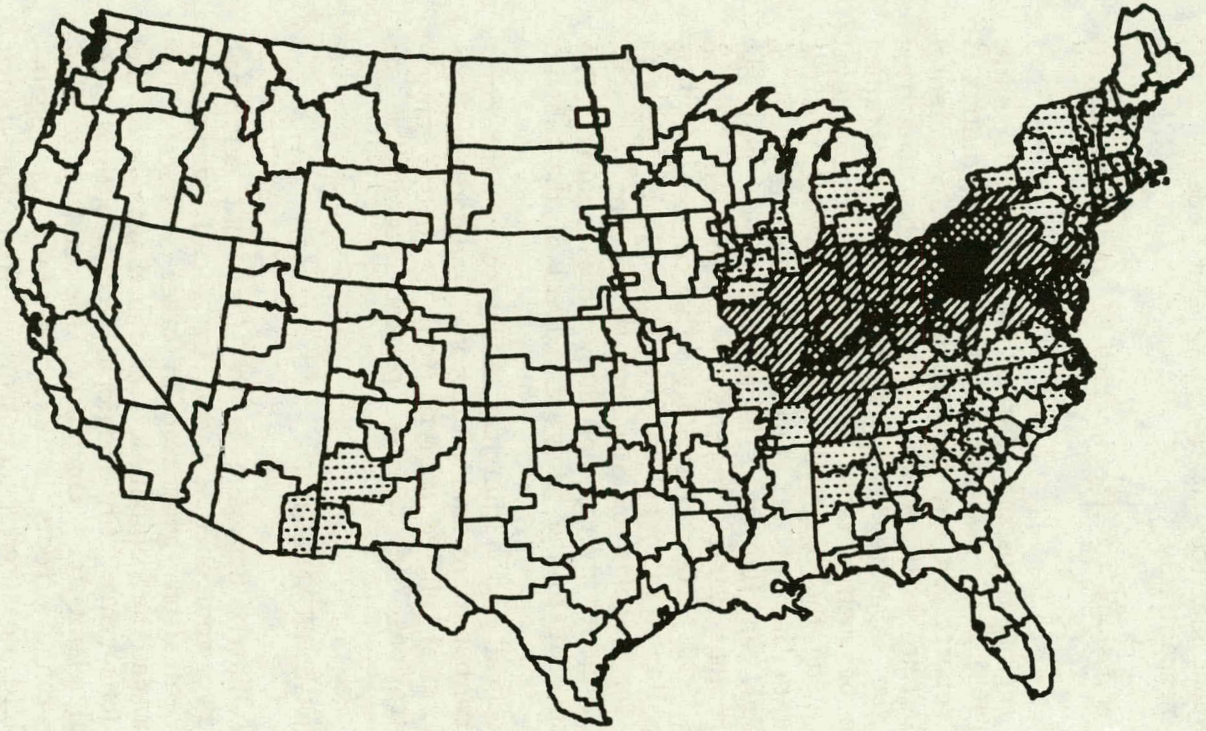

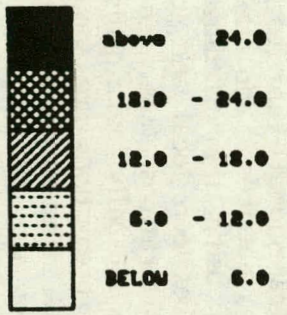

Note: Concentrations predicted by transport matrix method for average of January and July 1974 meteorology. Emission data from DOE/FERC (electric utilities) and EPA/NEDS (other sources) (1975).

FIGURE 2-1. PREDICTED AVERAGE SULFATE CONCENTRATIONS

i = receptor region (state)

j = source region (state)

k = source class (utility, industrial, or area source)

x denotes weighting by either area or population

T^k_{ij} and $T^k_{\alpha\beta}$ are transport matrices at the state and Federal regional levels, respectively

E^k_j and E^k_β are total emissions for the k class of sources in region j and β

The values of a Federal region transport matrix for fine particulates for four months are shown in Table 2-1. A sample state transport matrix is included as Appendix A of this report. At any geographic level, incremental contributions to concentration from each source area can be identified separately. These are simply the separate products $T^k_{ij}E^k_j = \Delta C_{ij}$ obtained before summation. An example of such a table at the Federal region level is shown in Table 2-2. Terms along the diagonal (i=j) in this table are the intraregional contributions. Summation of off-diagonal contributions for a receptor area gives the imported contribution. Table 2-2 shows that the imported fraction to Federal regions varies from 6 to 92 percent. The area-weighted national average is 50 percent for SO_4. The comparable SO_2 average is 27 percent. A similar treatment at the state level gives a national average of 73 percent for imports of SO_4 and 40 percent for SO_2. All of these figures apply to a 2-month average of BNL model results. The concept of import and local is specific to the geographic level of the matrix.

In summary, state and Federal region matrices allow convenient computation of imported and local contributions and of region-to-region relationships. In addition, they provide a simplified analytic tool for quick computation of regionwide concentrations (e.g., by pocket calculator or microcomputer).

2.7 LOCAL VERSUS LONG-RANGE TRANSPORT

A major advantage of the matrix approach is the fact that computations can easily be split into two components: one for locally generated concentrations and one for concentrations generated in other AQCRs. The local (intraregional) contributions can be computed from the diagonals of the transport matrices, and the long-range (interregional) contributions are computed using the off-diagonal elements. Obviously, the ability to distinguish between local and long-range effects is very important for regulatory considerations. Because field-measured concentrations from long-range sources are usually indistinguishable from concentrations due to local sources, computer predictions are sometimes the only information available on source resolution. The use of a "square" matrix allows substitution of more detailed models for the local source contributions (diagonal terms), while retaining off-diagonal elements for the interregional contributions.

Table 2-1. Fine Particulate Transport Matrix
(Federal Region Level)

RECEPTOR REGIONS	EMITTER REGIONS 1	2	3	4	5	6	7	8	9	10
1	4.6602	2.9563	0.9966	0.1832	0.4789	0.0566	0.1434	0.0380	0.0134	0.0129
2	1.5096	6.5138	3.3305	0.3370	0.8170	0.0856	0.2470	0.0460	0.0149	0.0275
3	0.0529	1.2046	4.1547	0.9090	1.2668	0.1162	0.2220	0.0302	0.0069	0.0067
4	0.0110	0.0286	0.1875	2.1851	0.4149	0.2842	0.1837	0.0267	0.0063	0.0023
5	0.0000	0.0022	0.0370	0.2098	1.8340	0.2777	1.1157	0.2449	0.0400	0.0596
6	0.0016	0.0032	0.0138	0.0930	0.0206	1.5116	0.2183	0.2136	0.1460	0.0369
7	0.0000	0.0007	0.0073	0.0499	0.1915	0.7962	2.4965	0.5670	0.0882	0.0845
8	0.0	0.0000	0.0001	0.0011	0.0166	0.0570	0.1371	1.8181	0.3213	0.6316
9	0.0	0.0000	0.0000	0.0002	0.0001	0.0050	0.0001	0.0824	2.4288	0.1037
10	0.0	0.0	0.0000	0.0000	0.0000	0.0002	0.0000	0.0536	0.2933	3.4032

Note: Based on PNL model, using annual average, area-weighted data. Units are micrograms per cubic meter per million metric tons of emissions.

Table 2-2. Interregional Contributions to Sulfate Concentrations (Federal Region Level)

	Receptor									
Emitter	1	2	3	4	5	6	7	8	9	10
1	0.453	0.059	0.009	0.002	0.000	0.000	0.000	0.000	0.000	0.000
2	0.540	1.199	0.328	0.037	0.009	0.000	0.000	0.000	0.000	0.000
3	1.232	2.212	4.728	0.518	0.171	0.012	0.001	0.000	0.000	0.000
4	0.646	0.934	2.559	3.832	1.042	0.256	0.209	0.007	0.000	0.000
5	2.817	4.120	5.640	1.730	4.420	0.121	0.617	0.026	0.000	0.000
6	0.035	0.058	0.098	0.228	0.293	1.032	0.755	0.278	0.068	0.003
7	0.174	0.295	0.322	0.283	0.966	0.169	1.113	0.050	0.000	0.000
8	0.008	0.014	0.007	0.006	0.114	0.059	0.243	0.530	0.026	0.061
9	0.008	0.019	0.014	0.011	0.041	0.484	0.287	0.791	1.848	0.250
10	0.000	0.000	0.000	0.000	0.007	0.004	0.012	0.080	0.026	0.316
Local	0.453 (8%)	1.199 (13%)	4.728 (34%)	3.832 (58%)	4.420 (63%)	1.032 (48%)	1.113 (34%)	0.530 (30%)	1.848 (94%)	0.316 (50%)
Import	5.461 (92%)	7.712 (87%)	8.976 (66%)	2.815 (42%)	2.642 (37%)	1.105 (52%)	2.124 (66%)	1.232 (70%)	0.121 (6%)	0.314 (50%)
Total	5.914	8.911	13.704	6.647	7.062	2.137	3.237	1.762	1.969	0.630

Note: Values are from BNL model for average of January and July 1974 meteorology; units are micrograms per cubic meter.

The relative fractions of local and long-range contributions varies greatly among regions, with as much as 99 percent of SO_4 due to imports. On a national average basis, model runs give about 89 percent of concentrations of SO_4 contributed by imports and 62 percent for SO_2 at the AQCR level.

2.8 ERROR ANALYSIS

The matrix approach greatly simplifies some aspects of error analysis. Errors in computed concentrations may be regarded as arising from errors in the emission vector and from errors in estimation of atmospheric transport properties, which are reflected in the transport matrix elements. The form of the matrix representation makes it possible to compute the error variances in concentrations that would result from given errors in either of these two sources. More complicated models, such as the BNL and PNL parent models are not as convenient for direct computation of such error variances. They must be estimated from laborious sensitivity runs of the model. However, the parent models are essential for calculating the magnitudes of possible errors caused by uncertainties in various transport parameters (e.g., wind field errors, transformation rates).

2.9 OPTIMIZATION

The matrices provide a tractable mathematical form that can be incorporated into formal optimization algorithms. The parent models are too cumbersome to be used in this manner. When and if sound economic data are available and optimization criteria are developed, the efficiency of the transport matrix method will be very important.

2.10 INTEGRATED GRAPHICS

The matrix method output has been interfaced with three different computer programs to produce plots. Contour plotting from the DISSPLA* package is being developed to provide maps similar to Figure 3-1. Shaded maps at the AQCR level (such as Figure 2-1) are generated by the SEEDIS** system. The SAS*** package provides scatter plots directly from terminal printers (Figure 5-3). Scatter plots are frequently used to investigate x-y data trends, and the first two plotting styles are used to aid perception of spatial trends. Each style has its own strengths; the combination of all three linked to matrix method output is an effective tool.

---

* DISSPLA is a software package for graphic data display marketed by Integrated Software Systems Corp., San Diego, California.

** SEEDIS is the Socioeconomic Environmental-Demographic Information System developed by Lawrence Berkeley Laboratory, University of California.

*** SAS is a commercial computer software package developed by SAS Institute, Inc., Cary, North Carolina.

2.11 INFERENCE OF TRANSPORT PROPERTIES

A transport matrix represents a mathematical transformation of an emission field into a concentration field. A transport matrix summarizes a large amount of information about the transport properties of a given period and of the parent transport model. (Much more information than one resulting concentration field.) Examination of matrices for different periods should aid in understanding the relationship between meteorological patterns and their transport characteristics and the transport processes in the parent model. Hence, the matrices may become important tools in understanding and improving models.

2.12 TRANSPORT DISPLAY

A visual display of transport relationships among regions can be obtained by use of a pseudo mass transport scheme. If emissions in region j cause an average concentration of SO_4 in region i of $T_{ij} \cdot E_j$, then the average suspended mass in the air above region i is approximately $M_{ij} = h \cdot A_i \cdot T_{ij} \cdot E_j$, where h is the height of the assumed mixing layer and A_i is the area of region i. In a crude way, one may say that M_{ij} is the impact of region j on region i. A map of M_{ij} values represented as vectors from one region to another is shown in Figure 2-2.

The flows given in Figure 2-2 are useful in visualizing the relative magnitudes of transport relationships. The width of each vector is proportional to the magnitude of M_{ij}. However, these values do not give true mass transport. For this, one needs information on deposition and transformation. Such information is planned for future implementaton to permit sulfur budget calculations. Displays of M_{ij} as in Figure 2-2 are intended only for qualitative visualization.

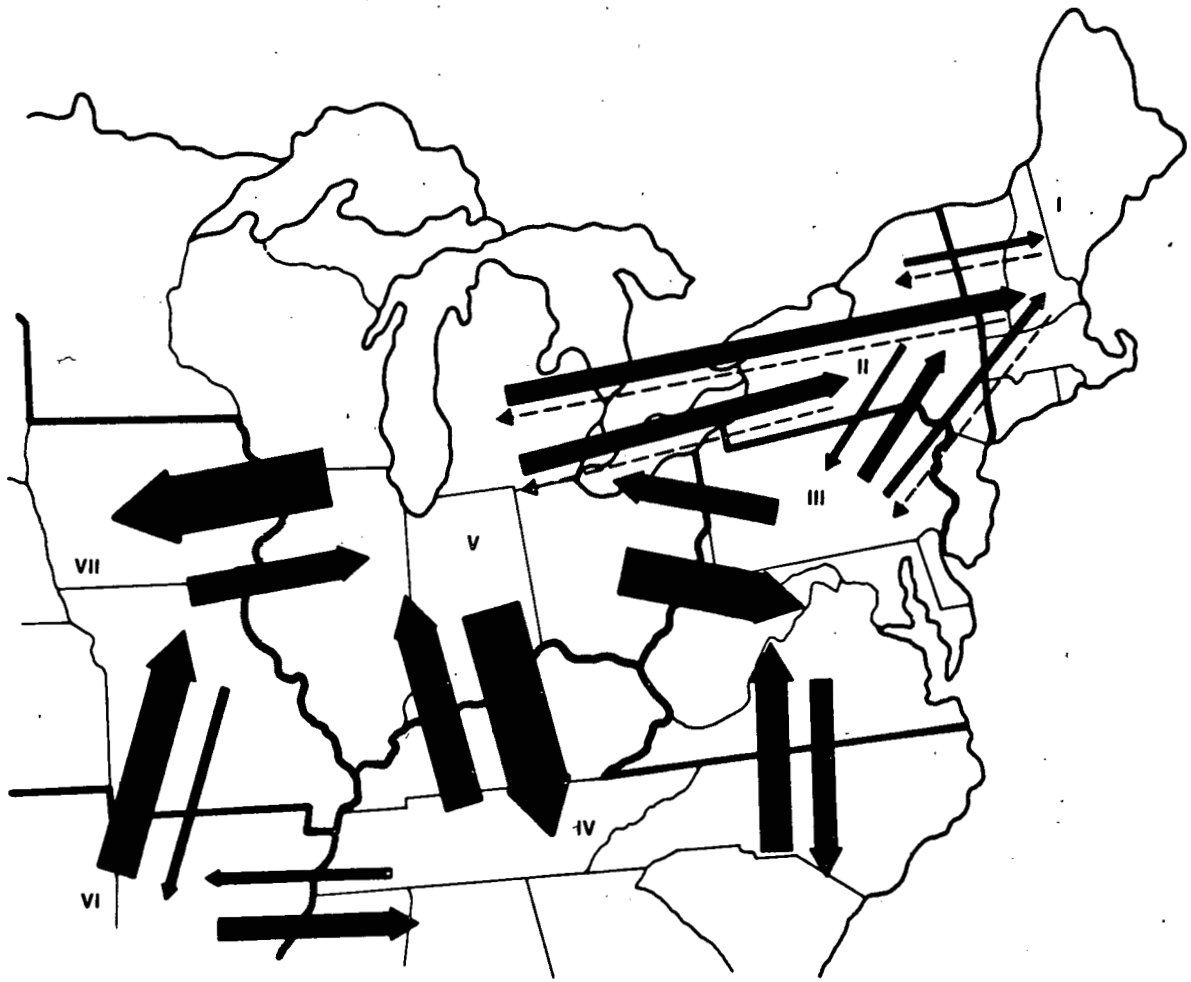

Note: Opposing parallel arrows indicate flow in both directions between regions. Width of each vector is proportional to the pseudo-mass transport. Very small flows are indicated by dashed lines. Data are from BNL AIRSOX model using January and July averaged, area-weighted, utility values.

FIGURE 2-2. SULFATE MASS TRANSPORT BETWEEN FEDERAL REGIONS

3. INFERENTIAL CAPABILITIES OF LONG-RANGE TRANSPORT MATRICES

3.1 GENERAL

In addition to their use in estimating concentrations, matrices can be used to infer other properties of transport that are less obvious. Several such uses are discussed here. The individual elements of a matrix represent transport coefficients, coupling pairs of regions as emitter and receptor. A number of properties of the transport process can be inferred from these matrix elements and combinations thereof. These properties or "measures" can be computed readily from the transport matrices, sometimes supplemented by regional population data.

3.2 TRANSPORT POTENTIAL OF AN EMITTER

This "measure" is a conceptual interpretation of the columns of the transport matrices. By scanning down the j^{th} column, one can see the potential influence of the j^{th} region on each of the other regions. Because no actual emissions are involved, this measure is only a potential. It represents the amount of pollution ($\mu g/m^3$) that would be added to each region by unit emission of 1 million metric tons annually in the j^{th} region. An analyst posed with the problem, "How would each of the regions be impacted by emissions from the j^{th} region?", could gain quick insight from a map of transport potentials for that region. Figure 3-1 shows such a map for AQCR 183, Zanesville, Ohio. A different map could be generated for each AQCR viewed in turn as an emitter.

3.3 RECEPTOR POTENTIAL

Each region has potential to receive pollutants as well as emit them. When considering one region as a receptor, its potential for being affected by the other region can be seen by looking at the corresponding row of the transport matrix. Each element in this row shows the potential of some region to transport pollutants into the selected region. Figure 3-2 shows receptor potential for AQCR #43, New York City, New Jersey, and Connecticut.

3.4 IMPACT POTENTIAL

Integral measures of potential impacts may be inferred directly from the matrices. Suppose one has a function, V_i, representing the susceptibility to impact of a population or crop. If we assume that V_i times C_i is a measure or surrogate for impact, then total impact (I) for the United States would be given by

$$I = \sum_i V_i \cdot C_i = \sum_i V_i \sum_j T_{ij} \cdot E_j$$

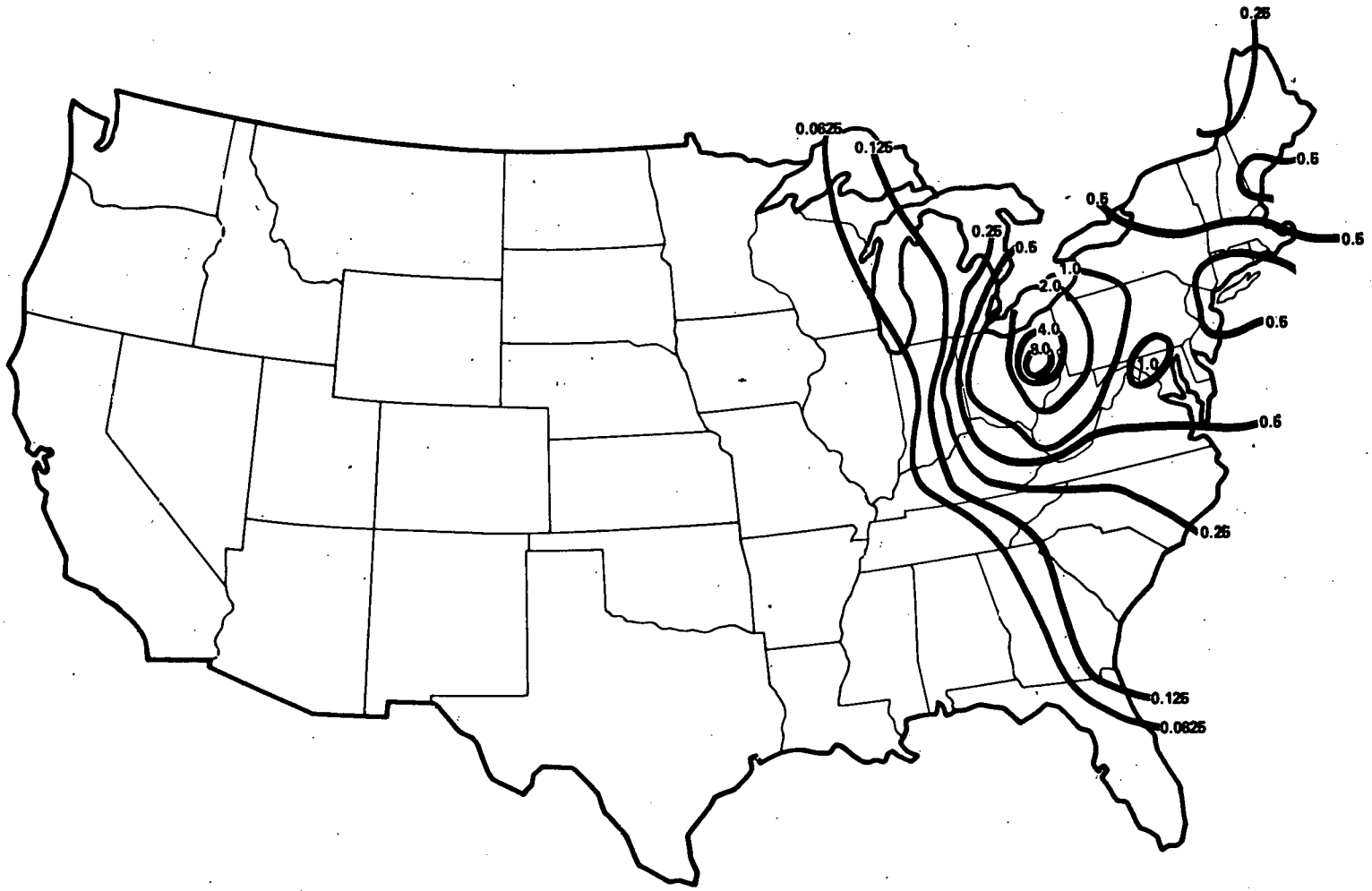

Note: Contours show incremental suspended sulfate (SO_4) concentration ($\mu g/m^3$) averaged over one month due to a hypothetical tall stack source emitting one million metric tons per year of SO_2, located in Ohio (AQCR #183, "Zanesville"). Meteorological data are for the month of January 1974. Concentrations based on calculations with Brookhaven National Laboratory AIRSOX model.

FIGURE 3-1. SULFATE TRANSPORT POTENTIAL

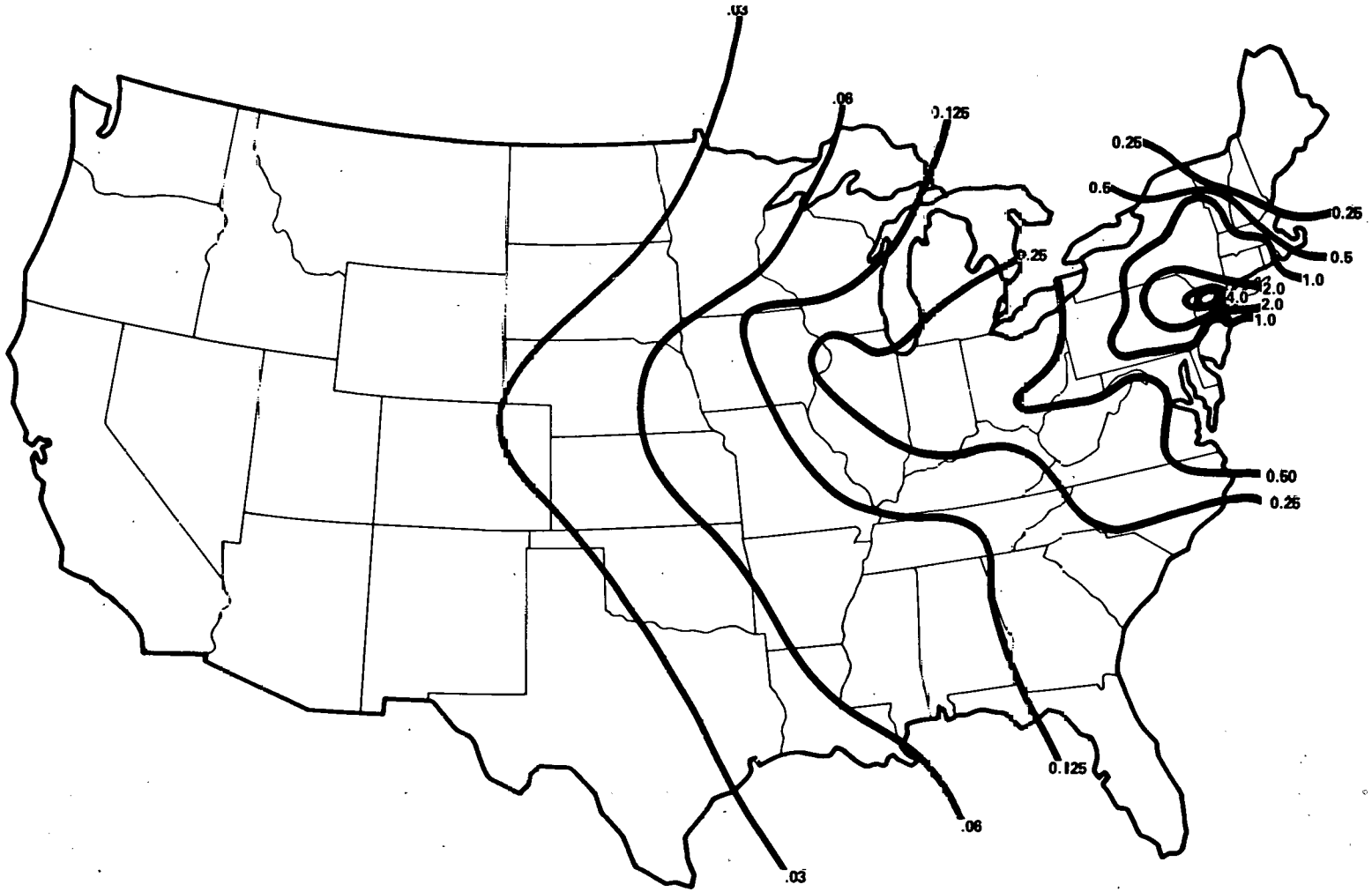

Note: Contours show incremental average sulfate (SO_4) concentrations ($\mu g/m^3$) expected in New York metropolitan area (AQCR #43) for a single source located in vicinity of the contour emitting one million metric tons of SO_2 per year. Concentrations are a one-month average based on January 1974 meteorology.

FIGURE 3-2. SULFATE RECEPTOR POTENTIAL

where:

V_i = measure of susceptibility to impact of receptor region i
C_i = pollutant concentration in receptor region i
E_j = pollutant emissions from emitter region j
T_{ij}= transport potential from emitter j to receptor i

The utility of a matrix formulation is that one can rearrange this formula in terms of a potential impact measure per unit of emissions, Φ_j, as follows:

$$I = \sum_j \Phi_j \cdot E_j$$

where

$$\Phi_j = \sum_i V_i \cdot T_{ij}$$

In this form, one is able to directly express impact everywhere in the conterminous United States due to unit emissions in any region (j).

Measures of susceptibility to pollution damage are still a controversial subject; therefore, few generally accepted measures are available. Mapping of crops and ecosystems susceptible to damage is under development at Argonne and Oak Ridge National Laboratories.

3.4.1 Population Exposure Potential

Human health damage is difficult to quantify due to the uncertainty of human response to pollutant dosage. One can use population as the measure of susceptibility (V_i) in the equation above, in which case Φ_j becomes a measure of population exposure potential.*

For each region viewed as an emitter, one can define a single number (rather than a row or column) that represents its nationwide potential for exposing human population to pollution. For a selected region, the corresponding T-matrix column is multiplied element by element by the populations of the regions. These products are then summed to one number (Φ_j):

$$\Phi_j = \sum_i P_i \cdot T_{ij}$$

---

* The population exposure potential concept was developed by M.D. Rowe of Brookhaven National Laboratory using the Brookhaven parent model (Rowe, 1980) rather than the matrix method.

where

ϕ_j = exposure potential for j^{th} region
P_i = population in i^{th} region
T_{ij} = transport from j^{th} to i^{th} region

Regions having high ϕ_j values would tend to be bad locations for increased emissions insofar as this measure is concerned. If increased emissions are necessary, the implication is that they should be located in regions with low exposure potential. Because there is one value for each region, exposure potentials can be summarized for all regions in one map. Figure 3-3 illustrates the potential for a single pollutant, sulfates. This figure shows strong local maxima near population centers, especially Los Angeles and New York. This occurs because the urban exposure potentials are matrix products of the large urban population values and high local (intraregional) sulfate transport values. The high intraregional transport values indicate that some sulfates tend to be produced close to the emission sources (generally near urban centers) and affect their immediate locality. It is also true, however, that sulfates are transported further downwind than SO_2, partly because of the continuing generation of sulfates as the SO_2 migrates.

3.4.2 National Population Exposure

This measure (NPE) is the sum of products formed by multiplying the concentrations predicted for each region by the population in that region. It can also be viewed as the sum of population exposure potential times emissions over all emitting regions:

$$NPE = \sum_i P_i \cdot C_i = \sum_j \phi_j \cdot E_j$$

National population exposure is a single, aggregate measure of consequences that may be useful in judging the relative effects of policy alternatives.

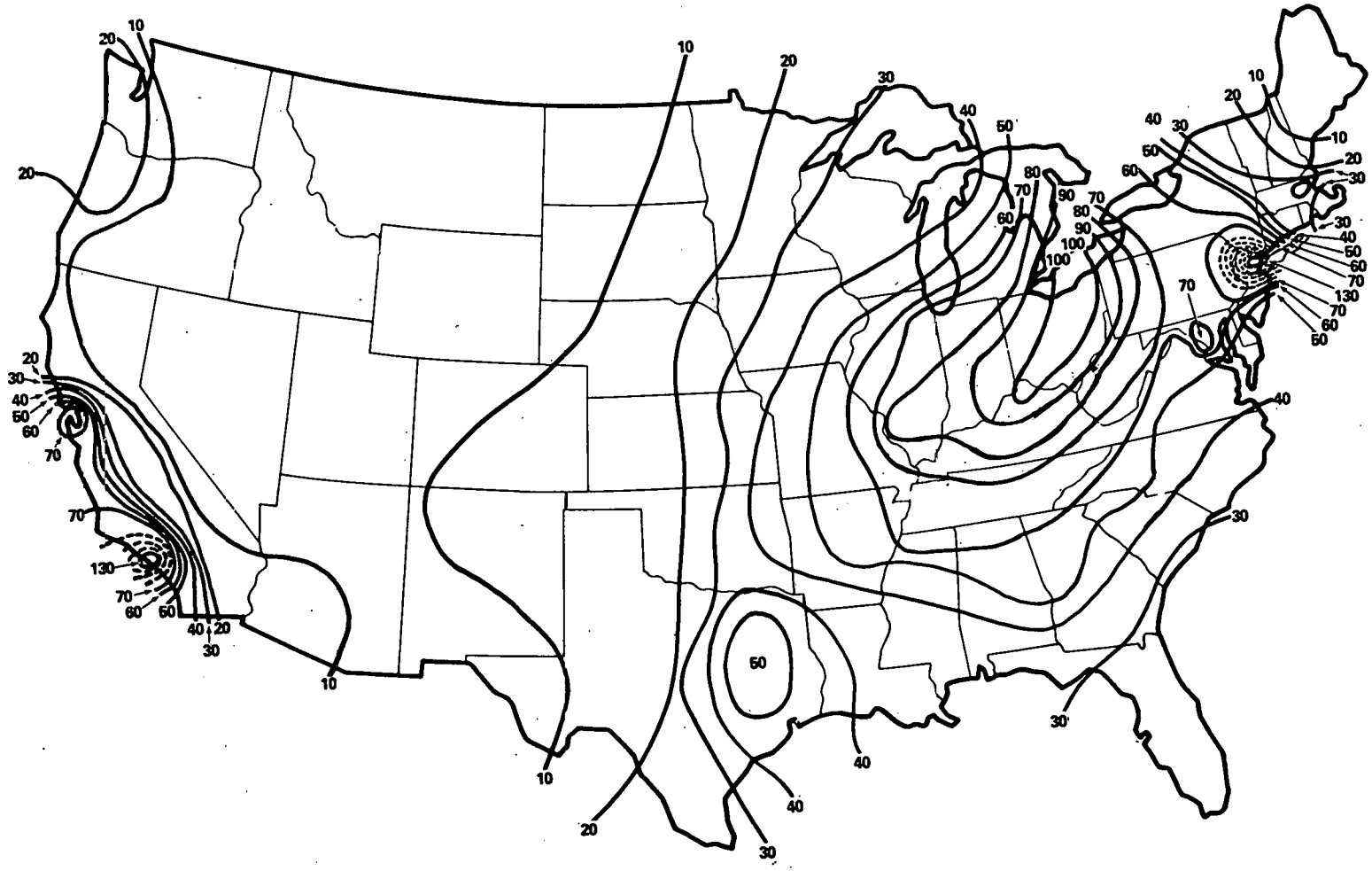

Note: Contours show the integrated U.S. population exposure (sum over number of persons exposed to each value of monthly average sulfate concentration throughout contiguous U.S.) predicted for a hypothetical source of SO_2 emissions located in vicinity of contour. Units are person-$\mu g/m^3$ of SO_4 per ton/year of SO_2 emitted (July 1974 meteorology).

FIGURE 3-3. POPULATION EXPOSURE POTENTIAL

4. APPLICATION OF THE MATRIX METHOD

4.1 LONG-RANGE TRANSPORT STUDIES

The matrix method has been emphasized as a practical tool for fast response policy analysis support. Several analyses have been conducted making practical use of the matrices. Summaries of two studies conducted in May 1980 are presented in the next two sections as illustrations of some applications of this method.

Generally, how the matrices are used and which measures are computed depends on the requirements of the study and on what questions are asked. The two studies presented use only the most straightforward applications of the matrix methodology.

4.2 STUDY NO. 1: CONTRIBUTIONS OF LONG-RANGE TRANSPORT TO NONATTAINMENT OF AIR QUALITY STANDARDS

This analysis was part of an assessment of long-range transport issues. It quantifies the amount of pollution caused by local sources versus sources outside local AQCRs for a region in Ohio, Pennsylvania, and West Virginia that has a history of air pollution problems. Because the purpose is to get an approximation to the effects of local versus imported pollution, only the predicted concentrations are needed from the matrix method.

Many of the pollutants and effects involved in long-range transport are not currently regulated by the National Ambient Air Quality Standards (NAAQS). However, for several pollutants, transport is substantial enough at moderate distances (100 km or so) to contribute concentrations that are at least a significant fraction of the ambient standards. Where this transport occurs across AQCR and state boundaries, legal, regulatory, and institutional issues are engendered.

The gases sulfur dioxide and ozone appear to cause the most obvious long-range transport problems, but violation of particulate (TSP) standards also may be exacerbated by long-range transport.

Identification of the role of long-range transport in areas experiencing nonattainment problems is often difficult because of a lack of reliable regional scale models and/or insufficient observed data. Many of the problem areas occur in or near industrialized areas of the northeastern United States, where a multiplicity of local and distant emission sources confuses the identification problem. However, as state governments and local interests become more aware of the external impacts on their environment and economic growth, increased attention and analysis is being focused on identifying the causes of their local problems.

4.2.1 Sulfur Dioxide

Nonattainment problems occur for sulfur dioxide in about 49 different counties in the United States, although often in only a small portion of the

total area. Many of the cases appear to be due to local effects of a large source, such as a primary metal smelter or a collection of sources in a poorly ventilated area. In a few parts of the northeastern United States, however, there appears to be substantial transport across AQCR and state boundaries. Local sources and long-range transport combine to provide high values of SO_2 as well as of sulfates.

A prime example of interstate SO_2 transport problems is the tri-state area of eastern Ohio, western Pennsylvania, and northern West Virginia. Nonattainment areas for SO_2 have been declared in portions of many of the AQCRs within this region, as indicated in Table 4-1. Both annual and short-term standards are violated in this region, although more often the latter.

Long-range transport matrices cannot describe the short-term situation, but analysis of monthly average values gives important clues about the degree of transport. Table 4-1 lists results for several AQCRs in this region derived by applying two monthly average matrices to a national SO_2 emission vector. The emission estimate is for 1975 and the meteorological data are for January and July 1974. The average calculated concentrations for the two months can be compared with observed annual average values for the years 1974 and 1975. The model calculations provide separate estimates of the imported and local contributions to the concentration.

Model calculations in Table 4-1 indicate that imported SO_2 makes a substantial contribution to total SO_2 concentrations even in areas with high emissions. These figures suggest that imports are able to tip the balance to nonattainment when combined with high local emissions. However, in the two regions in West Virginia with low emissions, total concentrations were moderate and there were no recorded violations. Generally speaking, the proportions of imported concentration calculated may be expected to be more applicable to violations of the annual SO_2 standard than the 24-hour standard.

4.2.2 Sulfate/TSP

Calculated SO_4 levels show an even larger proportion of imported versus local contribution because of the lag time in their formation. Imports account for more than two-thirds of the concentration in this region, even in AQCRs having the highest emissions. As the wind flow changes direction, from one period to another, different regions may exchange roles as emitters and receptors. Although regions with no emissions show some concentrations due to import, they did not approach nonattainment status.

The maximum predicted total level of SO_4 found here was 27 $\mu g/m^3$, but values of the imported component were all in the 16 to 20 $\mu g/m^3$ range. This suggests that imported sulfate alone would account for one-third and one-fourth of the annual TSP secondary and primary standards (60 $\mu g/m^3$ and 80 $\mu g/m^3$), respectively. Of course, long-range transport of nitrates, organics, and emitted fine particulates must be added to sulfates to capture the full effect of long-range transport on TSP.

Table 4-1. Import of Sulfur Into Areas in Ohio, Pennsylvania, and West Virginia

#	Name	(State)	Estimated 1975 SO_2 Emissions (1,000 Tons)	Nonattainment Status For SO_2 (as of 3-79)	Annual Avg. Observed SO_2 Conc. ($\mu g/m^3$)		Calculated Concentrations: AQCR Average For 2 Months (January & July 1974) of Meteorological Data ($\mu g/m^3$)					
							SO_2			SO_4		
					1974	1975	Total	Local	Import	Total	Local	Import
174	Gr. Met. Cleveland	(Ohio)	650	Nonattainment	56	57	52	36	16	22	06	16
183	Zanesville-Cambridge	(Ohio)	239	Nonattainment	-	82	44	16	28	22	02	20
179	Parkesburg-Marietta	(Ohio)	367	Nonattainment	-	32	47	19	27	21	03	18
181	Steubenville-Weirton-Wheeling	(Ohio-W. Vir)	858	Nonattainment	79	79	84	54	29	27	08	19
178	N.W. Penn. - Youngstown	(Ohio-Penn.)	356	Nonattainment	52	41	38	10	29	20	02	18
197	S.W. Pennsylvania		981	Nonattainment	27	28	82	39	42	23	05	18
195	Central Pennsylvania		212	Nonattainment	32	36	30	05	25	18	01	17
233	Eastern Panhandle	(W. Vir.)	009	O.K.	-	31	23	01	22	17.5	00.1	17.4
235	N. Central W. Vir.		398	O.K.	13	25	59	31	28	25	05	20
232	Central W. Vir.		002	O.K.	13	16	24	00	24	17	00	17

4.2.3 Caveats

Caution is advised in interpreting the values in Table 4-1 due to a number of technical limitations of the model and the fact that only two months of meteorology have been utilized. Furthermore, one should not conclude that imports will contribute the same fractional amount to short-term concentration maxima as found here for monthly averages.

4.3 STUDY NO. 2: EFFECTS OF INCREASED SO_2 EMISSIONS DUE TO CONVERSION FROM OIL TO COAL

This analysis addressed questions generated from draft legislation proposing that a number of powerplants convert from oil to coal. Rough estimates of the increases in SO_2 that would result for each powerplant were extracted from informal Environmental Protection Agency analyses, and the increases were assigned to the AQCRs where the powerplants are located. Proposed policies and emission estimates are subject to change, and the emissions estimates used here subsequently changed with evolving legislative proposals. The important point was to obtain rough estimates of potential consequences quickly.

Calculations were made of SO_2 and SO_4 concentrations by AQCR, population exposures by AQCR, and national averages. Because these measures are linear with respect to emissions, an estimate of the effect due to increased emissions can be computed directly by multiplying appropriate matrices by the emission change vector. It is not necessary to predict what the total emissions will be with and without the changes.

4.3.1 Overview

Preliminary Environmental Protection Agency estimates of increased SO_2 emissions due to the oil backout initiative have been analyzed with the aid of Brookhaven's sulfur long-range transport matrices. Results indicate that changes in monthly average concentrations of SO_2 and SO_4 averaged over AQCRs will amount to as much as 3 $\mu g/m^3$ of SO_2 and less than 1 $\mu g/m^3$ of SO_4. National population exposure over the United States is estimated to increase by 91 x 10^6 person-$\mu g/m^3$ of SO_2 and 22 x 10^6 person-$\mu g/m^3$ of SO_4.* Almost half of the SO_2 population exposure and one-third of the SO_4 population exposure occurs in the New York/New Jersey/Connecticut AQCR (#43). The percent increase in SO_2 population exposure is almost double the percent increase in SO_2 emissions. (This results from the predominantly urban locations for the converted plants.) The percent increase in SO_4 exposure is about equal to the SO_2 emission increase.

The geographic distribution of concentration increments shows the largest percentage increases, relative to the 1975 baseline, in urban areas rather than rural areas where ecological resources are at risk (e.g., New

---

* National population exposure is the sum of population times concentration over all regions. This measure is described further in Section 3.4.2.

England and upper New York State). In the absence of reliable dose-response function for human health and ecological damage and of acid deposition predictions, it is not possible to infer the magnitudes of health or ecological damages. One can only say that the effect of these conversion-related emissions is more skewed toward urban SO_2 levels than are average (1975 base case) emissions.

4.3.2 Ambient Impacts

A simple analysis of ambient air quality impacts of increased sulfur dioxide emissions has been made for the utility oil conversion issue. The analysis is based on unofficial Environmental Protection Agency estimates of increased SO_2 due to the oil backout initiative. Altogether, 345,000 tons/yr of emissions in 21 air quality control regions are involved.

For this analysis, emissions from the plants were aggregated to totals for their respective AQCRs (see Table 4-2). This vector of emissions was multiplied by the air transport matrices developed by Brookhaven National Laboratory with their AIRSOX model. Matrices that give monthly concentration averages based on meteorological data from July 1974 and January 1974 were used.

The results of the matrix transport analysis are shown in Table 4-2. Incremental, population-weighted concentrations for a January and July 2-month average are shown for both SO_2 and SO_4. Values are shown for the 21 AQCRs that had non-zero emissions and for other AQCRs that showed substantial concentrations and/or population exposure values. Note that the highest concentrations were about 3 $\mu g/m^3$ for SO_2 and 0.5 $\mu g/m^3$ for SO_4. These SO_2 and SO_4 values are small compared with annual primary and secondary standards for SO_2 and TSP, respectively, and with typical observed annual maximum values of SO_4 of 10 to 20 $\mu g/m^3$. The primary annual standard for SO_2 is 80 $\mu g/m^3$. The primary and secondary annual standards for TSP are 75 and 60 $\mu g/m^3$, respectively. Sulfates, of course, are only one small component of TSP. Long-range transport will add fine particulate nitrates, organics, and emitted fine particulates to local fine and coarse particulates. Allocable increments under Prevention of Significant Deterioration (PSD) regulations for annual SO_2 averages are 2, 20, and 40 $\mu g/m^3$ for Classes I, II and III, respectively.

Several areas have SO_2 concentrations greater than PSD Class I increments, but do not contain Class I areas. The increases would use 10 to 15 percent of the Class II increment in a few areas. Increases in SO_4 are relatively small (5 to 10 percent) compared with the prevailing annual values in the northeastern United States. In the upper New York State area (AQCR #159 and #158), increases are of the order of 0.10 to 0.15 $\mu g/m^3$, or about 1 to 2 percent of currently observed values. This suggests that acid rain effects would not be unusually important, i.e., not out of proportion to the relative increase in total U.S. emissions and not large in absolute magnitude.

Table 4-2. Selected Impacts of Incremental Sulfur Emissions

Federal Region	AQCR#	Name	Emissions of SO_2 (1,000 tons/year)	Annual Average Base Ambient Concentration of SO_2 ($\mu g/m^3$) in 1975*	Average Concentration Increases (January-July Average)($\mu g/m^3$)		Population Exposure (January-July Average) (person-$\mu g/m^3$ x 10^6)	
					SO_2	SO_4	SO_2	SO_4
I	41	East. CONN.	0.61	16	0.72	0.21	0.2	0.07
I	42	Hartford/NewHaven/Spring.	10.54	31	0.84	0.21	2.1	0.51
I	44	N.W. CONN.	0.00	26	0.53	0.17	0.1	0.02
I	119	Metro. Boston	2.72	23	0.59	0.17	1.9	
I	120	Metro. Providence	7.74	24	0.61	0.19	0.9	
I	121	Merrimack Valley-S.N.H.	6.80	33	0.41	0.15	0.2	
II	43	N.J./N.Y./CONN.	56.66	40	2.69	0.42	46.1	7.22
II	158	Cent. N.Y.	4.80	25	0.25	0.13	0.3	
II	159	Champlain Valley	0.00	28	0.07	0.09	0.0	
II	161	Hudson Valley	16.00	40	0.60	0.18	1.0	0.31
III	45	Metro. Philadelphia	12.67	37	0.74	0.23	4.2	1.28
III	46	Southern Delaware	0.00	3	0.51	0.25	0.1	
III	47	National Capital	2.07	17	0.58	0.23	1.7	0.70
III	114	Eastern Shore	0.00	13	0.60	0.24	0.1	
III	115	Metro. Baltimore	22.52	20	1.41	0.31	3.0	0.66
III	116	Southern Md.	0.00	8	0.39	0.23	0.1	
III	197	S.W. PENNA.	0.00	70	0.03	0.07	0.1	
III	223	Hampton Roads	21.95	23	1.74	0.35	2.0	0.40
III	224	N.W. VA.	0.00	13	0.46	0.20	0.2	
III	225	State Capitol (VA.)	33.16	22	2.15	0.37	1.3	
III-IV	103	Hunt.-Ashland-Portland	3.90	14	0.12	0.09	0.1	
IV	18	Metro. Memphis	0.00	22	1.35	0.39	1.1	0.33
IV	49	Jacksonville/Brunswick	0.06	13	0.05	0.06	0.1	
IV	52	West. Cent. Florida	15.77	14	0.78	0.14	1.5	
IV	58	Savannah-Beaufort	0.37	8	0.02	0.05	0.0	
IV	209	Western TENN.	0.00	27	0.80	0.26	0.4	
V	81	N.E. Indiana	13.41	22	0.89	0.17	0.5	
V	123	Metro. Detroit	11.89	29	0.45	0.12	2.2	0.49
VI	20	N.E. Arkansas	76.35	3	1.47	0.38	1.1	0.33
VII	94	Metro. Kansas City	25.00	18	1.14	0.17	1.6	
		TOTAL	344.99			U.S. TOTAL	80.0	21.60

* Ambient values represent averages over all population-oriented monitors in AQCR; violations not necessarily reflected.

It is noteworthy that several AQCRs with no emissions show substantial values on the order of 1 $\mu g/m^3$ of SO_2. The worst such case is metropolitan Memphis with 1.6 $\mu g/m^3$ in January and 1.4 for the two months. The overall highest SO_2 values occur in the metropolitan New York City AQCR (#43, New Jersey/New York/Connecticut), 3 $\mu g/m^3$ in January and 2.7 overall. This region alone accounts for almost half of the total SO_2 population exposure due to the initiative. In this region, the contribution to SO_2 from interregional transport is 0.42 $\mu g/m^3$, or 14 percent in January and 10 percent in July.

For sulfate, incremental concentrations are widespread at about 0.33 $\mu g/m^3$, reaching the highest values again in the New York City area (AQCR #43) at 0.42 $\mu g/m^3$, in the Virginia State capital area (0.47 in January), Memphis, Tennessee (0.49 in July), and northeastern Arkansas (0.47 in July). The New York City area accounts for one-third of total U.S. population exposure to sulfate (6×10^6 person-$\mu g/m^3$) due to the initiative emissions. About 24 percent of this is due to imports to this region. Values of SO_4 comparable to those in the emitting regions (0.1 to 0.3 $\mu g/m^3$) occur in a number of nonemitting regions, such as in Maryland, Delaware, Tennessee, and parts of New England and the Midwest.

Total population exposure is also calculated. This represents the sum over the whole United States of number of persons times average pollutant level in each area. The incremental values due to the oil backout initiative are 80 million person-$\mu g/m^3$ for SO_2 and 22 million for SO_4. These values may be compared with the calculated U.S. totals for the 1975 base case, which are 3580 million person-$\mu g/m^3$ for SO_2 and 1730 million for SO_4. Thus, initiative emissions, which are about 1.3 percent of the 1975 total, produce 2.2 percent of 1975 SO_2 population exposure and 1.3 percent of 1975 SO_4 exposure. Hence, initiative emissions are more effective in exposing people to SO_2 and are average in exposing people to SO_4.

4.3.3 Caveats

Population exposure, as calculated here, is a linear measure of dose that is thought to be significant for long-term, cumulative health effects. Acute effects should be analyzed in terms of peak concentrations to which population groups are exposed, usually at a microscale level. The model used here cannot estimate peak concentration values occuring over short time intervals and small-scale spatial regions. The spatially and temporally averaged concentration values estimated here will underestimate such peak values systematically. The concentration increments cannot be used to estimate regulatory violations.

Estimates of urban sulfate levels, and hence of population exposure to sulfate, are likely to be underestimated. The BNL model assumed a constant SO_2 to SO_4 transformation rate, which usually is an underestimate for urban areas in which high oxidant levels greatly increase transformations. Therefore, it is likely that actual SO_4 exposure is larger. Although base case SO_4 exposure is based on this model, the distribution of initiative emissions is more urban, which suggests that actual SO_4 exposure might be out of proportion to emissions.

5. LONG-RANGE TRANSPORT MATRIX METHODOLOGY

5.1 MATRIX REPRESENTATION OF LONG-RANGE TRANSPORT

5.1.1 Matrix Equation

The advantages of a matrix representation of long-range transport models, as indicated in Section 2, led OEA, with the assistance of BNL and PNL, to develop a matrix analysis capability. These matrices are derived from the Lagrangian trajectory models at BNL and PNL and, therefore, are subject to any limitations inherent in those models. General descriptions of those models can be found later in this section; detailed mathematical descriptions may be found in Appendixes B and C.

The basic computational concept is that the spatial and temporal average concentrations ($C(t)_i$) in a geographic region (i) depend linearly on the emission rate from this and every other region, or

$$C(t)_i = \sum_j \sum_k T^k_{ij} \cdot E^k_j(t)$$

where $E^k_j(t)$ is the average emission rate of the precursor pollutant from source category k in region j during period t and T^k_{ij} is the transport coefficient calculated by the model for transport from region j to region i for sources of type k. Three types of sources (k) are distinguished according to their average effective stack heights: utility (200 m effective stack height), industrial (100 m), and area (20 m).

5.1.2 Spatial Units

Because the basic purpose of this matrix method is to permit modification of emission scenarios, the matrix should permit specification of a set or vector of emission strengths at the level of detail predicted in assessment scenarios. Many OEA scenarios have been projected at the level of air quality control regions,* so this spatial unit of aggregation was chosen for description of emission sources. Other spatial units are possible, including the original plant source points from which many trajectories are calculated. However, that approach requires new trajectories to be calculated when new plant sites are added for any scenario if a consistent level of resolution is to be retained. Furthermore, it is impractical to obtain specific site level data and calculate trajectories for all important sources, such as the large number of industrial combustion sources. Aggregation of emissions to the AQCR level is more practical and consistent with available emission data

* There are 247 air quality control regions in the United States, but only 238 are in the conterminous states.

such as the Environmental Protection Agency's National Emission Data inventory. However, coefficients for individual plant sites may still be of interest in some cases, and isolated cases have been studied in several OEA analyses.

At the receptor end, an appropriate spatial unit should be consistent with the resolution available from the air transport model to be used and with the type of air quality analyses to be performed. The BNL and PNL air transport models record concentrations on a regular grid spaced about 32 to 38 kilometers. This spacing is generally too large for counties, but adequate for most air quality control regions. AQCRs are also more convenient because they are usually air quality planning units and are much fewer in number.

An additional consideration in selection of spatial units is that of symmetry between source and receptor units. Using the same units for both results in a "square" matrix, which has several advantages. First, it provides a clear interpretation of influence of each emitter region on each receptor region. Second, it permits selective replacement of the diagonal, intraregional transport coefficient with alternative estimates for intraregional effects.

For the above reasons, AQCRs were selected as the smallest spatial unit of aggregation for both source and receptor classifications. Aggregated matrices at the state and Federal region levels have also been generated.

5.1.3 Theoretical Basis

An ideal air quality model for applied use in assessment and policy analysis arguably would be one that predicts air quality based solely on input of the variables subject to control or affected by policies. These variables typically include emissions, perhaps the location and height of releases, and more rarely, the timing and mix of pollutants released. Other variables not subject to control, such as meteorology and uncontrolled pollutants, would be factored into the model as constants or probability distributions. As an example, if the controllable variables are the magnitudes of emissions at several locations, E_1, E_2, . . . E_n, then the desired results would be measures of ambient quality. For example, mean concentration (C) would be represented as a function of the E values.

The general form of matrix representation is based on the assumption that certain statistical measures, usually expected values or mean values, are linear functions of a set of emission values. Matrices cited in this report represent estimated mean values for particular months of historical meteorological conditions. While these actual months are useful in validating or comparing against observed data, the goal for future assessment purposes would be matrices that represented expected values for periods of time in the future. (Expected annual average, expected monthly average for any July, etc.). It would also be useful to have predictions of the fluctuations about this mean value, such as the standard deviation about the mean. However, such measures are not necessarily expected to be representable as linear functions of the E values.

A fundamental question in developing matrix approaches is the following: for which pollutants, impact measures, and emission descriptions is the linear representation a valid approximation? More generally, air quality management strategy requires an understanding of the dependence of pollution management objectives on the controlled variables. Photochemical oxidant levels, for example, are predicted to vary as a nonlinear function of both NO_x and hydrocarbon emissions. Hence, a linear representation of oxidant formation could be very misleading (although even in this case linearity might be a suitable approximation for hydrocarbon variations in a limited range when NO_x is held constant).

Air transport processes tend to be linear at the microscopic level, in terms of pollutant concentrations, when concentrations are not too large and there are no reactions among constituents. However, atmospheric transformation and deposition processes of a given pollutant proceed at rates that depend on values of atmospheric variables and concentrations of other pollutants. They may also vary nonlinearly with the concentration of the given pollutant. The dependence on atmospheric variables and other pollutants does not necessarily introduce nonlinearity into the overall statistical description (although matrix coefficients might then depend on the general levels of other pollutants), but processes that are nonlinear in the given pollutant tend to invalidate a matrix representation. An evaluation of the effect of nonlinear processes on the overall functional dependence requires detailed consideration of processes and of the statistical correlations among pollutant levels and sources.

The BNL and PNL long-range transport models used in generating the present matrices are linear in their representation of all processes. Hence, there is no loss in representing their results linearly as far as processes are concerned. Sulfate might depend nonlinearly on SO_2 concentrations, but a regional study of correlations among SO_2, SO_4, and TSP showed no clear preference for this (Meyers and Ziegler, 1978).

The long-term, regionwide spatial and temporal averages are likely to vary approximately linearly with emissions. Extreme values such as the worst-case station values or short-term temporal maximum values usually are not simply additive with respect to emissions; hence, linear representation would not be justified.

The transport matrices (T_{ij}) depend on the detailed source distributions that produce E_j. Important changes in the value of T_{ij} with changes in source distribution would be expected mainly for intraregional and adjacent region relationships (i.e., for $i = j$ or region i next to region j). Problems are expected to be less serious for the longer term (monthly and annual) temporal and broad regional averages used in the present method.

5.1.4 Calculation of Matrices

Matrices might be generated by any appropriate model or by empirical methods. Analysis of observed data is unlikely to provide enough information to infer all of the interregional contributions, so long-range transport models

must be used to estimate interregional coupling. BNL and PNL were asked to generate matrices for SO_2 and SO_4 from their models (PNL also developed matrices for respirable particulates).

It was initially contemplated that the intraregional effects might not be well resolved by the long-range transport models. Hence, empirical methods using hybrid rollback models were considered for generation of diagonal elements. Initial testing of rollback concepts for SO_2 did not give good results, at least with the available 1974 empirical data bases. A major problem is that the position of the monitoring stations does not yield data representative of the AQCR average. Further testing and analysis and use of later data may improve this for SO_2. Sufficient data do not exist to use the rollback method for fine particulates, while SO_4 data require further examination. Hence, current matrix calculations are based on diagonal coefficients derived from the long-range transport models with the off-diagonal terms.

5.2 MATRIX GENERATION TECHNIQUE

5.2.1 General

The first matrices were generated by calculating concentrations of SO_2 and SO_4 with BNL's AIRSOX model. Values are calculated at grid points of about 32 km spacing across the conterminous United States and surrounding areas based on transport trajectories from a set of sources in one AQCR. One month of meteorological data at a time is used for computing wind trajectories and precipitation, and the average concentrations for that month are recorded. Grid point values are interpolated, mapped onto a polygon of counties, and then aggregated to form AQCR averages. Concentrations are normalized to unit emissions from the AQCR source, resulting in one column of the matrix T_{ij}. Repetition for other source areas yields one 238 x 238 matrix each for SO_2 and SO_4. In the county-to-AQCR aggregation, counties are weighted either by area or by their population to form two classes of matrices. (Different weightings are useful for different types of impact analyses.)

Matrices have also been generated for respirable particulates, SO_2, and SO_4 by PNL with their long-range transport model. Their matrix generation procedure is similar to the BNL procedure in principle, but streamlined to reduce computational effort. Only one source category is assumed and actual trajectories are calculated for a smaller number of source points. Resolution of source regions is obtained by generating additional, pseudo-source points through a special method of interpolation from the calculated source points (see Appendix C).

Results derived from matrices of this type are limited in accuracy by the assumptions of linearity, the constant sub-AQCR source and receptor patterns, and the limited spatial resolution, as well as by any limitations of the transport models used to generate them. Use of meteorological data for specific months requires that many additional months be examined to determine the degree of validity achieved and to formulate statistical probabilities for future concentration predictions.

5.2.2 Model Comparison

Matrices for SO_2 and SO_4 were generated by both BNL and PNL and include 2 months of meteorological data in common for both models (January and July 1974). Results from the two methods are found to differ somewhat, which may be due to differences in the parent model algorithm, choice of parameters, and methods used to generate the matrices. The matrix generation methods used by PNL were chosen deliberately, at DOE's request, to reduce computer requirements by reducing the number of trajectories calculated. Sensitivity tests were performed by PNL to verify the accuracy of the pseudo-source methods, as described in Appendix C.

In addition to the pseudo-source method for calculating intermediate trajectories, PNL also used a simpler, less realistic distribution of sources than BNL used in their utility matrices (PNL used a uniform 200-m stack height). Further testing of the effect of intra-AQCR source patterns used in the two methods is planned to establish their consequences on accuracy and resolution.

The two parent models also differ in many respects, although both are of the Lagrangian or trajectory model type and use similar grid sizes. The following two sections and Appendices B and C summarize the basic model algorithms and matrix generation techniques. Greater detail of the parent models is given in model descriptions for BNL AIRSOX (Meyers et al., 1979a) and PNL (Powell et al., 1979a). Horizontal and vertical diffusion are treated differently in the models. Those differences make it difficult to compare transformation and deposition parameters directly, because their effect is modified by the diffusion algorithms.

Empirical comparison of predicted concentrations of the two parent models, made at a selected set of points, showed high correlation (R^2=0.92) for both SO_2 and SO_4. However, PNL values of SO_4 were about two-thirds of the BNL values in magnitude.

Comparison of matrices shows additional differences, which are being investigated. Sulfate transport coefficients are smaller for PNL, especially the diagonal (intraregional) term, but patterns of transport are similar. Figures 5-1 and 5-2 show typical SO_4 transport patterns for a particular source calculated from BNL and PNL matrices, respectively. These figures are each derived from a column of the matrix corresponding to AQCR #183 as the source region.

The models differ significantly in their individual transport coefficients. Figure 5-3 illustrates a comparison of the two models' intraregional (diagonal) SO_2 coefficients in the form of a scatter diagram. There is a systematic tendency toward higher values for BNL. A least-squares line forced through the origin and fitted to this data gives an R^2 of 0.87 and a slope of 1.14. Thus, BNL matrices tend to predict about 14 percent larger local impact than the PNL matrices. In contrast, when the predicted values of SO_2 concentrations are compared, using a 1975 SO_2 emission estimate,

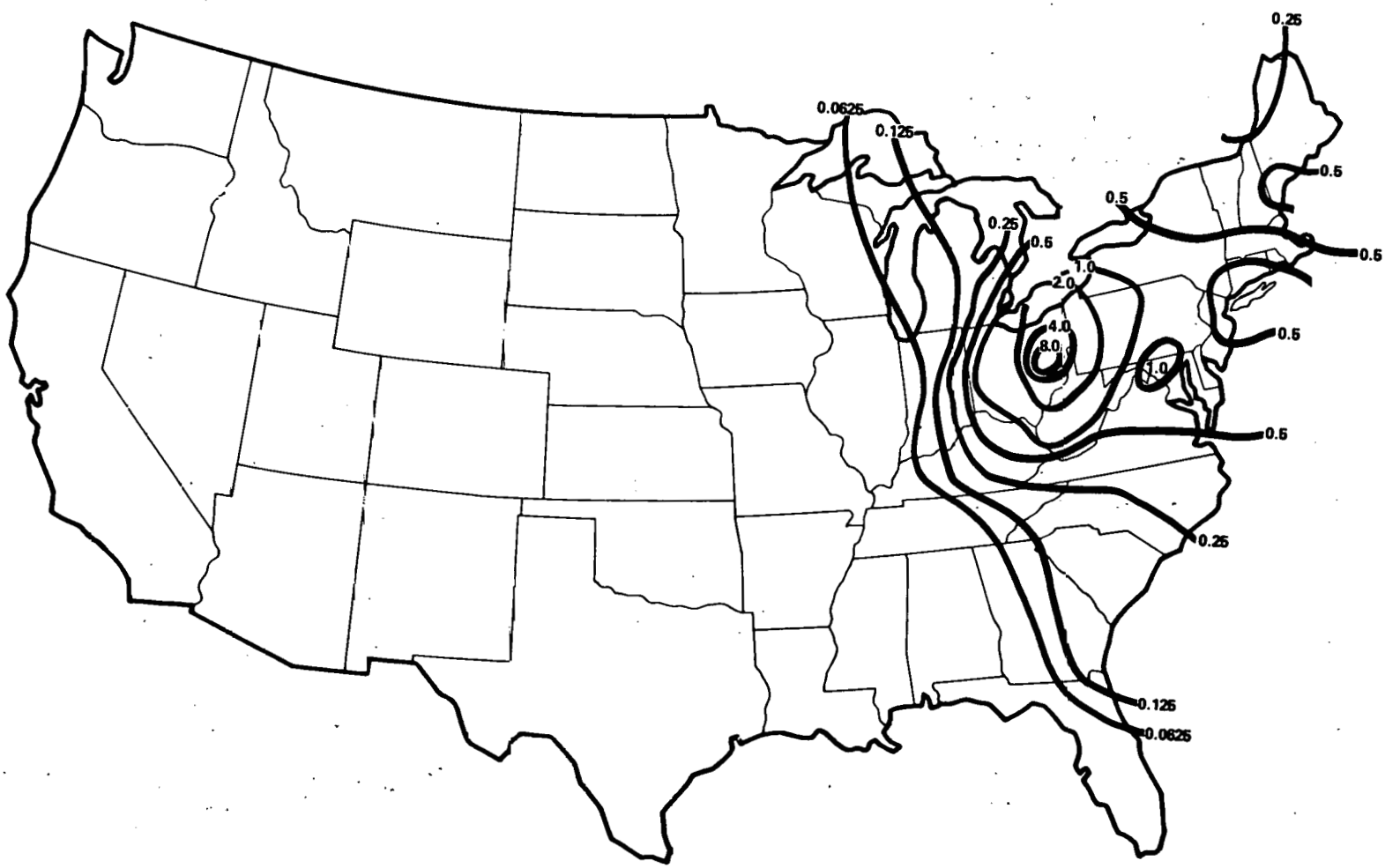

Note: Contours show incremental suspended sulfate (SO_4) concentration ($\mu g/m^3$) averaged over one month due to a hypothetical tall stack source emitting one million metric tons per year of SO_2, located in Ohio (AQCR #183, "Zanesville"). Meteorological data are for the month of January 1974. Concentrations based on calculations with Brookhaven National Laboratory AIRSOX model.

FIGURE 5-1. BNL MODEL (SULFATE TRANSPORT POTENTIAL)

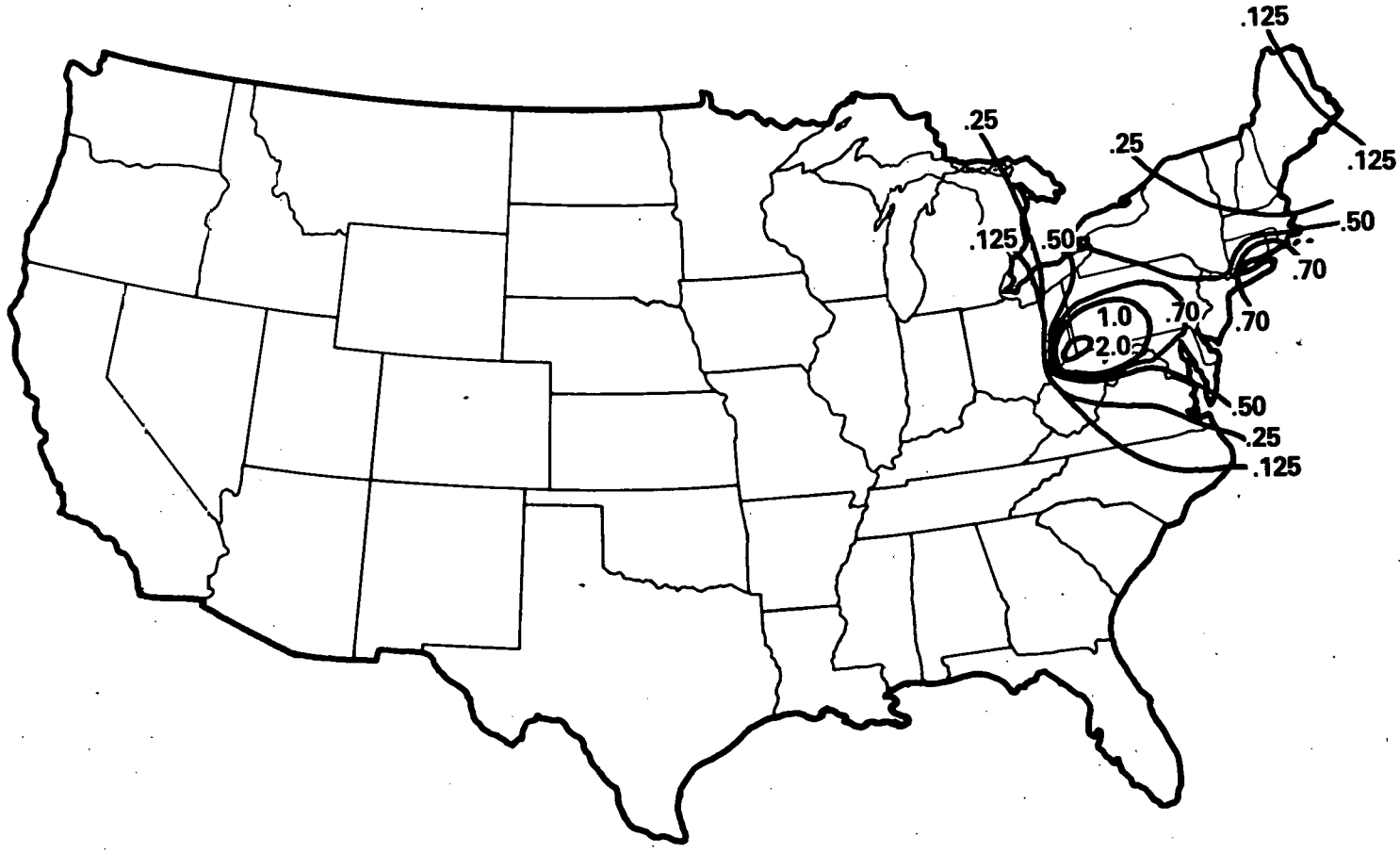

Note: Contours show incremental suspended sulfate (SO_4) concentration ($\mu g/m^3$) averaged over one month due to a hypothetical tall stack source emitting one million metric tons per year of SO_2, located in Ohio (AQCR #183, "Zanesville"). Meteorological data are for the month of January 1974. Concentrations based on calculations with Pacific Northwest Laboratory air transport model.

FIGURE 5-2. PNL MODEL (SULFATE TRANSPORT POTENTIAL)

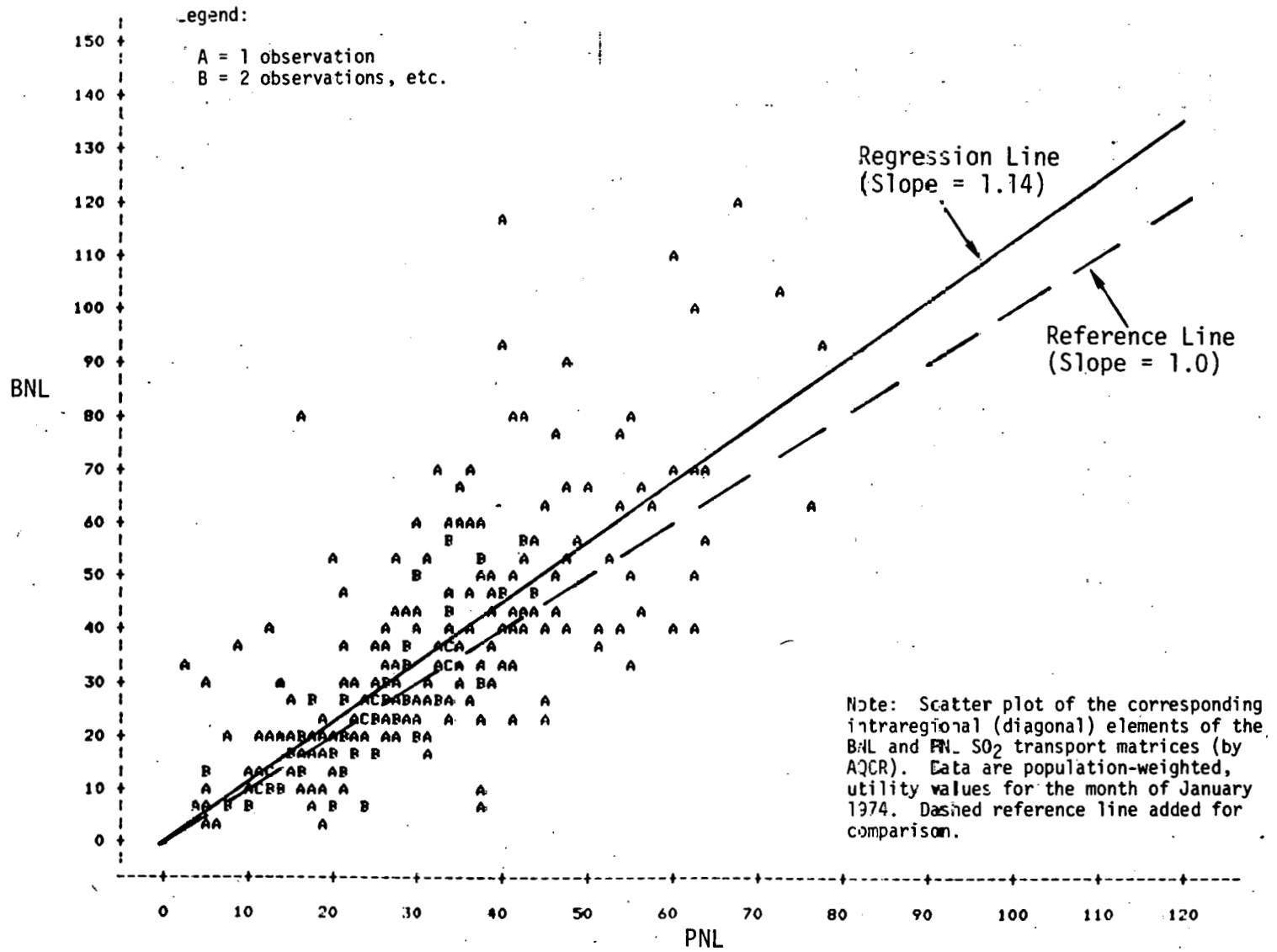

FIGURE 5-3. BNL VS PNL INTRAREGIONAL TRANSPORT

the correlation between models is much better, as shown in Figure 5-4. Calculation of a best fit to the scatter points gives a slope equal to 1.06 (i.e., BNL predicts 6 percent larger concentration) and an R^2 of 0.925.

Differences in model patterns and values can arise due to parameter selection. At the present state of knowledge of atmospheric processes and observed data, it was not feasible to unambiguously calibrate the separate parameters for chemical conversion and deposition of SO_x. Ongoing studies with more recent data might improve this situation.

5.2.3 BNL AIRSOX Model

Brookhaven National Laboratory developed the computerized, trajectory-based model, Atmospheric Impact of Residual SO_x (AIRSOX), primarily for use in calculating the transport, diffusion, and transformation of sulfur oxides on regional and continental scales. Sulfur dioxide and small particulates such as sulfate (largely a secondary pollutant formed by atmospheric chemical conversion) may be carried by the wind over distances of hundreds to thousands of kilometers before being deposited on the surface. Estimates of the long-term average oxidation rate for SO_2 in the atmosphere ranges from 0.1 percent/hr to about 2 percent/hr (Calvert et al., 1978; Beilke and Gravenhorst, 1978). The removal of the SO_2 and SO_4 may be caused by the dry deposition process or precipitation scavenging. The mathematical model AIRSOX is capable of providing estimates of the population-weighted concentrations of SO_2 and SO_4 occurring in the conterminous United States for a specified emission inventory.

a. Physical Processes

To compute the concentrations of SO_2 and SO_4, several pertinent physical processes are simulated; these are, in general, atmospheric transport, diffusion, and transformation (oxidation, surface removal, and precipitation). Figure 5-5 depicts how the fate of SO_2 emitted into the atmosphere is affected by these physical processes.

(1) Atmospheric Transport

The meteorological data used in AIRSOX to compute the plume trajectories are obtained from the National Oceanic and Atmospheric Administration and the National Center for Atmospheric Research. During the time period over which concentrations of SO_2 and SO_4 are calculated, puffs are emitted every 6 hours representing the emissions for that entire period. The puff experiences different velocities due both to changes in the wind field and its motion within the field. Wind data are updated every 6 hours. The direction and length of each segment of the puff's trajectory are determined by interpolation of the observed upper air winds at the location of the trajectory segment from a data set of approximately 80 stations in and around the United States.

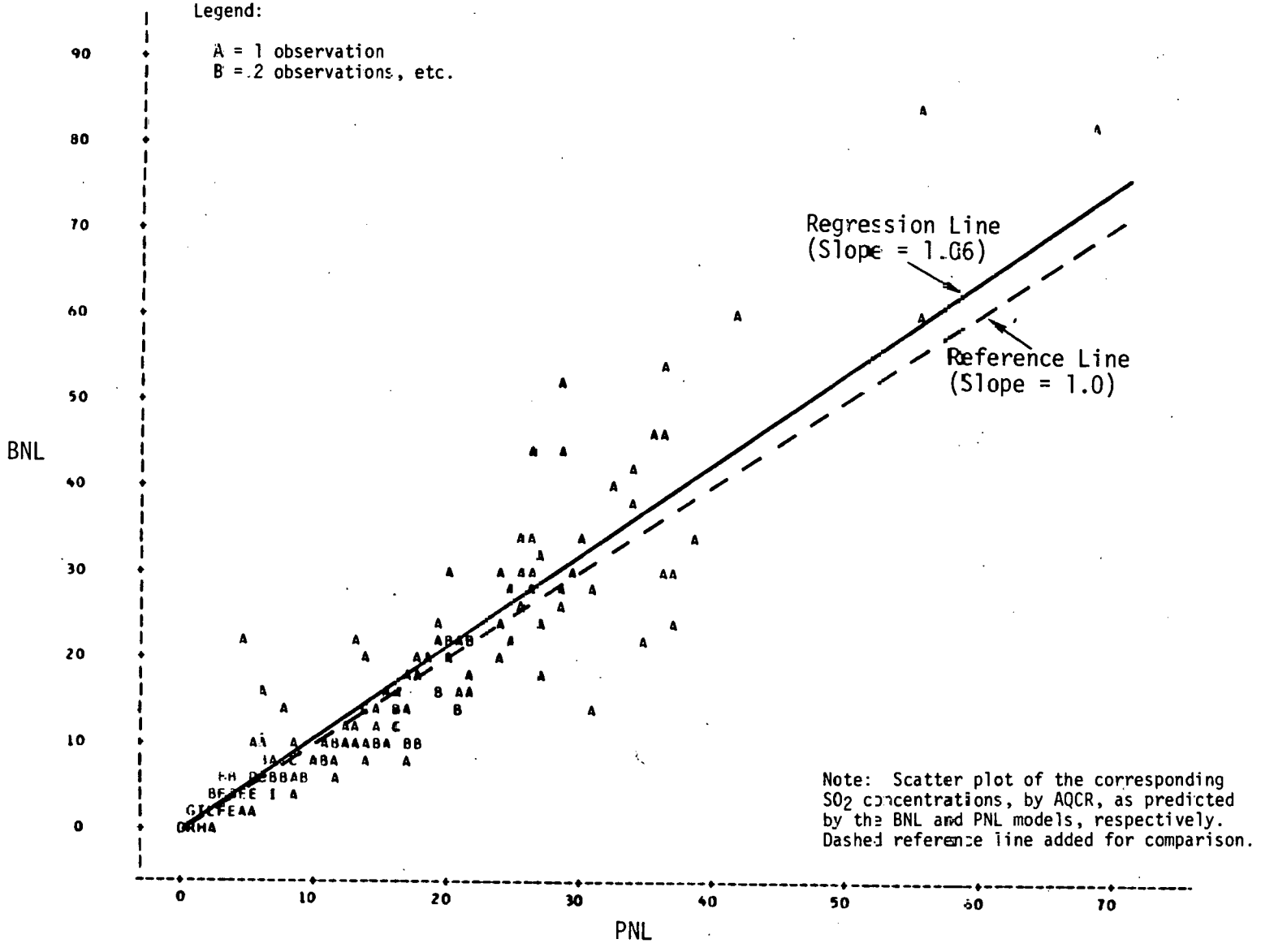

FIGURE 5-4. BNL vs PNL PREDICTED SO_2 CONCENTRATIONS

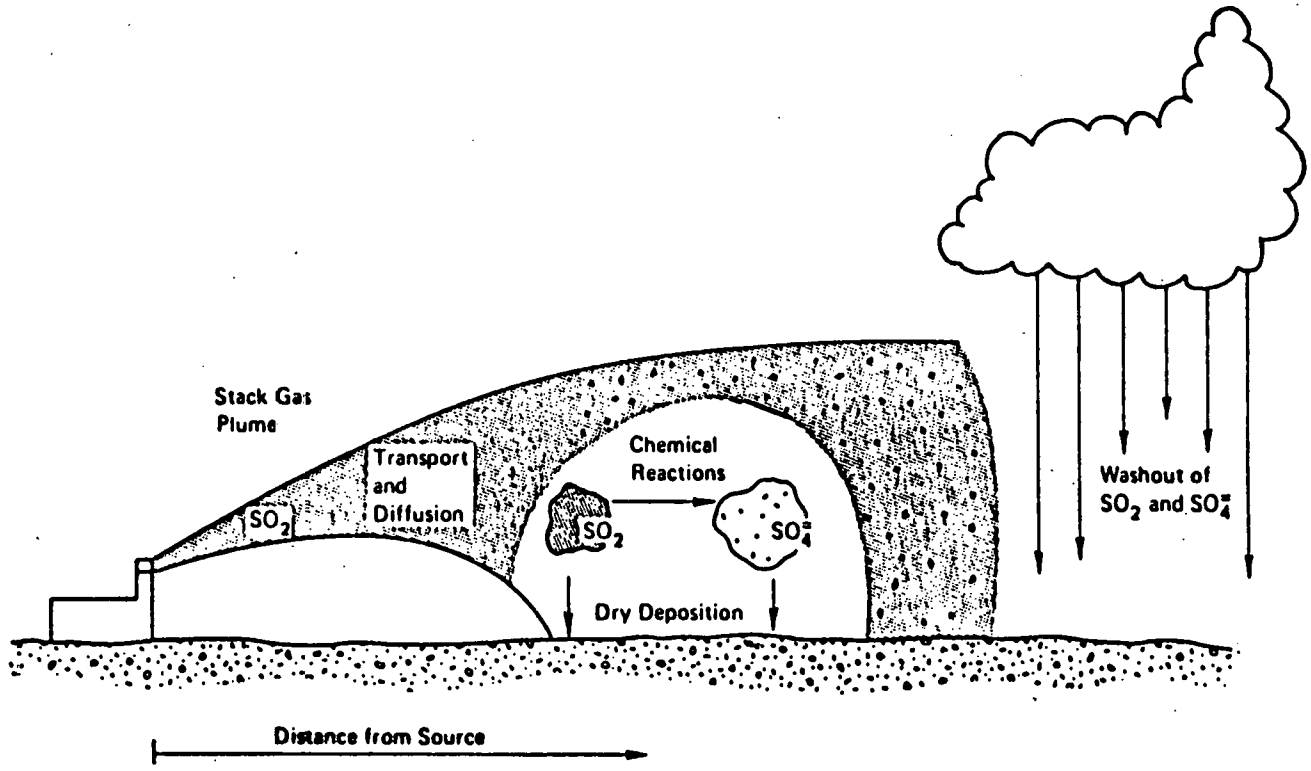

FIGURE 5-5. PLUME TRANSPORT DIAGRAM

In the model calculation, SO_2 and SO_4 are assumed to be transported over large distances by the average wind in the mixing layer. The average wind in the mixing layer at each station is computed from the observed winds linearly weighted by height increments. The average wind at a station, $\vec{V}_m$, can be expressed as

$$\vec{V}_m = \frac{\sum_k^n \vec{V}_k \Delta Z_k}{\sum_k^n \Delta Z_k}$$

where k is the vertical observation level, n is the total number of observed wind levels below the mixing height for that station, and ΔZ_k is the difference in height between adjacent mixing levels.

The trajectory segments are linked together to form a complete puff trajectory. The first segment starts from the source and each following segment starts from the end point of the segment before it. Trajectories terminate after the desired duration (for example, 120 hr), or when the specified criteria are not met, for example lack of input wind data or trajectories extending beyond the boundary of simulation.

The trajectory segment (T_S) is computed from the observed winds using Heffter and Taylor's technique (1975) as follows:

$$T_S = \frac{\sum_i^n f(S_i) f(\theta_i)\ T_i}{\sum_i^n f(S_i) f(\theta_i)}$$

where $T_i = \vec{V}_i \Delta t$, is the contribution of trajectory segment from station i

$\vec{V}_i$ is the average wind at station i
Δt is the segment time interval
$f(S_i)$ is the distance weighting function
$f(\theta_i)$ is the alignment weighting function

The trajectory segment contributions are calculated using layer-averaged observed winds from stations within a fixed radius from the segment origin (e.g., 300 nautical miles). The distance weighting function is $f(S_i) = 1/S_i^2$, where S_i is the distance from an observed wind station to the midpoint of the trajectory segment. The closest observations are thus given the greatest weight. The alignment weighting function is defined as $f(\theta_i) = 1 - 0.5 |\sin \theta_i|$, where θ_i is the angle formed between segment i and a line drawn from the segment origin to the observed wind station. Observations upwind and downwind are therefore given more weight.

Figure 5-6 depicts trajectories of the center of mass of hypothetical SO_2 puff releases from a source near Chicago, Illinois, on October 17, 1974. The trajectories labeled A, B, C, and D were released at times 00Z, 06Z, 12Z, and 18Z, respectively. The numbers on each trajectory indicate the length of travel time in days (Meyers and Cedarwall, 1975).

(2) Diffusion

The parameter involved in solving the atmospheric diffusion equation is eddy diffusivity, which is a function of stability, mixing height, and surface roughness. Neutral atmospheric stability conditions were used throughout the calculations in the AIRSOX model because of the simulation of an average well-mixed boundary layer with a constant mixing height. The vertical diffusion is calculated using eddy diffusivity or the "K" theory. The eddy diffusivity used in the model for neutral conditions follows the formulation by Bolin and Persson (1975):

$$K = \begin{cases} ku_*z & z_0 \leq z \leq 85m \\ 85\ ku_* \text{ for} & 85m \leq z < H \\ 0 & z \geq H \end{cases}$$

where k is the von Karman constant, $k = 0.4$, u_* is the friction velocity, and H is the mixing height. The friction velocity, $u_* = 0.4$ m/s, and the surface roughness, $z_0 = 25$ cm, were chosen in the model calculation to represent neutral conditions averaged over the United States.

The height of the mixed layer defines the upper limit of the dilution of material released below it. In the AIRSOX model, the eddy diffusivity goes to zero at the mixing height, which in some applications is assumed to be equal to the climatological height of the inversion. Holzworth (1972) summarized vertical temperature sounding data for numerous locations in the United States from 00Z to 12Z observations over a 5-year period. He objectively determined the height of the mixing layer from the intersection of the dry adiabat extrapolated from the adjusted surface temperature and the observed temperature profile. The morning and afternoon mixing heights for selected locations in the Eastern United States over four seasons are presented in Table 5-1. A striking feature is the persistence of a low-level morning inversion across seasons, as compared with the variability of the afternoon mixing height with season. Further, the diurnal variability would appear to be greater than the seasonal variability. The average seasonal mixing heights range from 650 to about 1000 m. In the AIRSOX model for July, for example, a constant mixing height of 1000 m was employed because it represents the characteristic average value for that month.

(3) Transformation

The parameters governing the transformation of pollutants, SO_2 and SO_4, are chemical reaction, dry deposition, and wet deposition.

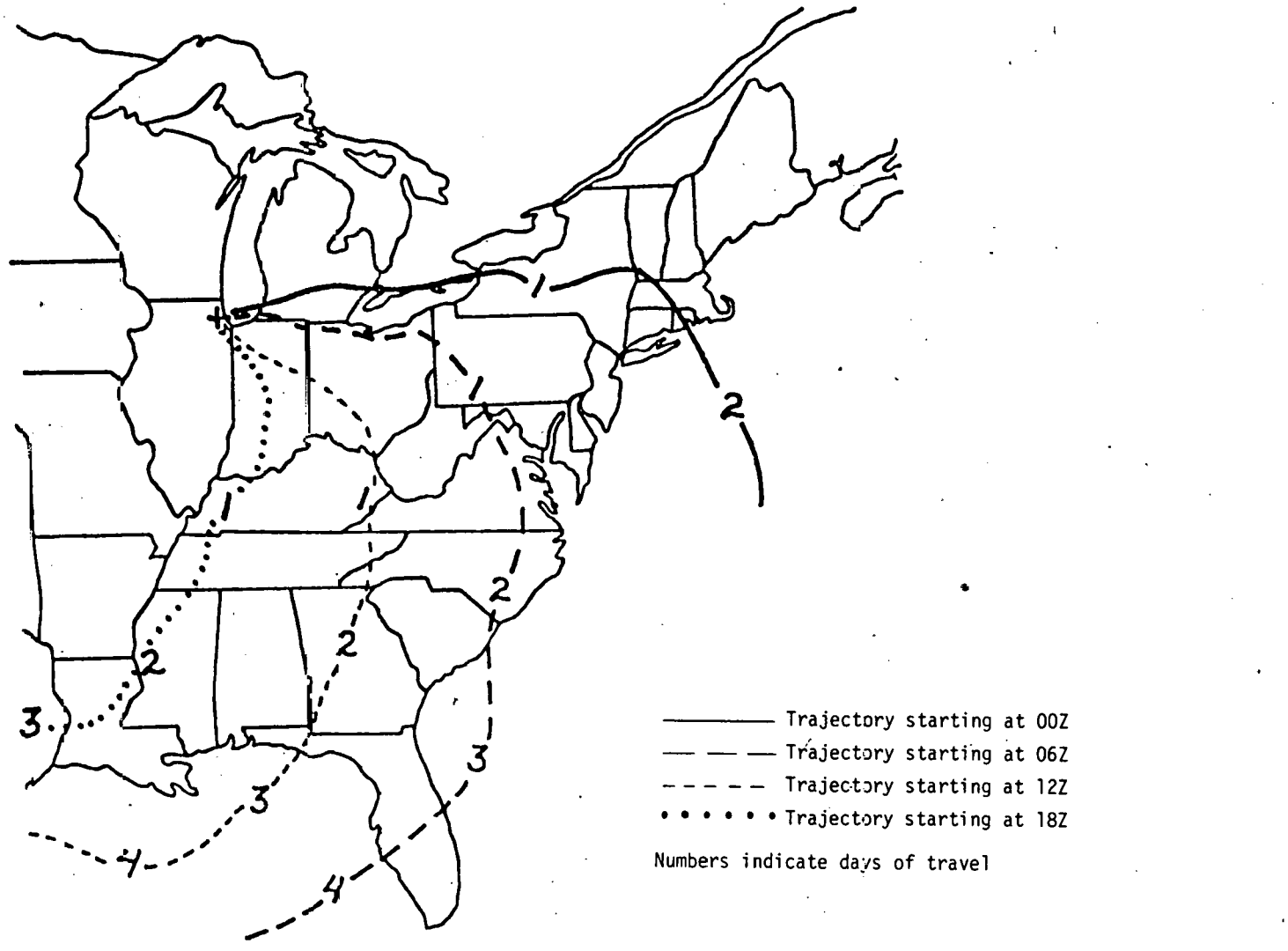

FIGURE 5-6. TYPICAL PUFF TRAJECTORIES (CHICAGO SOURCE)

Table 5-1. Selected Mixing Heights

Season and Time of Day		New York, New York	Pittsburgh, Pennsylvania	Dayton, Ohio	Peoria, Illinois	Charleston, South Carolina	Nashville, Tennessee	Average	Daily Average
Winter	a.m.	875	419	461	327	296	440	470	650
	p.m.	901	811	749	533	951	1035	830	
Spring	a.m.	788	404	462	361	339	500	476	1010
	p.m.	1360	753	1570	1353	1519	1713	1545	
Summer	a.m.	662	333	349	272	411	417	407	1017
	p.m.	1512	1794	1661	1498	1447	1945	1626	
Fall	a.m.	675	404	360	273	264	301	380	815
	p.m.	1086	1365	1315	1068	1222	1438	1249	

Note: Mixing heights are in meters. Data are from Holzworth, 1972.

Chemical reaction -- The mechanism for the chemical conversion of SO_2 to SO_4 in the atmosphere is not well understood, particularly in relation to the relative contributions of homogeneous and heterogeneous reactions. The gross conversion rate has, however, been measured under a variety of atmospheric conditions. Literature values for the temporally and spatially averaged linear reaction rate are clustered around a mean of approximately 0.5 percent/hr. For use in the AIRSOX model, a linear reaction rate of 0.57 percent/hr was chosen for July 1974 and 0.50 percent for January, on the basis of sensitivity calculations and comparison with observations. In addition to the SO_4 produced by chemical conversion (secondary sulfate), 2 percent of the initial SO_2 (by mole) is assumed to be emitted directly as SO_4 to simulate primary production of SO_4.

Dry deposition -- A derivative boundary condition is used at the bottom boundary in the vertical diffusion to allow for dry deposition removal. Because dry deposition is a result of SO_2 and SO_4 impacting on the land, the use of a bottom boundary condition to allow for dry deposition (surface depletion model) is, on physical grounds, preferable to the phenomenological approach of using a bulk deposition velocity (source depletion model). It should be noted that in a model versus model comparison the bulk deposition velocity (source depletion model) calculation requires a lower deposition velocity as compared with the bottom boundary calculation (surface depletion model), in order to yield similar results (Horst 1977). In some regional applications, deposition velocities of 3.4 cm/sec for SO_2 and 0.23 cm/sec for SO_4 were chosen on the basis of sensitivity calculations, literature values, and comparison with observations. These values were used in the July matrix calculations. For January, the SO_2 value was reduced to 2.5 cm/sec to account for the reduced absorption rate and vegetation in winter.

Wet deposition (precipitation) -- A linear rainout model is used to remove SO_2 and SO_4 from the vertical column whenever a plume segment encounters rainfall. There exists considerable uncertainty as to the mechanism of SO_2 and SO_4 incorporation into rainfall. For this reason, the BNL AIRSOX model has used a set of rainout parameters previously applied to calculate acid rainfall, albeit in a different geographical location (Johnson et al., 1977; Johnson et al., 1978; Mancuso et al., 1978). The wet deposition depends on the rainfall rate, P, and is assumed to be constant with height. The wet deposition coefficient, λ_w, used in AIRSOX, is 0.216P and 0.07P for SO_2 and SO_4, respectively.

b. Computer Implementation of the Model

The AIRSOX model computes the concentrations of SO_2 and SO_4, assuming a puff is released every 6 hours from individual sources during the simulation period. The height of releases typically used are 200 m for utility sources, 100 m for industrial sources, and 20 m for area sources. The advection of the puff is calculated at 3-hour intervals using historical data. Vertical diffusion, chemical transformation, dry deposition, and wet deposition are calculated at hourly intervals. At the completion of a 3-hour advection step, the horizontal diffusion of the puff is calculated. The

time intervals used in the calculation represent a compromise between the desire to limit calculation complexity and computer expense and the desire for sufficient temporal-spatial accuracy. A summary of the input parameters employed in the AIRSOX model is shown in Table 5-2. The effects of multiple sources are calculated by combining the SO_2 and SO_4 fields from individual sources into composite concentration fields. Population in each grid cell is tagged by county so that population-weighted concentrations and population exposures can be aggregated from county level to state or Federal region levels according to the emitter or receptor locations.

5.2.4 PNL Long-Range Transport Model

The PNL long-range transport, transformation, and removal model was developed by Wendell et al. (1976). Sensitivity and verification studies with the model have been conducted by Powell et al. (1979) and McNaughton (1980) for sulfur dioxide and sulfate air concentrations and depositions in the northeastern United States. The model has been adapted to provide assessments of the air quality impacts of energy development in the western United States by Renne et al. (1978) and Sandusky et al. (1979). This PNL model was then modified to provide AQCR-to-AQCR transfer matrices for SO_2 and SO_4, applying many of the techniques that were used to generate AQCR-to-AQCR transfer matrices for emitted fine particulates (Eadie and Davis, 1979).

The PNL long-range transport model simulates the airborne transport, diffusion, transformation, and removal of SO_2 and SO_4 from point emission sources. Transport is simulated by following trajectories in a 100 to 1000 m layer average wind field with reference to a fixed grid. Trajectories originate hourly at each source and calculations of diffusion, transformation, and wet and dry deposition are calculated hourly using coupled mass conservation equations. The resultant mass distributions are accumulated over a month at each grid square to which the plumes contribute.

The grid system in the PNL long-range model adopted for this program is based on the National Meteorological Center (NMC) Northern Hemisphere grid. The NMC grid is a regularly spaced grid laid out on a polar stereographic projection. The PNL advection grid (Figure 5-7) upon which layer-averaged winds are mapped every 12 hours is a subset of the NMC grid and spans the United States and adjacent areas. The dimensions of the PNL grid are 14 NMC grid units in the x direction and 12 NMC grid units in the y direction. The sampling grid upon which pollutant air concentrations and depositions are predicted has linear dimensions one-tenth of the advection spacing, making a 140 x 120 array of grid squares. The precipitation data used in the wet removal calculations in the model is also mapped on the sampling grid. The sampling grid spacing is approximately 38 km at 60°N and 32 km at 35°N latitude.

Some significant features of the model in the generation of the AQCR-to-AQCR transfer matrices for SO_2 and SO_4 are

- Dry deposition of SO_2 and SO_4 is constant with deposition velocities of 1.0 cm/sec and 0.1 cm/sec (Garland, 1978).

Table 5-2. BNL AIRSOX Model Parameters

Parameter	Value
1. Effective release height (height of stabilized plume after emission processes)	
Utility	200 meters
Industrial	100 meters
2. Amount of SO_4 in effluent	2% of emitted SO_2 (by mole)
3. Meteorology and precipitation data	July 1974, January 1974
4. Mixing layer height above terrain	1000 m (July), 600 m (Jan)
5. Atmospheric stability	Neutral
6. Number of vertical levels	12 (July), 8 (Jan)
7. Conversion rate of SO_2 to SO_4	0.57%/hr (July), 0.50%/hr (Jan)
8. Dry deposition velocity	
for SO_2	3.4 cm/sec (July), 2.5 cm/sec (Jan)
for SO_4	0.23 cm/sec
9. Wet removal rate	
for SO_2	0.216 P*
for SO_4	0.07 P
10. Grid resolution, approximate	32 x 32 km

* P = rainfall (mm/hour).

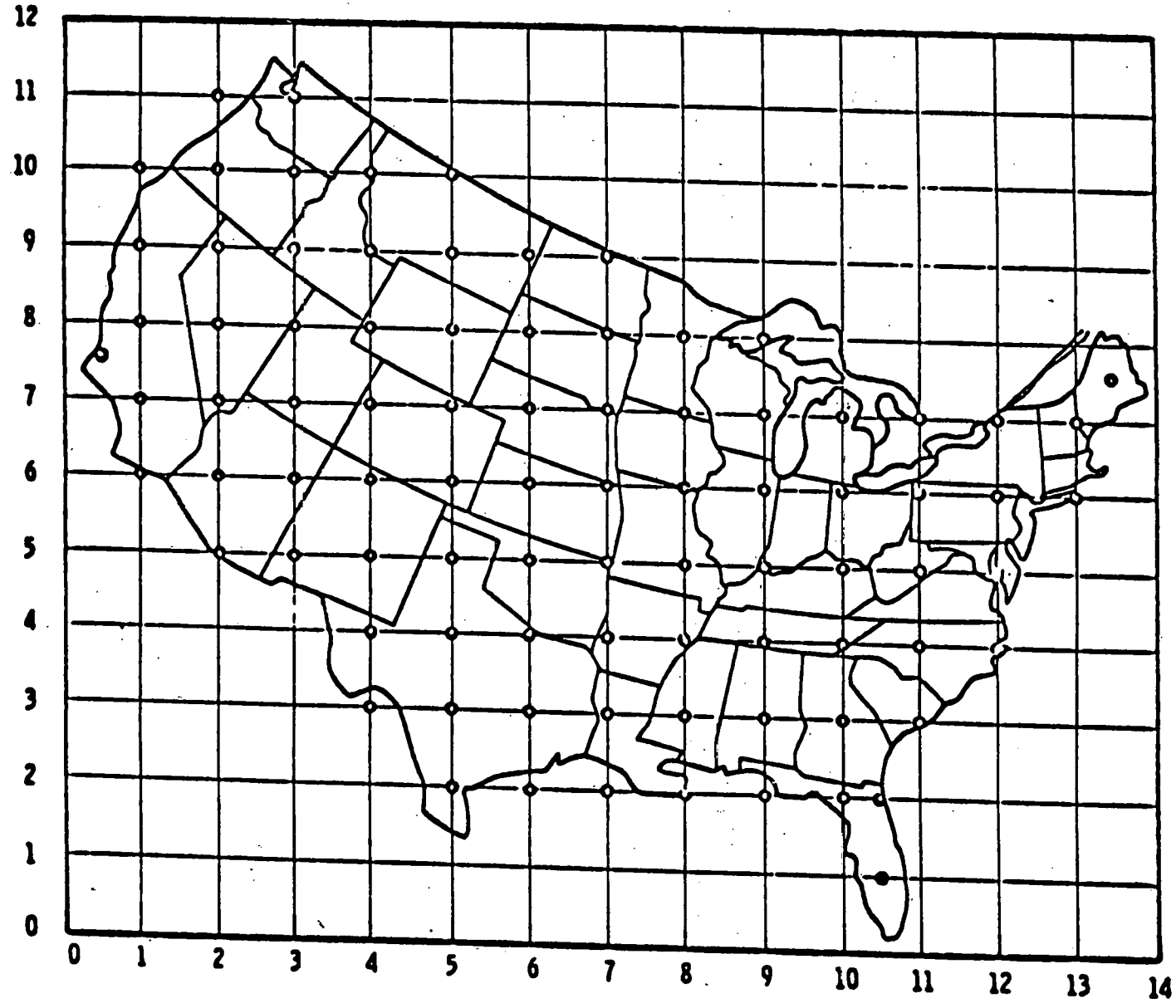
12
11
10
9
8
7
6
5
4
3
2
1
0
0 1 2 3 4 5 6 7 8 9 10 11 12 13 14

- SO_2 to SO_4 transformation is linear as a function of SO_2 mass with a daytime rate of 2 percent/hr and low transformation at night (0.25 percent) (Husar, 1978).

- Wet removal of SO_2 is given by $w_1 = 0.005\ P(t)$ (Dana et al., 1975) of SO_4 as determined from a formulation by Scott (1978) for Bergerontype clouds, $w_2 = 0.232\ P(t)^{0.625}$.

- A diurnal stability cycle is specified giving unstable conditions in the afternoon, neutral conditions in the morning and late afternoon, and stable conditions at night. Mixing height is given by a sinusoidally varying cycle representing the building of a stable nocturnal layer and a daytime mixed layer from the surface.

Model input include wind data and hourly precipitation data. Wind data are obtained by averaging radiosonde data in a 100 m to 1000 m layer, objectively analyzing the data and interpolating the data each hour between observations taken at 12-hour intervals by weighting their position in the observational period.

Precipitation data are obtained from National Weather Service cooperative observers. The model uses hourly gridded precipitation fields derived from approximately 3000 observing stations in the United States.

The PNL long-range transport model parameters used in the generation of the SO_2 and SO_4 transfer matrices are summarized in Table 5-3.

5.3 ANALYSIS OF MATRICES

5.3.1 General

In the development and application of long-range transport models and analytical methodologies, it is important to bear in mind the constraints related to those methods. The matrix techniques can be used, to some extent, to analyze the models and their constraints. This section deals with analyses of the transport matrix (T_{ij}) from various perspectives, independent of emission inputs (E_j) or resulting concentration outputs (C_i), which are treated in Section 5.4.

5.3.2 Temporal Variations

As described in Section 5.2, the meteorology data processed to date in both the BNL and PNL models is very limited in scope. The data used represents only four select months out of a single year. This data base is, of course, insufficient to ascertain systematic seasonal variations in the transport matrix or to determine whether the transport changes significantly from year to year. However, it does provide a preliminary basis for estimating the degree of variability from one month to another. Figures 5-8 and 5-9 are contour maps of the transport from a fixed Midwest source, from the same model, for meteorology from January and July of the same

Table 5-3. PNL Model Parameters

Time periods for meteorological data	1-31 January 1974 1-30 April 1974 1-31 July 1974 1-31 October 1974
Advection grid spacing (35°N latitude)	321 km
Grid spacing for sampling results and for precipitation data (35°N latitude)	32 km
Source emission rate	1.0 kiloton/yr
Source locations (86)	Advection grid intersections for interpolation to centroids of AQCR
Effective source stack height	200 m
Maximum daytime mixing height	1500 m
Minimum daytime mixing height	200 m
Maximum nighttime stable layer height	400 m
Minimum nighttime stable layer height	100 m
Stability	Varied through the diurnal cycle
SO deposition velocities:	
SO_2	1.0 cm/sec
SO_4	0.1 cm/sec
Wet removal coefficients:	
SO_2	0.005 P*/hr
SO_4	0.23 $P^{5/8}$/hr
Transformation rate of SO_2 to SO_4	0.02/hr (daytime) and 0.0025/hr (nighttime)
Percentage of SO_4 in original emissions	0.0
Puff release rate from source, advection time step, and sampling rate of puffs for results	1 per hr
Maximum number of hours a puff trajectory will be continued if it stays on grid	200 hr
Averaging period for air concentration fields of SO_2 and SO_4	1 mo
Units of air concentrations of SO_2 and SO_4	$\mu g/m^3$

* P = rainfall rates, mm/hr. Temporal and spatial variations in P were determined from hourly precipitation data.

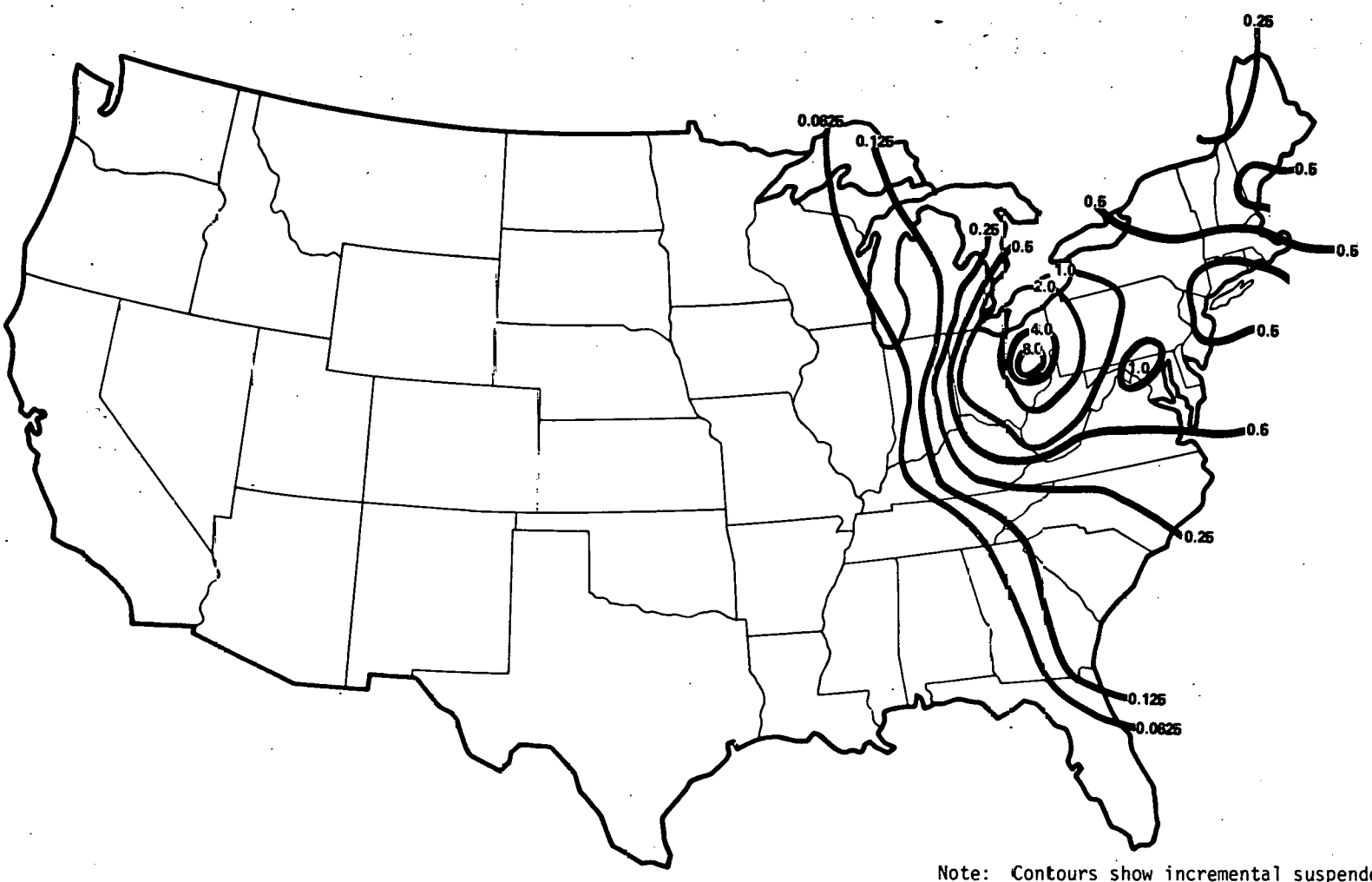

Note: Contours show incremental suspended sulfate (SO_4) concentration ($\mu g/m^3$) averaged over one month due to a hypothetical tall stack source emitting one million metric tons per year of SO_2, located in Ohio (AQCR #183, "Zanesville"). Meteorological data are for the month of January 1974. Concentrations based on calculations with Brookhaven National Laboratory AIRSOX model.

FIGURE 5-8. JANUARY TRANSPORT CONTOURS (BNL-MIDWEST SOURCE)

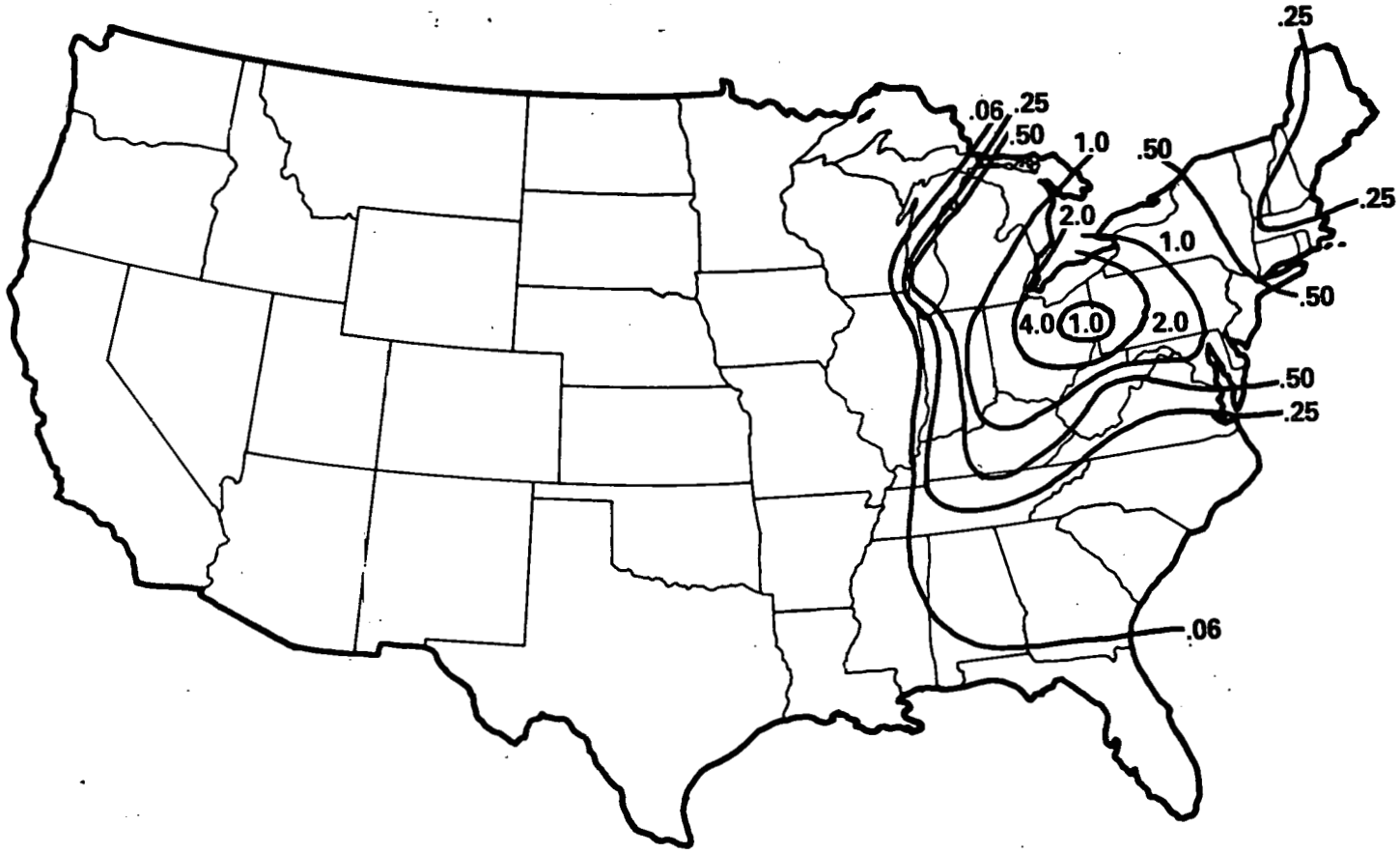

Note: Contours show incremental suspended sulfate (SO_4) concentration ($\mu g/m^3$) averaged over one month due to a hypothetical tall stack source emitting one million metric tons per year of SO_2, located in Ohio (AQCR #183, "Zanesville"). Meteorological data are for the month of July 1974. Concentrations based on calculations with Brookhaven National Laboratory AIRSOX model.

FIGURE 5-9. JULY TRANSPORT CONTOURS (BNL-MIDWEST SOURCE)

year. As data from other time frames become available, mapping and general statistical analysis techniques can be applied to determine whether there are seasonal, annual, and/or random aspects to the transport matrix. This determination can then be used to apply the appropriate factors to the matrix generation.

5.3.3 Local/Long-Range Variation

Because of the necessarily gross grid employed in the generation of these matrices, some inaccuracies may arise in the local (diagonal element) transport calculations that do not affect the long-range (off-diagonal element) transport to the same extent. This class of problems is related to the siting of emission sources within a region in the process of generating the matrices. Due to the additive nature of long-range transport, these problems tend to cancel and be masked in the interregional transports, especially among regions separated by greater distances. Table 4-1, in the preceding chapter, presents some initial data showing values of local and long-range effects for SO_2 and SO_4 in a particular area.

5.3.4 Source (Stack Height) Variation

In most cases, increasing the stack height of a pollutant-emitting source should result in the pollutant's being deposited further from the source. Furthermore, higher release should give less chance for ground-level absorption of SO_2 (dry deposition) and lead to greater conversion to SO_4. In these analyses, the three classes of source have different stack height: utility (200 m), industrial (100 m), and area (20 m). The resulting pollutant deposition from the utility sources should, on the average, be deposited further away and more in the form of SO_4 than the other two source classes. In the matrix representation, low stacks result in high values for the diagonal matrix elements; conversely, high stacks yield high values for off-diagonal matrix elements.

The source classes also differ in their spatial distribution of sources within a region. The spatial distributions are reflected to some extent in the BNL matrices, where individual utility sources and some large industrial sources were explicitly modeled. This spatial distribution also affects the concentration patterns, especially the intraregional, diagonal elements. Population-weighted matrices are likely to be more sensitive to differences in intra-AQCR source distribution than area-weighted matrices because of correlations between population and source locations. Stack height effects may vary by location; however, the general tendencies of local versus long-range effects are expected to be manifested statistically rather than uniformly.

Because of the tendency of emissions from low stacks to reach ground level before leaving the emitter region, the diagonal elements of industrial transport matrices (100-m stacks) should be larger than the corresponding diagonals of the utility matrices (200-m stacks). Diagonals of the July BNL transport matrices for industry and utilities are compared in Figure 5-10. The data follow the expected trend. Utility diagonals tend to be about 76 percent as large as the industry diagonals as can be seen from the slope

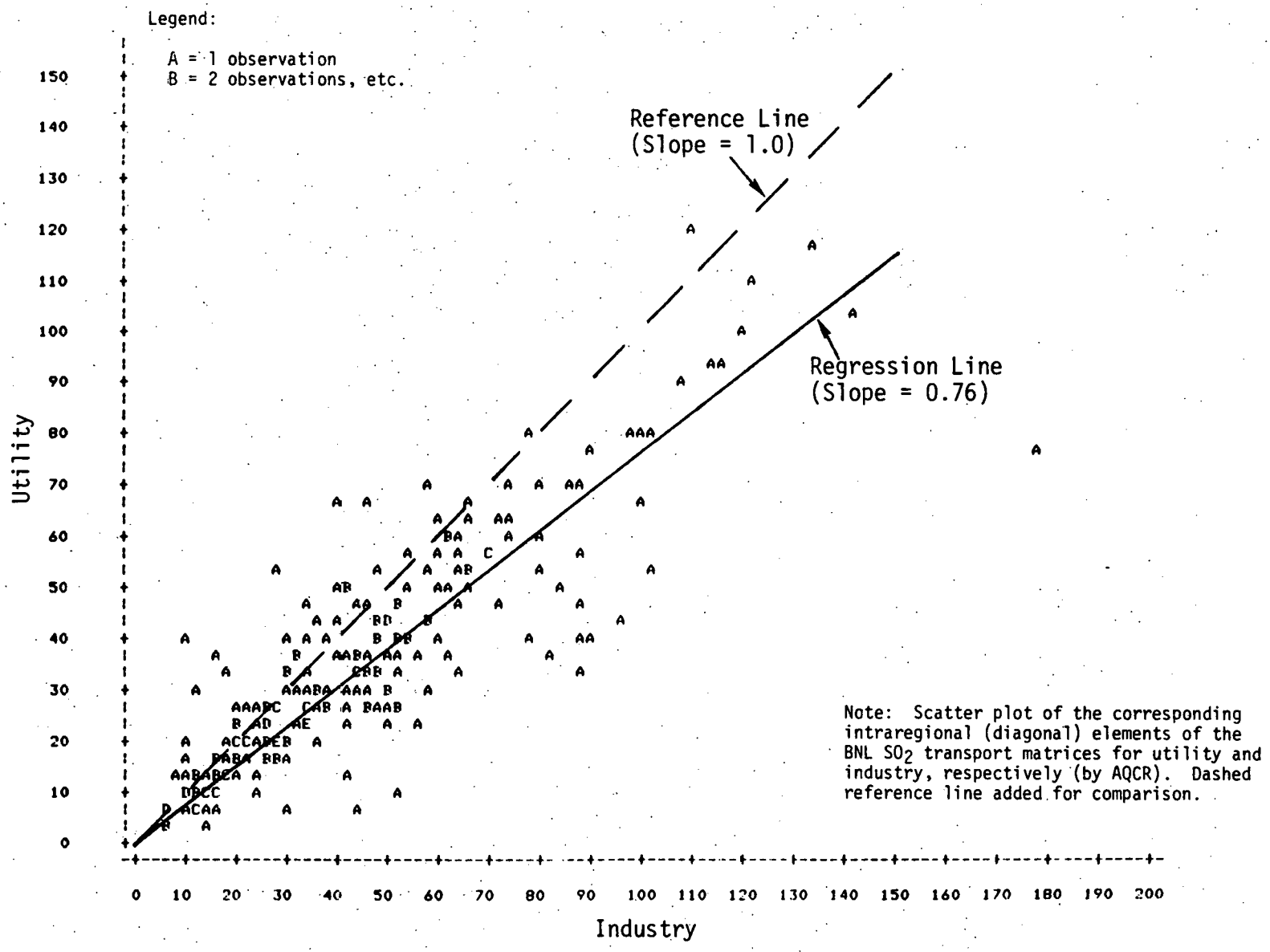

FIGURE 5-10. UTILITY VS INDUSTRY INTRAREGIONAL TRANSPORT

of the regression line. (The regression line was forced through the origin, has an R^2 of 0.924, and a slope of 0.763). The smaller utility diagonals reflect the tendency of the high stacks of the utilities to reduce local impacts.

5.4 DATA ANALYSIS AND MODEL VALIDATION

5.4.1 General

Validation of predicted concentrations against observed data cannot be carried out effectively because of limitations in all three components of such a comparison -- i.e., the matrices, the emission vectors, and the observed concentrations.

The matrices currently available are based on a small sample of meteorology, only January and July 1974 for BNL and 4 months of 1974 for PNL. A larger statistical sample is needed, especially for later years that can be compared with better emission and concentration data. Monitoring stations in the early years were generally clustered in urban areas and near emission sources; they were not well distributed for estimating average concentrations over AQCRs. Furthermore, SO_4 measurement techniques for that period sometimes allowed transformation of SO_2 to SO_4 within the instruments, creating false readings.

A further difficulty with current validation attempts is the quality of available emission data. Two agencies collect emission data: the Environmental Protection Agency has the National Emissions Data System (NEDS), and the DOE Federal Energy Regulatory Commission (FERC) collects utility data. NEDS data collection was just starting in 1974, so their procedures may not have been well established during the period corresponding to the meteorological data used in the available transport matrices. There are major discrepancies between NEDS and FERC utility emissions for that period. In this study, emissions for 1974 are approximated by a combination of 1975 NEDS and FERC data as discussed in the next section.

Even with these reservations, it is tempting to compare computed and measured concentrations (see Section 5.4.3). As new matrices are developed using recent meteorology and as better emissions and measured concentrations are analyzed, genuine validation trials may be possible.

5.4.2 Emissions

The matrix method requires input values corresponding to annual emissions from each of the regions. A single AQCR-level vector of 238 emissions multiplied by the appropriate transport matrix produces a vector of 238 concentrations.

Transport matrices have been developed for 20-m, 100-m, and 200-m stack heights (permitting the use of input emissions, which are also divided into three stack height categories) and then adding the resulting three sets of concentrations. Actual sources have a wide variety of stack heights but

can be assigned to one of the three categories as a useful approximation. NEDS provides a detailed inventory of such emissions for every AQCR. Table 5-4 is a copy of a typical NEDS inventory for 1975 (EPA, 1978).

In addition to the detailed classification shown, NEDS aggregates emissions into two broad categories: "area" and "point." The NEDS data for "area" were used for the 20-m class input vector; the NEDS "point" category includes both industrial and utility sources. The utility portion is easily identified under the heading "Electric Generation." The industrial component is assumed to be all "point" categories except electric generation (i.e., industry = point - electric generation).

A second source of utility emissions is also available from FERC. The FERC data should be identical to NEDS, but in fact often differ considerably. Because NEDS data are compiled from FERC information, it was decided that, temporarily, any discrepancies would be resolved in favor of FERC. Reconciliation of these discrepancies by the responsible agencies is being pursued.

In summary, the three components of emissions were taken from NEDS and FERC as follows:

- 20-m stack from NEDS "area"
- 100-m stack from NEDS "point" minus NEDS "electric generation"
- 200-m stack from FERC "utilities"

The current transport matrices are based on 1974 meteorology. NEDS was not fully operational in 1974, but the 1975 data presented in the Environmental Protection Agency 1975 National Emissions Report were a reasonable approximation to 1974 emissions. NEDS 1976 data are also available in published form (EPA, 1979), and data later than 1976 can be obtained by request from the Environmental Protection Agency. It is important to obtain transport matrices for more recent years along with good emission inventories for the same periods.

Two pollutants from the NEDS inventory are of major interest: SO_x and particulates. The particulate emissions cannot be used directly with the particulate matrices without correction for the respirable fraction. The SO_x emissions are used with both SO_2 and SO_4 matrices. Initially, SO_x emissions are predominantly SO_2. The BNL matrices account for chemical transformation to SO_4 within the plume, as well as for computing deposition and transport.

Figure 5-11 shows an AQCR map of the NEDS/FERC 1975 emission densities (emission per unit area). These data were used in the comparison of computed and observed data discussed in the next section.

5.4.3 Concentrations

a. SO_x

Figures 5-12 and 5-13 show 1974 annual average SO_2 concentrations predicted by the matrix method and observed from the SAROAD data base,

Table 5-4. Emissions Data Format
(1975 National Emissions Data System)

AQCR 183 ZANESVILLE-CAMBRIDGE (OHIO)

Emission categories	Pollutant, tons per year				
	Particulates	Sulfur oxides	Nitrogen oxides	Hydro-carbons	Carbon monoxide
GRAND TOTAL	**70,908**	**320,648**	**82,997**	**34,759**	**130,961**
-AREA	**2,902**	**3,000**	**17,898**	**33,951**	**115,231**
-POINT	**68,006**	**317,648**	**65,099**	**808**	**15,730**
FUEL COMBUSTION-AREA	608	2,052	1,303	442	1,973
-POINT	63,062	314,815	64,188	808	2,216
External Combustion-area	608	2,052	1,303	442	1,973
-point	63,055	314,800	63,982	788	2,091
Residential Fuel-area	505	1,899	584	419	1,886
Anthracite Coal	23	50	7	6	206
Bituminous Coal	339	1,612	51	339	1,527
Distillate Oil	81	233	97	24	41
Residual Oil	0	0	0	0	0
Natural Gas	53	3	425	43	106
Wood	9	1	4	7	7
Electric Generation-point	49,951	301,758	62,823	572	1,916
Anthracite Coal	0	0	0	0	0
Bituminous Coal	49,947	301,731	62,767	571	1,915
Lignite	0	0	0	0	0
Residual Oil	0	0	0	0	0
Distillate Oil	4	27	56	1	1
Natural Gas	0	0	0	0	0
Process Gas	0	0	0	0	0
Coke	0	0	0	0	0
Solid Waste/Coal	0	0	0	0	0
Other	0	0	0	0	0
Industrial Fuel-area	25	1	448	7	42
-point	12,054	10,999	941	197	129
Anthracite Coal-area	0	0	0	0	0
-point	0	0	0	0	0
Bituminous Coal-area	0	0	0	0	0
-point	12,052	10,999	941	197	129
Lignite-point	0	0	0	0	0
Residual Oil-area	0	0	0	0	0
-point	0	0	0	0	0
Distillate Oil-area	0	0	0	0	0
-point	0	0	0	0	0
Natural Gas-area	25	1	448	7	42
-point	2	0	0	0	0
Process Gas-area	0	0	0	0	0
-point	0	0	0	0	0
Coke-point	0	0	0	0	0
Wood-area	0	0	0	0	0
-point	0	0	0	0	0
Liquid Petroleum Gas-point	0	0	0	0	0
Bagasse-point	0	0	0	0	0
Other-point	0	0	0	0	0
Commercial-Institutional Fuel-area	78	151	271	16	45
-point	1,050	2,643	218	19	46
Anthracite Coal-area	40	37	16	0	10
-point	0	0	0	0	0
Bituminous Coal-area	0	0	0	0	0
-point	1,050	2,643	218	19	46
Lignite-point	0	0	0	0	0
Residual Oil-area	12	93	32	2	2
-point	0	0	0	0	0
Distillate Oil-area	11	21	43	2	3
-point	0	0	0	0	0
Natural Gas-area	15	1	181	12	30
-point	0	0	0	0	0
Wood-area	0	0	0	0	0
-point	0	0	0	0	0
Liquid Petroleum Gas-point	0	0	0	0	0
Miscellaneous-point	0	0	0	0	0
Internal Combustion-point	7	15	206	20	125
Electric Generation	7	15	206	20	125
Distillate Oil	0	0	0	0	0
Natural Gas	0	0	0	0	0
Diesel Fuel	7	15	206	20	125
Industrial Fuel	0	0	0	0	0
Distillate Oil	0	0	0	0	0
Natural Gas	0	0	0	0	0
Gasoline	0	0	0	0	0
Diesel Fuel	0	0	0	0	0
Other	0	0	0	0	0
Commercial-Institutional	0	0	0	0	0
Diesel Fuel	0	0	0	0	0
Other	0	0	0	0	0
Engine-Testing	0	0	0	0	0
Aircraft	0	0	0	0	0
Other	0	0	0	0	0
Miscellaneous	0	0	0	0	0
INDUSTRIAL PROCESS-POINT	4,944	2,833	911	0	13,514
Chemical Manufacturing	0	0	0	0	0
Food/Agriculture	0	0	0	0	0
Primary Metal	817	0	0	0	0
Secondary Metals	1,070	0	0	0	13,514
Mineral Products	2,969	2,833	911	0	0
Petroleum Industry	0	0	0	0	0
Wood Products	76	0	0	0	0
Evaporation	0	0	0	0	0
Metal Fabrication	0	0	0	0	0
Leather Products	0	0	0	0	0
Textile Manufacturing	0	0	0	0	0
Inprocess Fuel	12	0	0	0	0
Other/Not Classified	0	0	0	0	0
SOLID WASTE DISPOSAL-AREA	599	50	163	1,189	3,426
-POINT	0	0	0	0	0
Government-point	0	0	0	0	0
Municipal Incineration	0	0	0	0	0
Open Burning	0	0	0	0	0
Other	0	0	0	0	0
Residential-area	459	20	110	1,030	3,002
On Site Incineration	180	3	6	506	1,519
Open Burning	279	17	105	524	1,483
Commercial-Institutional-area	94	22	33	98	257
-point	0	0	0	0	0
On Site Incineration-area	63	20	24	40	91
-point	0	0	0	0	0
Open Burning-area	31	2	12	59	166
-point	0	0	0	0	0
Apartment-point	0	0	0	0	0
Other-point	0	0	0	0	0
Industrial-area	46	8	17	62	168
-point	0	0	0	0	0
On Site Incineration-area	19	6	7	12	28
-point	0	0	0	0	0
Open Burning-area	26	2	10	50	140
-point	0	0	0	0	0
Auto Body Incineration-point	0	0	0	0	0
Other-point	0	0	0	0	0
Miscellaneous-point	0	0	0	0	0
TRANSPORTATION-AREA	1,661	898	16,424	20,505	109,551
Land Vehicles	1,640	875	16,320	15,922	99,844
Gasoline	1,199	344	11,113	15,235	97,616
Light Vehicles	1,128	316	10,302	13,639	82,908
Heavy Vehicles	48	16	551	864	6,407
Off Highway	23	12	260	732	8,301
Diesel Fuel	441	531	5,207	687	2,228
Heavy Vehicles	165	210	1,952	216	1,256
Off Highway	222	199	2,465	270	695
Rail	53	122	790	201	278
Aircraft	22	4	19	95	544
Military	0	0	0	0	0
Civil	22	4	19	95	544
Commercial	0	0	0	0	0
Vessels	0	20	85	2,882	9,163
Bituminous Coal	0	0	0	0	0
Diesel Fuel	0	0	0	0	0
Residual Oil	0	0	0	0	0
Gasoline	0	20	85	2,882	9,163
Gas Handling Evaporation Loss	0	0	0	1,606	0
MISCELLANEOUS-AREA	34	0	8	11,814	280
Forest Fires	34	0	8	48	280
Structural Fires	0	0	0	0	0
Slash Burning	0	0	0	0	0
Frost Control	0	0	0	0	0
Solvent Evaporation Loss	0	0	0	11,766	0

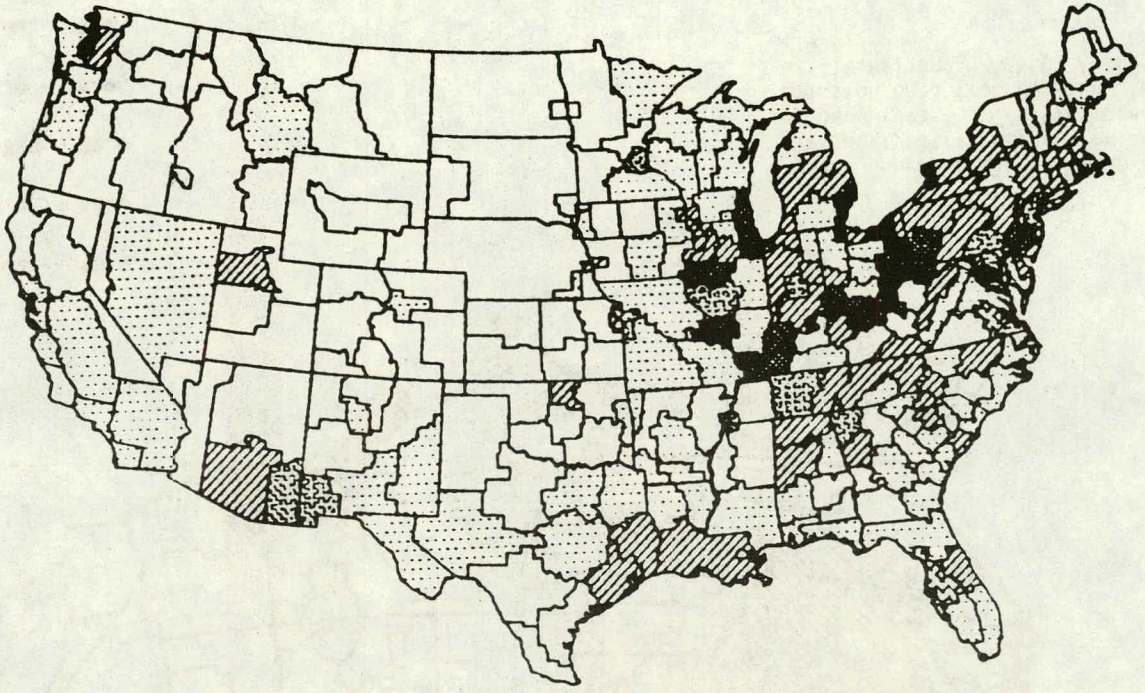

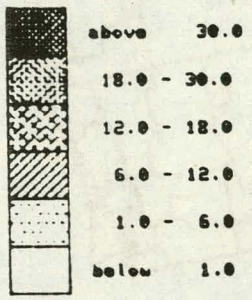

(tons/square kilometer)

Note: Emissions data by AQCR from DOE/FERC (electric utilities) and EPA/NEDS (other sources).

FIGURE 5-11. EMISSION DENSITIES

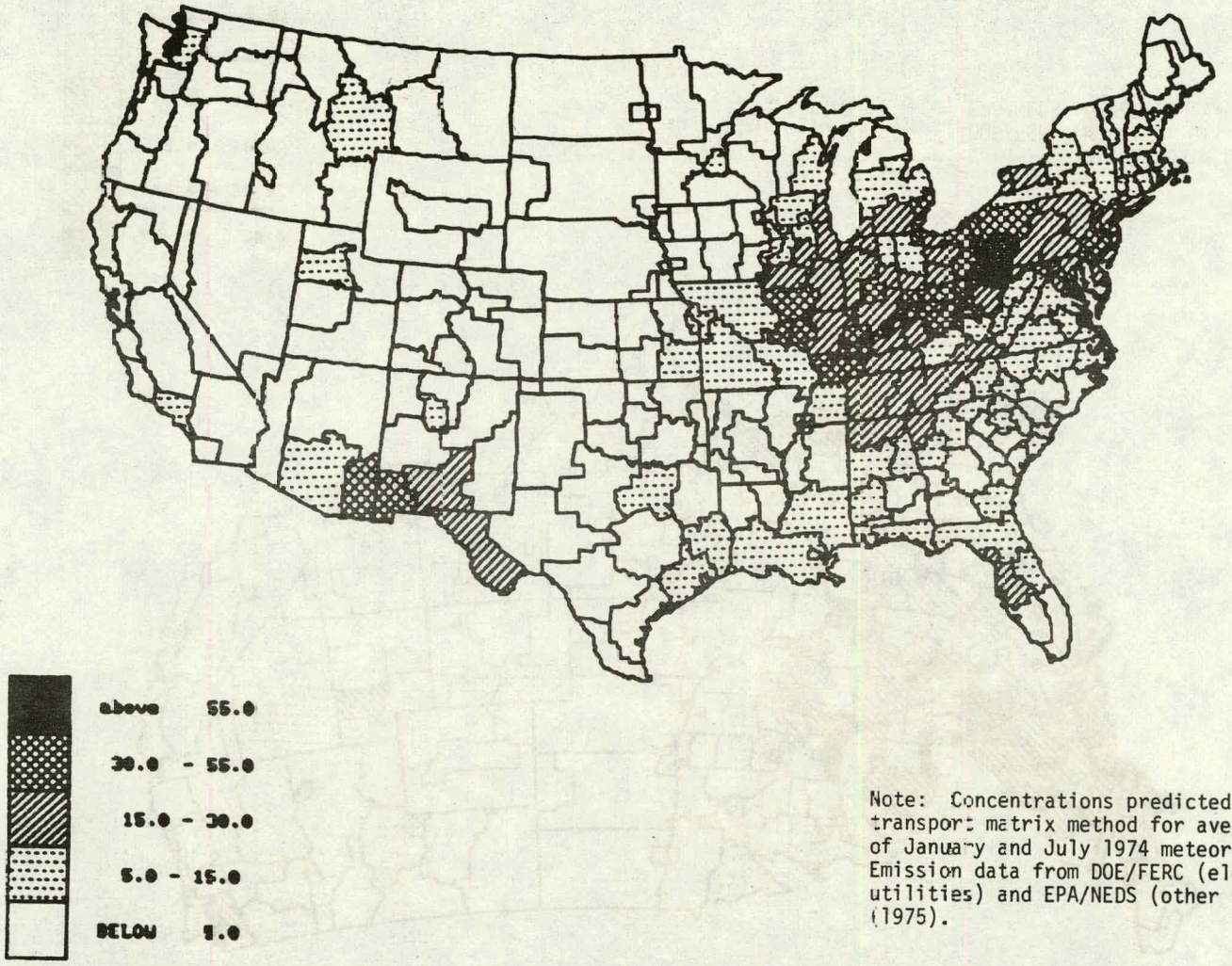

Note: Concentrations predicted by transport matrix method for average of January and July 1974 meteorology. Emission data from DOE/FERC (electric utilities) and EPA/NEDS (other sources) (1975).

FIGURE 5-12. PREDICTED SO_2 CONCENTRATIONS

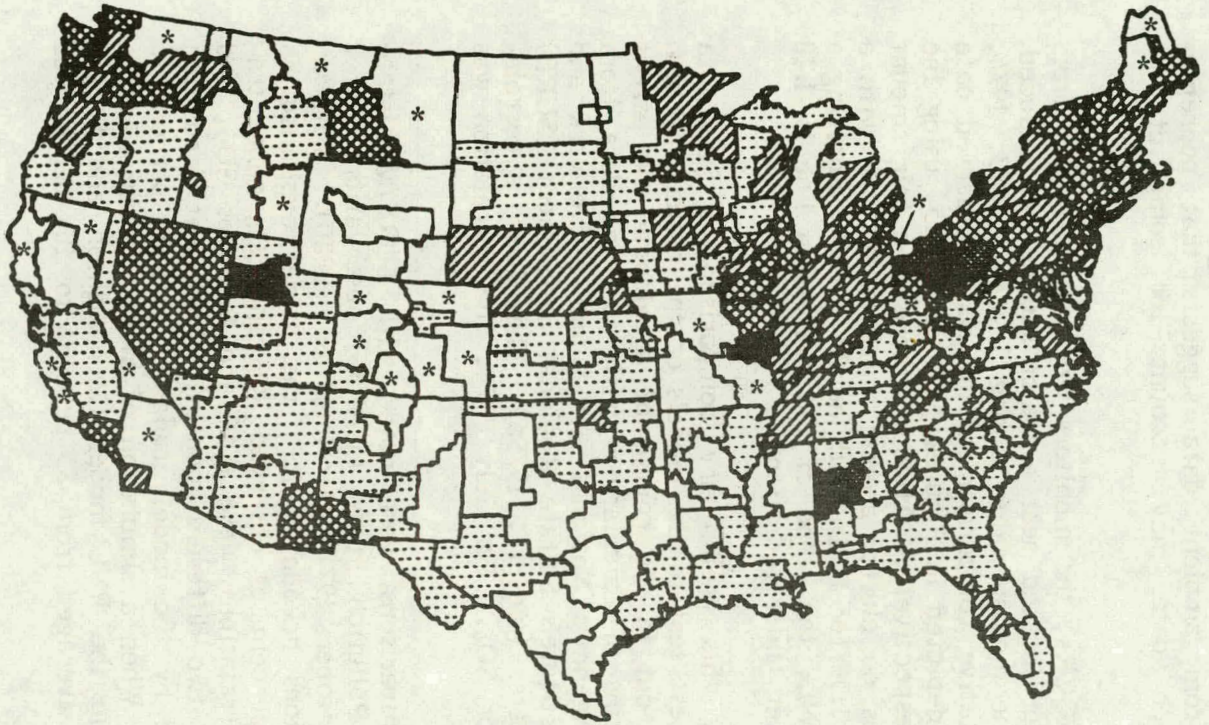

above 55.0
30.0 - 55.0
15.0 - 30.0
5.0 - 15.0
BELOW 5.0
* no data

(micrograms/cubic meter)

Note: Average of all population-oriented monitors in each AQCR.
Source: EPA SAROAD data base.

FIGURE 5-13. OBSERVED SO_2 CONCENTRATIONS

respectively. Comparison with SO_2 observations is not regarded as a satisfactory validation test of the matrix method for several reasons. First, the method was developed primarily to capture interregional effects; the intraregional effects, especially the local SO_2 concentrations, were not necessarily expected to be especially accurate. More importantly, however, the emission input data set and the observed SO_2 concentrations used have not been subjected to adequate quality controls. (Some of the problems with those data are described above.) Preliminary checking in a few regions where the model diverged substantially from ambient data suggests that nonrepresentative observed concentration data may account for some of the divergences.

For example, in several AQCRs, the monitors were clustered far from sources, or only a single monitor located near a major source was included. To eliminate spurious values, the median value among 3 years (1973, 1974, and 1975) was chosen. Quantitative comparison of the above observed data versus predicted SO_2 values is depicted in Figures 5-14 and 5-15, using the BNL and PNL SO_2 matrices, respectively. Although there is a fair amount of scatter, the 215 observations do cluster around a regression line with a slope close to 1. The slope is 1.06 for BNL, with an $R^2 = 0.64$, implying a slight under prediction. For PNL, the slope of the regression line is 1.18 and $R^2 = 0.63$, implying a greater underprediction.

For reasons given above, this preliminary comparison of SO_2 data should not be regarded as the best test of the models or the matrix method. Validation efforts were carried out in the course of developing the parent models. BNL compared 4 months of calculations with observed data from the Environmental Protection Agency's National Air Sampling Network and the Electric Power Research Institute's Sulfate Regional Experiment (SURE) data over the Eastern United States (Meyers, 1979a). They found a correlation of 0.7 for SO_2 and 0.6 for SO_4. For July 1974, the correlation was 0.57 for SO_2 and 0.81 for SO_4.

For the PNL model, comparisons were made with SURE/Multistate Atmospheric Power Production Pollution Study (MAP3S) observations for 2 months of data (August and October 1977) (McNaughton, 1980). With an estimated 65 percent of emissions accounted for, the model explained an average of 56 percent and 89 percent of observed SO_2 and SO_4 concentrations, respectively. Spatial correlations were 0.56 and 0.76 for SO_2, and 0.59 and 0.64 for SO_4, for the two different months. Total wet deposition was substantially underestimated by the model, ranging from 30 percent to 80 percent of observed values. When a simulation of incloud transformation of SO_2 to SO_4 was included in the PNL model (McNaughton and Scott, 1980), predicted wet deposition averaged from 85 percent to 104 percent of observed values.

Further validation work on the two parent models and the derived matrices is planned in the near future using more recent, better controlled observed data and corresponding meteorology. This work will examine both SO_2 and SO_4 concentration and wet deposition of sulfur. Comparison with SO_4 and deposition data for 1974 has not even been attempted here because such data was relatively sparse and systematic measurement errors occurred in SO_4 data during that period.

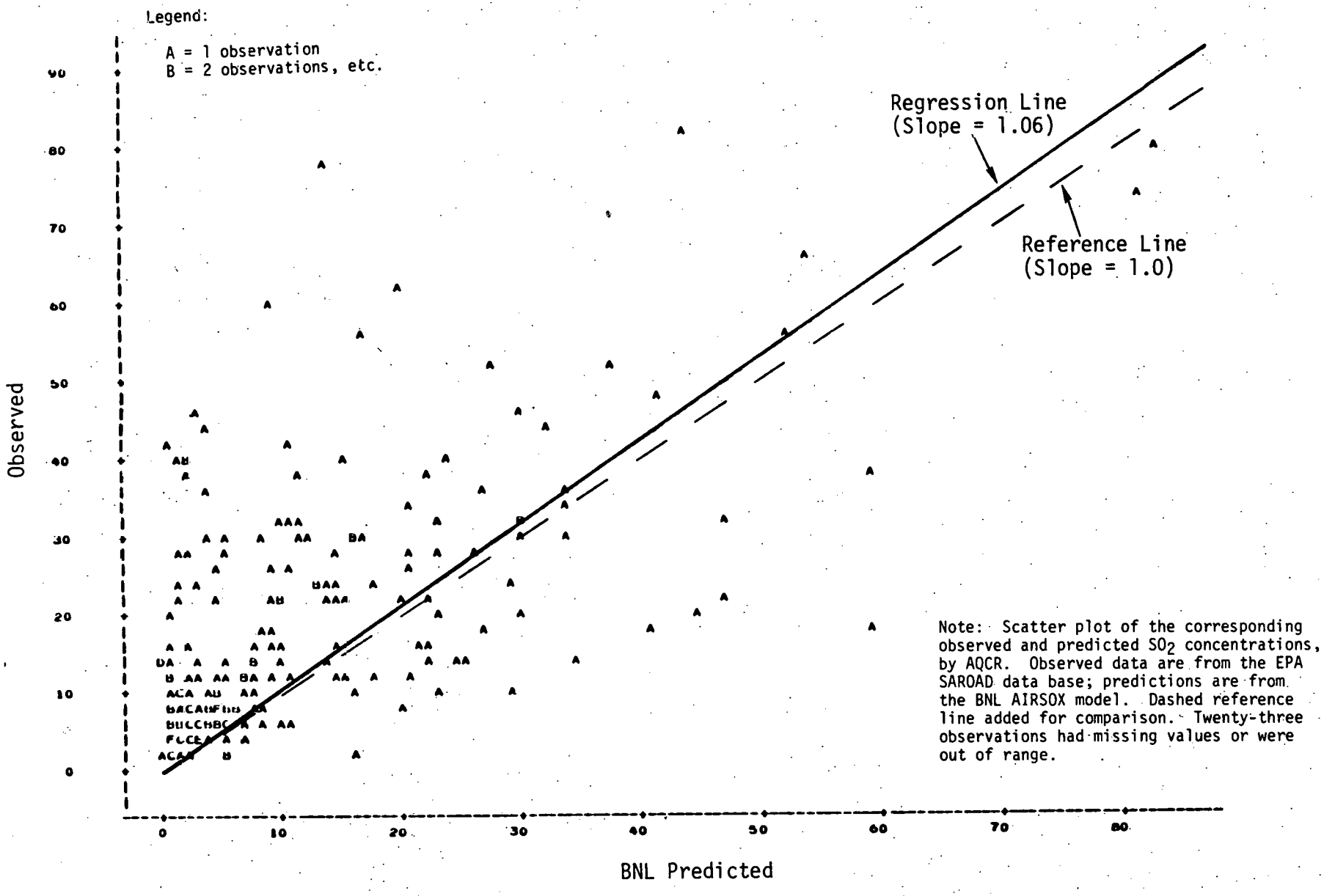

FIGURE 5-14. PREDICTED VS OBSERVED SO_2 CONCENTRATIONS (BNL)

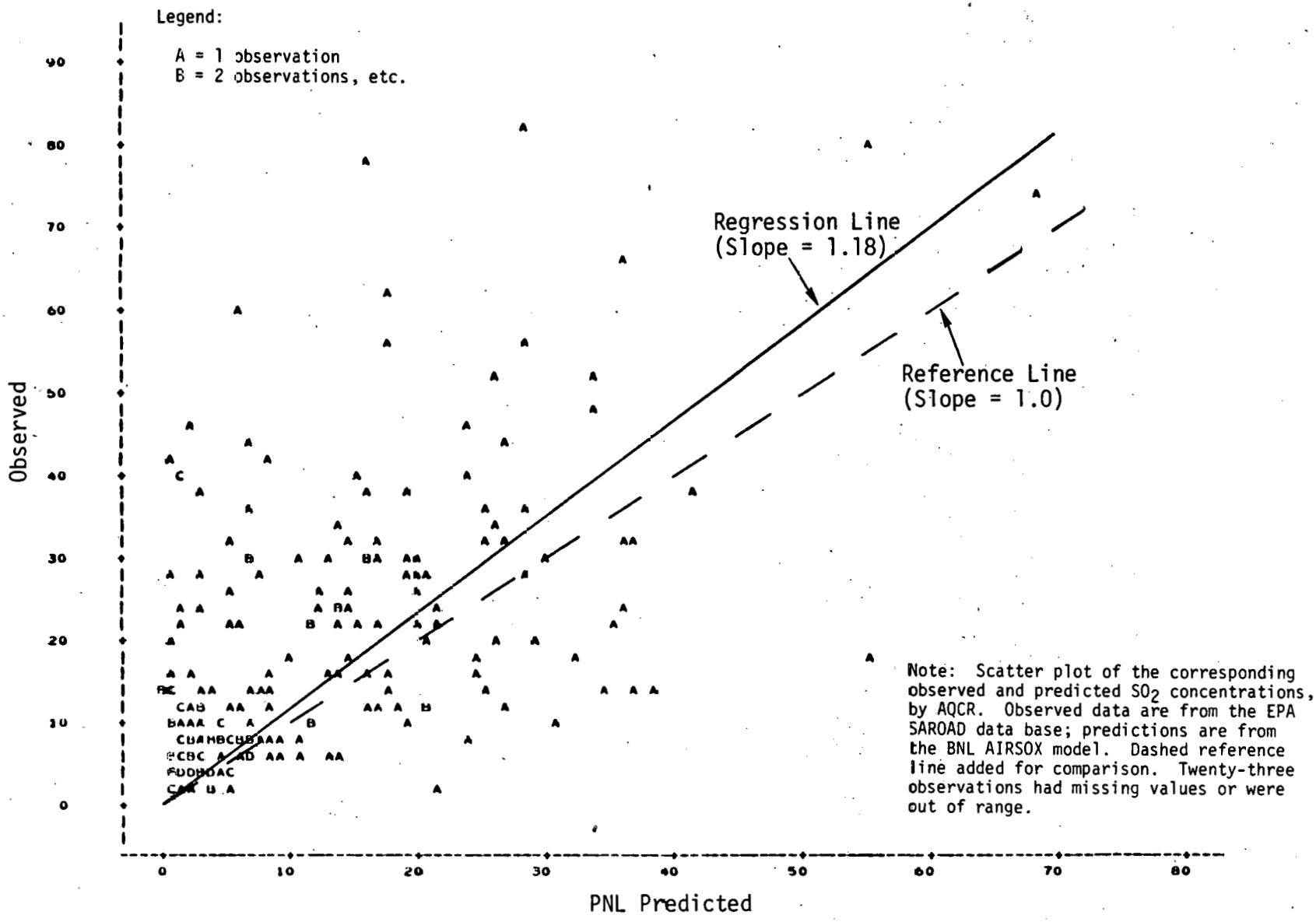

FIGURE 5-15. PREDICTED VS OBSERVED SO_2 CONCENTRATIONS (PNL)

The matrices developed by PNL for fine or respirable particulates have not been subjected to substantial testing due to the absence of comprehensive data for both emissions and ambient concentrations. The general method presumably could be used for any component of emitted particulates up to roughly 10 micron in size (where gravitational settling begins to become important), provided that appropriate rate parameters for wet and dry deposition are used and no significant transformations of form occur.

The fine particulate matrices have been used in DOE's Technology Assessment of Solar Energy (DOE, to be published). In this project, emission estimates for fine particulates were developed in terms of fractions of total particulate emissions for different sources. An example of the concentration results for the 1975 base year emissions is given in Figure 5-16. Large but uncertain sources of total particulates such as fugitive dust and forest fires are not included in these estimates. From Figure 5-16 it can be seen that primary fine particulate concentration estimates range from less than 0.5 to 10 $\mu g/m^3$ (annual average) over the United States.

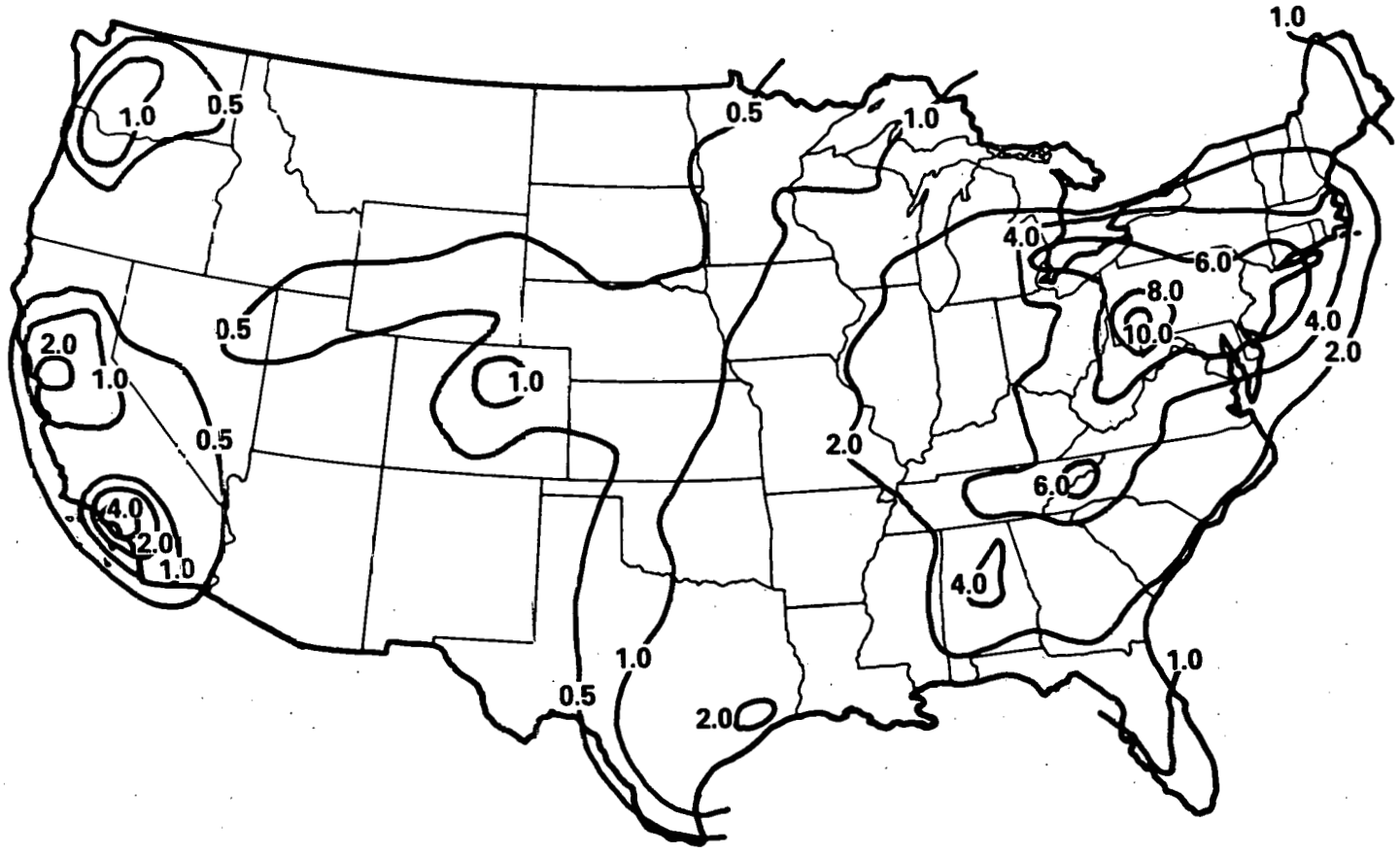

Note: Predicted primary fine particulate concentration (micrograms/cubic meter) based on annual average meteorology and emissions from the TASE low scenario.

FIGURE 5-16. FINE PARTICULATE CONCENTRATIONS

6. FUTURE DIRECTIONS

6.1 VALIDATION AND CALIBRATION

Validation of the matrix methodology and identification of its limits is an essential task to support future applications. Ideally, this work should be carried out in conjunction with validation and testing of the parent models for reasons of economy and to permit identification of limitations of the matrix method per se from those of the parent models.

An opportunity to do this exists because validation studies of the parent models are being carried out under the Environmental Protection Agency MAP3S program. Observations from the SURE monitoring network and an improved emission inventory should permit more accurate data for validation. Meteorological data and model runs will be made for July 1978. Development of new matrices for this period can be achieved with a relatively small increment of additional work and would provide improvements in long-term forecasting statistics plus an opportunity to check the matrix predictions against a better quality data base.

Validation work carried out in conjunction with the parent models not only establishes confidence limits on the models, but also provides the opportunity to select improved parameter values for atmospheric processes to improve models and derived matrices. This is especially important in view of current uncertainties in the relative value and magnitude of different transformation and removal processes. Simultaneous comparison with data bases for SO_2, SO_4, and deposition is especially important in separating the individual effects of transformation and removal rate parameters.

6.2 MODEL EXTENSIONS

Current matrices are limited in several ways:

- Geographic coverage is limited to the conterminous United States, excluding Canadian sources and receptors.
- Only SO_2 and SO_4 concentrations are provided. (Deposition values are not available at present but are being developed by BNL).
- Nitrate (NO_3^-) ions are not modeled, and these are presumed to be of growing importance to acid precipitation and visibility estimation in the future.
- Only monthly averages of air quality parameters are projected by present matrices; shorter term averages are important to regulatory analysis and estimation of acute effects.
- Only 4 months of 1974 meteorological data have been modeled and processed into matrices; further analysis of the range of effect of

meteorological variability on transport is required to establish representative annual, seasonal, and monthly averages and the statistics of probable fluctuations about those mean values.

- All emitted fine particulate species are treated as uniform in their behavior in the PNL respirable particulate matrices; further investigation of differences in behavior (e.g., deposition rates) among important substances is required, and important differences will be incorporated into the matrices.

- Emission estimates of fine particulates and available data on ambient concentrations need to be collected to validate and calibrate the respirable particulates matrices.

Limited coverage of Canadian sources and deposition values will be computed by BNL. Computation of July 1978 and additional spring and autumn months is also in progress. A preliminary study of methods for estimating short-term concentratons is underway at BNL. BNL matrices for wet and dry deposition of SO_2 and SO_4 will be described in a later report.

6.3 ANALYSIS OF VARIANCE IN AMBIENT CONCENTRATION

An important task for the future is to analyze the variance of observed SO_2, SO_4, and particulate data. This data is available from the Environmental Protection Agency in SAROAD and SURE data bases, but only cursory analysis has been conducted by OEA so far.

The statistical technique, analysis of variance, can be used on each pollutant to divide the total variance in the historical observations into components caused by factors such as the following:

- Monitor type (population, source, or background)
- Seasonal and monthly variation
- Year-to-year variation

6.3.1 Monitor Type

A significant fraction of the total variance might be attributable to monitor type. If so, rather than averaging all monitors together to represent the region, it might be better to average each type separately. Averages of background monitors might be the best data to use in comparisons with long-range transport predictions.

6.3.2 Seasonal Effects

Large variation between seasons would indicate the necessity to establish emissions by season rather than annually and to multiply seasonal emissions by seasonal transport matrices. Additionally, investigation of the variance between months provides information on how many monthly matrices are needed to establish a sound estimate of an average seasonal matrix.

6.3.3 Year-to-Year Variation

Variation between years indicates the number of annual matrices that must be averaged together to provide a sound estimate of a typical annual matrix. Furthermore, analysis of annual data is needed to develop corrections for long-term trends in the data.

If the observed ambient air quality data can be adjusted for the above factors, the data may prove useful in model validation testing. Even if validation cannot be accomplished, identification of major causes of data variability could help in refining the matrix methods.

6.3.4 Subsequent Tasks

If validation appears to be feasible on the basis of analysis of concentration data, then good estimates of emissions will also be needed for the same time periods. The Environmental Protection Agency NEDS and MAP3S data bases contain much of the needed information (quality unknown). A second task then is to establish effective computer access to these data bases. Once this is done, validation trials comparing model output concentrations with observed concentrations should be the third task.

APPENDIX A. STATE SULFATE TRANSPORT MATRIX

Interstate transport matrices have been developed by Brookhaven and Pacific Northwest National Laboratories as explained in Section 2.6. Table A-1 illustrates a typical state-level matrix. This matrix was generated by Brookhaven National Laboratory for utility sources and area-weighted receptors with transport averaged over January and July meteorology. Each matrix element represents a mathematical transformation of state emissions in units of millions of metric tons of SO_2 per year to annual average concentrations in the receptor state in micrograms of sulfate (SO_4) per cubic meter of air. Each state is listed as an emitter in the column headings and as a receptor in the row headings, allowing computation of transport from any emitter state to any receptor state. For example, the tabulated transport from Mississippi (3rd row in 2nd column) to Alabama (1st row) is 2.26739 micrograms/cubic meter/million metric tons of emissions.

Table A-1. Sample State Transport Matrix

	EMITTERS									
BAVSO4RE	AL	AZ	AR	CA	CO	CT	DE	FL	GA	ID
	IL	IN	IA	KS	KY	LA	ME	MD	MA	MI
RECEPTORS	MN	MS	MO	MT	NB	NV	NH	NJ	NM	NY
	NC	ND	OH	OK	OR	PA	RI	SC	SD	TN
	TX	UT	VT	VA	WA	WV	WI	WY		
ALABAMA	2.22525	0.00000	0.75012	0.00000	0.00020	0.01165	0.03708	0.79145	0.74510	0.00000
	0.19603	0.16652	0.01962	0.06231	0.33282	1.14235	0.00000	0.03281	0.00018	0.01957
	0.00421	2.26739	0.21414	0.00014	0.00874	0.00000	0.00000	0.03949	0.00024	0.02483
	0.12512	0.00133	0.05859	0.02427	0.00000	0.03836	0.00000	0.14462	0.00207	0.58460
	0.07069	0.00008	0.00000	0.06291	0.00000	0.08245	0.03154	0.00003		
ARIZONA	0.00000	1.67818	0.00000	0.51756	0.01522	0.00000	0.00000	0.00000	0.00000	0.00000
	0.00000	0.00000	0.00000	0.00000	0.00000	0.00000	0.00000	0.00000	0.00000	0.00000
	0.00000	0.00000	0.00000	0.00085	0.00000	0.64464	0.00000	0.00000	0.36128	0.00000
	0.00000	0.00000	0.00000	0.00010	0.00801	0.00000	0.00000	0.00000	0.00000	0.00000
	0.00119	0.17009	0.00000	0.00000	0.00004	0.00000	0.00000	0.03773		
ARKANSAS	0.02004	0.00338	1.42657	0.00000	0.03732	0.00000	0.00000	0.00664	0.00137	0.00000
	0.28929	0.06037	0.16795	0.48688	0.08296	0.15918	0.00000	0.00000	0.00000	0.00610
	0.02196	0.04679	0.56501	0.01518	0.16931	0.00036	0.00000	0.00000	0.03022	0.00000
	0.00028	0.03773	0.00092	0.35817	0.00000	0.00000	0.00000	0.00014	0.07790	0.18741
	1.77055	0.00921	0.00000	0.00011	0.00002	0.00034	0.06448	0.01729		
CALIFORN	0.00000	0.01437	0.00000	1.61300	0.00040	0.00000	0.00000	0.00000	0.00000	0.00000
	0.00000	0.00000	0.00000	0.00000	0.00000	0.00000	0.00000	0.00000	0.00000	0.00000
	0.00000	0.00000	0.00000	0.00000	0.00000	0.12516	0.00000	0.00000	0.00569	0.00000
	0.00000	0.00000	0.00000	0.00000	0.10600	0.00000	0.00000	0.00000	0.00000	0.00000
	0.00000	0.02311	0.00000	0.00000	0.05591	0.00000	0.00000	0.00092		
COLORADO	0.00000	0.75018	0.00000	0.05354	2.02669	0.00000	0.00000	0.00000	0.00000	0.00000
	0.00028	0.00004	0.00098	0.01599	0.00000	0.00000	0.00000	0.00000	0.00000	0.00003
	0.00006	0.00000	0.00315	0.08849	0.00556	0.36565	0.00000	0.00000	1.54868	0.00000
	0.00000	0.01656	0.00000	0.00126	0.01208	0.00000	0.00000	0.00000	0.01173	0.00000
	0.03565	1.06441	0.00000	0.00000	0.00740	0.00000	0.00028	0.57537		
CONNECTI	0.11084	0.00137	0.08897	0.00000	0.02193	3.52358	0.49760	0.06552	0.11717	0.00000
	0.22676	0.25644	0.19419	0.10402	0.17456	0.03317	0.10132	0.32459	0.89266	0.54398
	0.06293	0.05498	0.16129	0.01225	0.09018	0.00000	0.30625	0.92818	0.00528	1.18428
	0.21059	0.01733	0.36614	0.02207	0.00017	0.64862	0.89111	0.09235	0.03555	0.14004
	0.01468	0.01760	0.75694	0.28762	0.00000	0.35473	0.31783	0.02532		
DELAWARE	0.22449	0.00009	0.15117	0.00000	0.00761	0.21850	5.82902	0.15963	0.29815	0.00000
	0.19143	0.31179	0.10138	0.12379	0.45484	0.03028	0.01078	2.51493	0.03130	0.25940
	0.06339	0.08759	0.13811	0.00603	0.06805	0.00000	0.07659	1.19125	0.00005	0.58195
	0.73117	0.00390	0.79405	0.04140	0.00000	1.51366	0.07446	0.43521	0.01804	0.38197
	0.06359	0.00294	0.14171	1.62137	0.00000	1.17373	0.09353	0.00929		
FLORIDA	0.24636	0.00000	0.03514	0.00000	0.00001	0.02772	0.02180	2.44790	0.13397	0.00000
	0.01274	0.01848	0.00035	0.00077	0.02577	0.32243	0.00000	0.02574	0.00096	0.00633
	0.00000	0.49365	0.00749	0.00000	0.00001	0.00000	0.00000	0.03042	0.00000	0.02020
	0.08734	0.00002	0.02131	0.00020	0.00000	0.01392	0.00000	0.08129	0.00000	0.05379
	0.00197	0.00000	0.00000	0.04261	0.00000	0.02710	0.00395	0.00000		

Table A-1. Sample State Transport Matrix (continued)

	EMITTERS									
BAVSO4RE	AL	AZ	AR	CA	CO	CT	DE	FL	GA	ID
	IL	IN	IA	KS	KY	LA	ME	MD	MA	MI
RECEPTORS	MN	MS	MO	MT	NB	NV	NH	NJ	NM	NY
	NC	NB	OH	OK	OR	PA	RI	SC	SD	TN
	TX	UT	VT	VA	WA	WV	WI	WY		
GEORGIA	1.31874	0.00000	0.20644	0.00000	0.00000	0.01676	0.05652	1.30722	2.28775	0.00000
	0.07632	0.12651	0.00928	0.01010	0.23126	0.40552	0.00000	0.07902	0.00043	0.05819
	0.00139	0.88225	0.04224	0.00000	0.00213	0.00000	0.00000	0.05757	0.00000	0.04310
	0.26448	0.00154	0.09993	0.00369	0.00000	0.06843	0.00000	0.51869	0.00037	0.43146
	0.00789	0.00000	0.00000	0.13259	0.00000	0.12126	0.02263	0.00000		
IDAHO	0.00000	0.17616	0.00000	0.44663	0.01295	0.00000	0.00000	0.00000	0.00000	0.00000
	0.00000	0.00000	0.00000	0.00000	0.00000	0.00000	0.00000	0.00000	0.00000	0.00000
	0.00000	0.00000	0.00000	0.04737	0.00000	0.74606	0.00000	0.00000	0.08552	0.00000
	0.00000	0.00001	0.00000	0.00000	0.48441	0.00000	0.00000	0.00000	0.00169	0.00000
	0.00008	0.48990	0.00000	0.00000	0.34571	0.00000	0.00000	0.20501		
ILLINOIS	0.05542	0.00635	0.81469	0.00001	0.12385	0.00000	0.00000	0.00536	0.00147	0.00000
	2.14914	1.17608	0.99617	0.54980	0.78066	0.08602	0.00000	0.00000	0.00000	0.28007
	0.39449	0.08322	1.57316	0.07248	0.48673	0.00112	0.00000	0.00000	0.03745	0.00096
	0.00018	0.13841	0.06574	0.02449	0.00155	0.00142	0.00000	0.00017	0.21011	0.42499
	0.45048	0.02309	0.00000	0.00015	0.00161	0.00097	0.72840	0.05025		
INDIANA	0.26061	0.00672	0.63598	0.00000	0.07476	0.00000	0.00002	0.02472	0.06766	0.00000
	1.20545	2.58815	0.49818	0.37030	1.59385	0.08469	0.00000	0.00019	0.00000	0.52963
	0.22182	0.09917	0.83385	0.02655	0.26447	0.00143	0.00000	0.00000	0.01683	0.00637
	0.00255	0.05774	0.60204	0.28557	0.00187	0.01635	0.00000	0.00358	0.11655	0.62594
	0.29985	0.02693	0.00000	0.00317	0.00000	0.05387	0.49882	0.02006		
IOWA	0.00005	0.02386	0.02872	0.00037	0.20598	0.00000	0.00000	0.00001	0.00000	0.00000
	0.34141	0.06010	1.68640	0.84449	0.00420	0.00238	0.00000	0.00000	0.00000	0.05493
	0.62153	0.00090	0.59184	0.27656	1.70716	0.02219	0.00000	0.00000	0.06875	0.00012
	0.00000	0.34697	0.00164	0.71887	0.01529	0.00017	0.00000	0.00000	0.73369	0.00129
	0.31455	0.12969	0.00000	0.00000	0.01910	0.00001	0.44530	0.21608		
KANSAS	0.00000	0.23310	0.00987	0.00749	0.96399	0.00000	0.00000	0.00009	0.00000	0.00000
	0.05987	0.01240	0.29969	1.24283	0.00012	0.00131	0.00000	0.00000	0.00000	0.00697
	0.02178	0.00057	0.34030	0.23407	0.86301	0.02944	0.00000	0.00000	0.39356	0.00000
	0.00000	0.11647	0.00030	1.22236	0.00511	0.00000	0.00000	0.00000	0.17601	0.00062
	0.33694	0.29721	0.00000	0.00000	0.00550	0.00000	0.01619	0.42735		
KENTUCKY	0.79352	0.00114	1.14838	0.00000	0.00817	0.00019	0.00149	0.07204	0.57193	0.00000
	0.63713	1.09591	0.17586	0.21985	2.72443	0.33080	0.00000	0.01083	0.00001	0.18736
	0.09097	0.40280	0.52249	0.00229	0.10146	0.00000	0.00001	0.00127	0.00435	0.02087
	0.16499	0.02127	0.75574	0.05911	0.00013	0.07437	0.00002	0.09546	0.04049	1.81494
	0.39727	0.00148	0.00001	0.11946	0.00000	0.46235	0.23275	0.00090		
LOUISIAN	0.13820	0.00304	0.22427	0.00002	0.03752	0.00008	0.00057	0.07013	0.01935	0.00000
	0.05898	0.01356	0.02111	0.04132	0.01416	1.57899	0.00000	0.00041	0.00000	0.00046
	0.00063	0.29613	0.14869	0.00174	0.01130	0.00117	0.00009	0.00031	0.01452	0.00012
	0.00232	0.00361	0.00012	0.03727	0.00000	0.00011	0.00000	0.00814	0.00461	0.08055
	0.21775	0.00213	0.00000	0.00086	0.00000	0.00019	0.00815	0.00398		

Table A-1. Sample State Transport Matrix (continued)

	EMITTERS									
BAVSO4RE	AL	AZ	AR	CA	CO	CT	DE	FL	GA	ID
	IL	IN	IA	KS	KY	LA	ME	MD	MA	MI
RECEPTORS	MN	MS	MO	MT	NB	NV	NH	NJ	NM	NY
	NC	ND	OH	OK	OR	PA	RI	SC	SD	TN
	TX	UT	VT	VA	WA	WV	WI	WY		
MAINE	0.05593	0.00016	0.07547	0.00000	0.00487	0.18681	0.14769	0.01199	0.03230	0.00000
	0.22020	0.27874	0.12166	0.03029	0.17759	0.01377	1.76441	0.13662	0.37230	0.41114
	0.12071	0.02633	0.08191	0.00337	0.03273	0.00000	0.72515	0.15183	0.00050	0.30719
	0.05366	0.03463	0.24857	0.00998	0.00001	0.23693	0.27440	0.01916	0.06245	0.12305
	0.00372	0.00172	1.30895	0.08633	0.00155	0.16483	0.34962	0.00341		
MARYLAND	0.27491	0.00010	0.19305	0.00000	0.01090	0.15197	2.12234	0.13843	0.38147	0.00000
	0.24466	0.36441	0.09501	0.12770	0.55618	0.05194	0.00712	4.06042	0.02246	0.29877
	0.07259	0.11991	0.20100	0.00658	0.06459	0.00000	0.04532	0.61688	0.00013	0.40335
	1.03367	0.00431	0.96445	0.05818	0.00000	1.55595	0.05177	0.49878	0.02576	0.49945
	0.07662	0.00280	0.10244	2.18663	0.00000	1.81866	0.09245	0.00825		
MASSACHU	0.12065	0.00124	0.12812	0.00000	0.02299	1.39357	0.36534	0.05309	0.09644	0.00000
	0.30476	0.31173	0.21781	0.09613	0.19783	0.02694	0.41712	0.24492	2.73174	0.61870
	0.08462	0.05342	0.16767	0.00885	0.08296	0.00000	1.40417	0.63708	0.00395	0.84831
	0.14076	0.01990	0.33574	0.02497	0.00027	0.52231	2.78189	0.08754	0.05769	0.16725
	0.01228	0.01261	0.95475	0.24109	0.00002	0.26206	0.43133	0.02089		
MICHIGAN	0.04228	0.00963	0.11369	0.00000	0.09432	0.00005	0.00031	0.00548	0.02434	0.00000
	0.59432	0.63856	0.59095	0.37516	0.20210	0.01077	0.00000	0.00162	0.00000	1.34276
	0.62504	0.01900	0.42103	0.15549	0.38041	0.00786	0.00000	0.00008	0.01333	0.03929
	0.00184	0.21039	0.29553	0.16798	0.01166	0.06100	0.00001	0.00153	0.40415	0.08398
	0.14252	0.07979	0.00001	0.00253	0.00256	0.03871	1.02116	0.08902		
MINNESOT	0.00000	0.01187	0.00013	0.00136	0.21579	0.00000	0.00000	0.00000	0.00000	0.00000
	0.02159	0.00395	0.67494	0.33365	0.00001	0.00001	0.00000	0.00000	0.00000	0.02027
	1.31868	0.00000	0.10875	0.55478	0.95965	0.06994	0.00000	0.00000	0.04221	0.00000
	0.00000	1.10372	0.00009	0.40149	0.05807	0.00000	0.00000	0.00000	1.79299	0.00000
	0.07736	0.10900	0.00000	0.00000	0.07743	0.00000	0.23479	0.20501		
MISSISSI	0.51098	0.00022	0.74998	0.00000	0.00543	0.00016	0.00142	0.09677	0.15016	0.00000
	0.18497	0.08428	0.02660	0.09903	0.16953	1.90256	0.00000	0.00071	0.00000	0.00338
	0.00475	1.98172	0.24143	0.00155	0.01356	0.00013	0.00000	0.00134	0.00305	0.00027
	0.02735	0.00247	0.01036	0.05470	0.00000	0.00051	0.00000	0.01804	0.01066	0.39864
	0.26258	0.00043	0.00000	0.00700	0.00000	0.00904	0.03048	0.00059		
MISSOURI	0.00704	0.01142	1.04435	0.00010	0.11999	0.00000	0.00000	0.00057	0.00034	0.00000
	0.74917	0.16894	0.70313	1.86086	0.18539	0.05264	0.00000	0.00000	0.00000	0.03408
	0.19448	0.01905	1.95850	0.08931	0.79679	0.00292	0.00000	0.00000	0.03852	0.00000
	0.00011	0.10867	0.00404	0.67938	0.00165	0.00000	0.00000	0.00006	0.22858	0.15813
	1.09566	0.02787	0.00000	0.00005	0.00281	0.00017	0.21828	0.09096		
MONTANA	0.00000	0.19836	0.00000	0.19958	0.20364	0.00000	0.00000	0.00000	0.00000	0.00000
	0.00000	0.00000	0.00135	0.00060	0.00000	0.00000	0.00000	0.00000	0.00000	0.00000
	0.00017	0.00000	0.00001	1.18767	0.00612	0.41503	0.00000	0.00000	0.15503	0.00000
	0.00000	0.08567	0.00000	0.00396	0.42177	0.00000	0.00000	0.00000	0.04919	0.00000
	0.00377	0.36789	0.00000	0.00000	0.42396	0.00000	0.00000	0.52472		

Table A-1. Sample State Transport Matrix (continued)

BAVSO4RE / RECEPTORS	AL IL MN NC TX	AZ IN MS ND UT	AR IA MO OH VT	CA KS MT OK VA	CO KY NB OR WA	CT LA NV PA WV	DE ME NH RI WI	FL MD NJ SC WY	GA MA NM SD	ID MI NY TN
				EMITTERS						
NEBRASKA	0.00000	0.21608	0.00038	0.00924	1.14484	0.00000	0.00000	0.00000	0.00000	0.00000
	0.03157	0.00562	0.31980	0.39407	0.00000	0.00013	0.00000	0.00000	0.00000	0.00422
	0.06636	0.00001	0.11348	0.57363	0.99082	0.09238	0.00000	0.00000	0.40917	0.00000
	0.00000	0.36358	0.00009	0.44884	0.02474	0.00000	0.00000	0.00000	0.36636	0.00003
	0.11250	0.64732	0.00000	0.00000	0.02969	0.00000	0.02848	1.06189		
NEVADA	0.00000	0.03459	0.00000	1.20393	0.00062	0.00000	0.00000	0.00000	0.00000	0.00000
	0.00000	0.00000	0.00000	0.00000	0.00000	0.00000	0.00000	0.00000	0.00000	0.00000
	0.00000	0.00000	0.00000	0.00103	0.00000	1.47966	0.00000	0.00000	0.00626	0.00000
	0.00000	0.00000	0.00000	0.00000	0.19540	0.00000	0.00000	0.00000	0.00001	0.00000
	0.00002	0.07423	0.00000	0.00000	0.10952	0.00000	0.00000	0.00413		
NEW HAMP	0.12170	0.00117	0.23007	0.00000	0.02252	0.66812	0.28718	0.02632	0.04989	0.00000
	0.42157	0.45064	0.23989	0.10666	0.31722	0.02748	0.83654	0.25115	1.18958	0.64369
	0.15107	0.05200	0.24672	0.00871	0.09441	0.00000	3.50725	0.31519	0.00367	0.59287
	0.06108	0.03109	0.32471	0.02402	0.00012	0.32190	0.86925	0.03410	0.08587	0.23807
	0.00835	0.01284	2.12477	0.16931	0.00038	0.21224	0.57124	0.02277		
NEW JERS	0.14475	0.00063	0.09522	0.00000	0.00985	0.63038	1.85298	0.11507	0.17796	0.00000
	0.17671	0.28980	0.12759	0.10593	0.29292	0.03171	0.02447	1.02806	0.08068	0.24473
	0.05870	0.07146	0.15019	0.00851	0.06541	0.00000	0.03384	3.50308	0.00046	1.39797
	0.42162	0.00775	0.58873	0.02706	0.00000	1.37371	0.11703	0.22828	0.01656	0.18940
	0.03234	0.01063	0.25521	0.70737	0.00000	0.73948	0.12962	0.01525		
NEW MEXI	0.00000	0.73442	0.00000	0.06604	0.25223	0.00000	0.00000	0.00000	0.00000	0.00000
	0.00001	0.00000	0.00007	0.00123	0.00000	0.00000	0.00000	0.00000	0.00000	0.00000
	0.00000	0.00000	0.00015	0.00727	0.00074	0.16092	0.00000	0.00000	1.25682	0.00000
	0.00000	0.00080	0.00000	0.03416	0.00018	0.00000	0.00000	0.00000	0.00059	0.00000
	0.05527	0.15649	0.00000	0.00000	0.00014	0.00000	0.00001	0.05651		
NEW YORK	0.08565	0.00241	0.14777	0.00000	0.02740	0.56603	0.41262	0.02643	0.06141	0.00000
	0.36429	0.38417	0.29508	0.15922	0.21631	0.04353	0.02683	0.41345	0.14000	0.71263
	0.15378	0.05079	0.23437	0.02060	0.14322	0.00000	0.11002	0.73661	0.00524	1.40348
	0.12585	0.02508	0.52749	0.05044	0.00148	0.64884	0.14044	0.04919	0.09612	0.15038
	0.02920	0.02549	0.42531	0.28819	0.00017	0.38086	0.43419	0.03139		
N.CAROLI	0.43474	0.00001	0.12821	0.00000	0.00063	0.05829	0.29381	0.37567	1.13029	0.00000
	0.09011	0.18785	0.04689	0.04078	0.34249	0.06904	0.00580	0.44963	0.02962	0.15876
	0.02731	0.12871	0.06245	0.00058	0.02831	0.00000	0.02705	0.13045	0.00000	0.12067
	2.06385	0.00441	0.26189	0.01594	0.00000	0.28116	0.04991	1.48507	0.02114	0.61629
	0.02480	0.00029	0.02293	0.71014	0.00000	0.40097	0.05523	0.00124		
N.DAKOTA	0.00000	0.03678	0.00000	0.02078	0.29347	0.00000	0.00000	0.00000	0.00000	0.00000
	0.00016	0.00005	0.11240	0.02682	0.00000	0.00000	0.00000	0.00000	0.00000	0.00017
	0.07324	0.00000	0.00489	1.53471	0.35866	0.16141	0.00000	0.00000	0.07626	0.00000
	0.00000	2.29315	0.00000	0.26856	0.11938	0.00000	0.00000	0.00000	0.62246	0.00000
	0.03072	0.17819	0.00000	0.00000	0.17011	0.00000	0.00282	0.46805		

Table A-1. Sample State Transport Matrix (continued)

	EMITTERS									
BAVSO4RE	AL	AZ	AR	CA	CO	CT	DE	FL	GA	ID
	IL	IN	IA	KS	KY	LA	ME	MD	MA	MI
RECEPTORS	MN	MS	MO	MT	NB	NV	NH	NJ	NM	NY
	NC	ND	OH	OK	OR	PA	RI	SC	SD	TN
	TX	UT	VT	VA	WA	WV	WI	WY		
OHIO	0.26042	0.00933	0.49222	0.00000	0.09123	0.00102	0.00948	0.03008	0.18566	0.00000
	0.75370	1.38031	0.31262	0.34409	1.15988	0.13413	0.00004	0.05876	0.00006	0.71512
	0.14067	0.11692	0.63431	0.01295	0.19230	0.00026	0.00014	0.00295	0.00691	0.07096
	0.15086	0.02225	2.41358	0.27847	0.00104	0.35559	0.00008	0.06155	0.07185	0.59563
	0.24331	0.03573	0.00027	0.13116	0.00000	1.09260	0.39617	0.02101		
OKLAHOMA	0.00068	0.11620	0.00729	0.00325	0.39656	0.00000	0.00000	0.00210	0.00000	0.00000
	0.02407	0.00498	0.11702	0.77040	0.00043	0.00802	0.00000	0.00000	0.00000	0.00208
	0.00504	0.00506	0.23805	0.09193	0.41109	0.00728	0.00000	0.00000	0.37128	0.00000
	0.00000	0.09343	0.00008	2.42608	0.00091	0.00000	0.00000	0.00000	0.05658	0.00095
	1.12154	0.12095	0.00000	0.00000	0.00063	0.00000	0.00987	0.16826		
OREGON	0.00000	0.00035	0.00000	0.06968	0.00003	0.00000	0.00000	0.00000	0.00000	0.00000
	0.00000	0.00000	0.00000	0.00000	0.00000	0.00000	0.00000	0.00000	0.00000	0.00000
	0.00000	0.00000	0.00000	0.00001	0.00000	0.05422	0.00000	0.00000	0.00002	0.00000
	0.00000	0.00000	0.00000	0.00000	1.70440	0.00000	0.00000	0.00000	0.00000	0.00000
	0.00000	0.00205	0.00000	0.00000	0.93383	0.00000	0.00000	0.00012		
PENNSYLV	0.18858	0.00150	0.18575	0.00000	0.03211	0.15601	0.89006	0.04859	0.14221	0.00000
	0.38566	0.51597	0.21012	0.21878	0.46634	0.06958	0.00317	1.07791	0.01069	0.55817
	0.09800	0.09304	0.28824	0.01099	0.08664	0.00003	0.00726	0.68771	0.00311	0.70777
	0.49131	0.00890	1.43761	0.07867	0.00057	2.31123	0.01519	0.12347	0.05542	0.29653
	0.08039	0.01583	0.05489	0.78378	0.00000	1.52139	0.16393	0.02420		
RHODE IS	0.11903	0.00176	0.11653	0.00000	0.02258	2.64014	0.42922	0.06495	0.11968	0.00000
	0.27488	0.29239	0.20786	0.08585	0.19882	0.02694	0.33431	0.22576	2.38967	0.57228
	0.07060	0.05723	0.15461	0.00733	0.07388	0.00000	1.01300	0.83159	0.00399	0.95160
	0.20186	0.01259	0.33048	0.02215	0.00010	0.61012	4.60821	0.10945	0.04381	0.15592
	0.01017	0.01493	0.91980	0.28151	0.00000	0.32016	0.37376	0.02457		
S.CAROLI	0.76453	0.00000	0.08999	0.00000	0.00002	0.00803	0.17691	0.75116	1.78177	0.00000
	0.05889	0.13016	0.01838	0.01242	0.23032	0.07177	0.00000	0.23394	0.00144	0.09659
	0.00541	0.19154	0.03777	0.00000	0.00327	0.00000	0.00016	0.05427	0.00000	0.04780
	0.73582	0.00118	0.16112	0.00502	0.00000	0.14806	0.00061	2.58250	0.00329	0.45138
	0.00661	0.00000	0.00001	0.31232	0.00000	0.23615	0.02755	0.00000		
S.DAKOTA	0.00000	0.14690	0.00000	0.01415	0.83878	0.00000	0.00000	0.00000	0.00000	0.00000
	0.00491	0.00098	0.15091	0.10219	0.00000	0.00001	0.00000	0.00000	0.00000	0.00095
	0.06261	0.00000	0.02771	1.26141	0.32906	0.15015	0.00000	0.00000	0.26399	0.00000
	0.00000	1.14674	0.00001	0.33489	0.05660	0.00000	0.00000	0.00000	0.97512	0.00000
	0.08916	0.46889	0.00000	0.00000	0.06891	0.00000	0.01198	1.13505		
TENNESSE	1.51814	0.00004	1.79370	0.00000	0.00242	0.00020	0.00512	0.17186	1.12633	0.00000
	0.50083	0.57271	0.11660	0.17554	1.16911	0.54789	0.00000	0.00992	0.00001	0.08006
	0.03438	0.69857	0.48321	0.00239	0.06219	0.00000	0.00002	0.00273	0.00280	0.01555
	0.25037	0.01075	0.22050	0.10780	0.00002	0.04712	0.00001	0.16718	0.02668	2.48248
	0.30384	0.00040	0.00005	0.08880	0.00000	0.15736	0.14069	0.00055		

Table A-1. Sample State Transport Matrix (continued)

	EMITTERS									
BAVSO4RE	AL	AZ	AR	CA	CO	CT	DE	FL	GA	ID
	IL	IN	IA	KS	KY	LA	ME	MD	MA	MI
RECEPTORS	MN	MS	MO	MT	NB	NV	NH	NJ	NM	NY
	NC	ND	OH	OK	OR	PA	RI	SC	SD	TN
	TX	UT	VT	VA	WA	WV	WI	WY		
TEXAS	0.00298	0.17735	0.02886	0.01169	0.16879	0.00000	0.00000	0.00395	0.00002	0.00000
	0.00481	0.00021	0.01604	0.14558	0.00024	0.02185	0.00000	0.00000	0.00000	0.00012
	0.00037	0.01320	0.05092	0.02423	0.03898	0.04082	0.00000	0.00000	0.32116	0.00000
	0.00000	0.01172	0.00000	0.35998	0.00010	0.00000	0.00000	0.00001	0.01343	0.00268
	0.58709	0.07080	0.00000	0.00000	0.00020	0.00000	0.00196	0.07515		
UTAH	0.00000	1.21349	0.00000	0.50647	0.09029	0.00000	0.00000	0.00000	0.00000	0.00000
	0.00000	0.00000	0.00000	0.00000	0.00000	0.00000	0.00000	0.00000	0.00000	0.00000
	0.00000	0.00000	0.00000	0.01177	0.00000	2.02700	0.00000	0.00000	0.50368	0.00000
	0.00000	0.00004	0.00000	0.00002	0.08364	0.00000	0.00000	0.00000	0.00216	0.00000
	0.00187	2.08759	0.00000	0.00000	0.01722	0.00000	0.00000	0.35135		
VERMONT	0.06713	0.00106	0.15630	0.00000	0.02429	0.65708	0.19489	0.01567	0.03328	0.00000
	0.40453	0.37621	0.25792	0.12005	0.22972	0.03076	0.33660	0.27544	0.56443	0.57177
	0.18954	0.03832	0.24850	0.01303	0.11504	0.00000	1.14409	0.27244	0.00684	0.54144
	0.05929	0.04590	0.28449	0.02400	0.00026	0.29581	0.49841	0.02230	0.09343	0.15378
	0.01252	0.01368	3.52644	0.16036	0.00086	0.18303	0.57401	0.02241		
VIRGINIA	0.34823	0.00006	0.26218	0.00000	0.00466	0.08234	0.48203	0.19491	0.75248	0.00000
	0.16257	0.31085	0.06727	0.06975	0.57902	0.08463	0.00648	1.10749	0.02036	0.24004
	0.06255	0.16492	0.13105	0.00206	0.03694	0.00000	0.02370	0.20215	0.00003	0.20237
	1.93382	0.00526	0.57279	0.05295	0.00000	0.67148	0.03416	0.76544	0.02610	0.85700
	0.08609	0.00133	0.05549	2.16227	0.00000	1.31629	0.07721	0.00390		
WASHINGT	0.00000	0.00004	0.00000	0.02539	0.00001	0.00000	0.00000	0.00000	0.00000	0.00000
	0.00000	0.00000	0.00000	0.00000	0.00000	0.00000	0.00000	0.00000	0.00000	0.00000
	0.00000	0.00000	0.00000	0.00015	0.00000	0.00243	0.00000	0.00000	0.00001	0.00000
	0.00000	0.00004	0.00000	0.00000	1.54518	0.00000	0.00000	0.00000	0.00000	0.00000
	0.00000	0.00068	0.00000	0.00000	2.15578	0.00000	0.00000	0.00016		
W.VIRGIN	0.49710	0.00113	0.47403	0.00000	0.01680	0.00959	0.14009	0.08750	0.48096	0.00000
	0.28096	0.57227	0.07898	0.11130	1.14269	0.16674	0.00048	0.35251	0.00106	0.35887
	0.07484	0.26331	0.28678	0.00169	0.05431	0.00000	0.00234	0.05491	0.00050	0.13126
	0.83798	0.00858	1.62091	0.11507	0.00000	0.80398	0.00185	0.26128	0.02746	0.95960
	0.18684	0.00543	0.00408	0.69972	0.00000	3.32227	0.11159	0.00480		
WISCONSI	0.00213	0.01083	0.03080	0.00004	0.11918	0.00000	0.00000	0.00028	0.00003	0.00000
	0.35769	0.12782	0.77076	0.48777	0.02210	0.00781	0.00000	0.00000	0.00000	0.25837
	1.44454	0.01092	0.35045	0.26022	0.48590	0.01558	0.00000	0.00000	0.02111	0.00094
	0.00000	0.38028	0.00773	0.28563	0.02400	0.00137	0.00000	0.00000	0.79150	0.00948
	0.16829	0.08966	0.00000	0.00000	0.02142	0.00030	1.33400	0.17184		
WYOMING	0.00000	0.62581	0.00000	0.16739	0.63479	0.00000	0.00000	0.00000	0.00000	0.00000
	0.00000	0.00000	0.00004	0.00082	0.00000	0.00000	0.00000	0.00000	0.00000	0.00000
	0.00001	0.00000	0.00019	0.52965	0.00059	0.57896	0.00000	0.00000	0.69586	0.00000
	0.00000	0.01671	0.00000	0.00235	0.13074	0.00000	0.00000	0.00000	0.03759	0.00000
	0.00629	1.66361	0.00000	0.00000	0.06910	0.00000	0.00000	2.35385		

APPENDIX B. BROOKHAVEN NATIONAL LABORATORY MODEL

The AIRSOX model has been designed to efficiently calculate the transport, diffusion, and transformation of sulfur oxides emitted from a large number of area and point sources. Among other variables, the mdoel computes the gridded, population-weighted concentrations of SO_2 and SO_4 at the breathing level (2 m) occurring in the contiguous United States, using specified emission inventories for utility, industrial, and area sources.

The semi-empirical equation of atmospheric dispersion of pollutants on which the model is based is

$$\frac{\partial C(x,y,z,t)}{\partial t} + \nabla \cdot \vec{V}C(x,y,z,t) = K_H(x,y)\, \nabla_H^2 C(x,y,z,t)$$
$$+ \nabla_H K_H \cdot \nabla_H C(x,y,z,t) + \frac{\partial}{\partial z}\left[K(z)\, \frac{C(x,y,z,t)}{\partial z}\right] + S^+(x,y,z,t) \qquad (1)$$
$$+ S^-(x,y,z,t)$$

where

C is the mean concentration of pollutants
$\vec{V} = (U, V, W)$ is the mean wind vector
$K_H = K_H(x, y, z, t)$ is the horizontal eddy diffusivity
$K = K(x, y, z, t)$ is the vertical eddy diffusivity
∇_H^2 is the horizontal Laplacian operator
∇_H is the horizontal gradient operator
S^+ is the source term
S^- is the sink term
x, y are horizontal coordinates, z is the vertical coordinate t is the absolute time

The model approximates the long-term average plume from each pollutant source by a series of plume segments. In equation (1), the initial source strength for a plume segment for SO_2 is $Q_{ij1} = (1-\beta)\, Q_{ij}\, \delta(x-x_{io})\, \delta(y-y_{io})\, \delta(z-h_{ij})\, \delta(t-t_{ij})$, and the intial source strength for the SO_4 plume segment is $Q_{ij2} = 1.5\, Q_{ij}\, \beta\delta(x-x_{io})\, \delta(y-y_{io})\, \delta(z-h_{ij})\, \delta(t-t_{ij})$, where β is the fraction of SO_2 converted to SO_4 in the stack (primary sulfate), Q_{ij} is the source mass emitted over the release time interval, (x_{io}, y_{io}) is the horizontal location of source i, h_{ij} is the height of release of j^{th} plume segment from source i, t_{ij} is the time of release of j^{th} plume segment from source i, δ is the Dirac delta function, and the factor 1.5 is the ratio of the molecular weight of SO_4 to SO_2.

The horizontal and vertical diffusion are assumed to be independent, so that the dispersion can be expressed by the product of two independent functions. The concentration at each grid cell on an east-west, north-south projection map is computed from summing all the contributions of the plume segments to the grid cell. The approximate solution of equation (1) can be written as

$$C_k(x,y,z,t) \doteq \sum_{j=1}^{n} \sum_{i=1}^{m} q_{ijk} \, (C_H)_{ijk} \, (C_z)_{ijk} \qquad (2)$$

where

C is the pollutant concentration, the subscript k = 1 and 2 represents sulfur dioxide and sulfate, respectively
$(C_H)_{ijk} = C_{kH}\,(x - x_{ij},\ y - y_{ij},\ t,\ t - t_{ij})$
$(C_z)_{ijk} = C_{zk}\,(z,t,t - t_{ij})$
$q_{ij1} = Q_{ij}\,(1 - \beta)$ and $q_{ij2} = 1.5\,Q_{ij}\beta$ are the mass of SO_2 and SO_4, respectively, contained initially in each plume segment

The horizontal distribution, $(C_H)_{ijk}$, of pollutants, SO_2 and SO_4, is assumed to be a Gaussian function as follows:

$$(C_H)_{ijk} = f(x'_{ij},\ t'_{ij}) \left[\frac{1}{2\pi\sigma_{y'_{ij}}} \exp\left(-y'^{2}_{ij}/2\sigma^{2}_{y'_{ij}}\right)\right]$$

when $|\Delta x| \geq |\Delta y|$

$$= f(y'_{ij},\ t'_{ij}) \left[\frac{1}{2\pi\sigma_{x'_{ij}}} \exp\left(-x'^{2}_{ij}/2\sigma^{2}_{x'_{ij}}\right)\right] \qquad (3)$$

when $|\Delta y| > |\Delta x|$

where $f(x'_{ij},\ t'_{ij})$ and $f(y'_{ij},\ t'_{ij})$ are the along-wind factors and

$$f(x'_{ij},\ t'_{ij}) = \frac{1}{\ell_{ij}} \left\{u\left[(x_{ij}-x_{i0}) + \frac{\ell_{ij}}{2}\right] - u\left[(x_{ij}-x_{i0}) - \frac{\ell_{ij}}{2}\right]\right\}$$

$$f(y'_{ij},\ t'_{ij}) = \frac{1}{\ell_{ij}} \left\{u\left[(y_{ij}-y_{i0}) + \frac{\ell_{ij}}{2}\right] - u\left[(y_{ij}-y_{i0}) - \frac{\ell_{ij}}{2}\right]\right\}$$

where

u is a step function
$x'_{ij} = x - x_{ij}$, $y'_{ij} = y - y_{ij}$, and $t'_{ij} = t - t_{ij}$
v_{ij} is the initial velocity of the j^{th} plume segment from source i
$\ell_{ij} = \Delta t \cdot v_{ij}$ is the plume segment length
Δx is the projected segment length, ℓ_{ij}, on x axis
Δy is the projected segment length, ℓ_{ij}, on y axis
$\sigma_{y'_{ij}}$ and $\sigma_{x'_{ij}}$ are the crosswind standard deviations of the plume in the east-west and north-south direction, respectively (in meters)
Δt is the time interval over which a plume segment is released

The model uses the approximation for $\sigma y'_{ij}$ and $\sigma x'_{ij}$ of $\sigma y'_{ij} = \sigma x'_{ij} = 0.5\ (t-t_{ij})$, where $t-t_{ij}$ is the travel time (in seconds) of the plume segment, j, from the i^{th} source (Heffter, 1965). Distribution along the trajectory is dependent on the segment length, such that the amount of pollutant concentration decreases as the segment length increases due to higher initial along-wind velocities (ventilation). Diffusion in the along-wind direction is assumed to be unimportant.

The vertical distribution functions of pollutants are computed from integrating the finite difference form of the following equations under the initial conditions mentioned above:

$$\frac{\partial C_{z1}}{\partial t} = \frac{\partial}{\partial z}\left(K \frac{\partial C_{z1}}{\partial z}\right) - AC_{z1} - \lambda_{w1} C_{z1} \qquad (4)$$

$$\frac{\partial C_{z2}}{\partial t} = \frac{\partial}{\partial z}\left(K \frac{\partial C_{z2}}{\partial z}\right) - \lambda_{w2} C_{z2} + 1.5AC_{z1} \qquad (5)$$

where

$C_{z\ell}$ for $\ell = 1$ and 2 are the vertical distribution functions of the concentrations for SO_2 and SO_4, respectively
K is the eddy diffusivity, m^2/sec
z is the vertical coordinate, m
A is the chemical conversion rate of SO_2 to SO_4, per sec
$\lambda_{w\ell}$ are the wet deposition removal rates, $\ell = 1$ and 2 for SO_2 and SO_4, respectively, per sec

In general, $\lambda_{w\ell}$, K, A, Q and V_d are functions of space and time. Although in many past calculations they have been typically set as constants, the program is designed to accept them as varying in space and time.

The boundary conditions are

$$\lim_{z \to z_0} K \frac{\partial C_{z\ell}}{\partial z} = V_{d_\ell} C_{z_\ell} \qquad (6)$$

where $V_{d\ell}$ is the dry deposition velocity for SO_2 ($\ell = 1$) and SO_4 ($\ell = 2$) respectively, and

$$K \frac{\partial C_{z\ell}}{\partial z} = 0 \quad \text{at } z = H \qquad (7)$$

where H is the mixing height of the planetary boundary layer.

B.1 METHODS OF ANALYSIS

B.1.1. Numerical Methods

Vertical diffusion and transformation are calculated using a semi-implicit, variable grid, Crank-Nicolson, central finite-difference scheme similar to Shir and Shieh (1974), except that derivative boundary conditions, dry deposition, wet deposition, and chemical conversion are treated by the present schemes. The finite-difference approximation to the vertical concentration equations (4) and (5) are

$$\frac{C_{k,1}^{j+1} - C_{k,1}^{j}}{\Delta t} = \frac{\theta\left[\frac{K_{k+1/2}\left(C_{k+1,1}^{j+1} - C_{k,1}^{j+1}\right)}{\Delta z_{k+1/2}} - \frac{K_{k-1/2}\left(C_{k,1}^{j+1} - C_{k-1,1}^{j+1}\right)}{\Delta z_{k-1/2}}\right]}{z_{k+1/2} - z_{k-1/2}}$$

$$+ (1-\theta)\left[\frac{K_{k+1/2}\left(C_{k+1,1}^{j} - C_{k,1}^{j}\right)}{\Delta z_{k+1/2}} - \frac{K_{k-1/2}\left(C_{k,1}^{j} - C_{k-1,1}^{j}\right)}{\Delta z_{k-1/2}}\right] \qquad (8)$$

$$- AC_{k,1}^{j} - \lambda_{w1} C_{k,1}^{j}(1-\theta) - \lambda_{w1}\theta C_{k,1}^{j+1}$$

and,

$$\frac{C_{k,2}^{j+1} - C_{k,2}^{j}}{\Delta t} = \frac{\theta\left[\frac{K_{k+1/2}\left(C_{k+1,2}^{j+1} - C_{k,2}^{j+1}\right)}{\Delta z_{k+1/2}} - \frac{K_{k-1/2}\left(C_{k,2}^{j+1} - C_{k-1,2}^{j+1}\right)}{\Delta z_{k-1/2}}\right]}{z_{k+1/2} - z_{k-1/2}}$$

$$+ (1-\theta)\left[\frac{K_{k+1/2}\left(C_{k+1,2}^{j} - C_{k,2}^{j+1}\right)}{\Delta z_{k+1/2}} - \frac{K_{k-1/2}\left(C_{k,2}^{j} - C_{k-1,2}^{j}\right)}{\Delta z_{k-1/2}}\right] \qquad (9)$$

$$+ 1.5AC_{k,2}^{j} - \lambda_{w2} C_{k,2}^{j}(1-\theta) - \lambda_{w2}\theta C_{k,2}^{j+1}$$

where

θ is a parametric constant (as with Shir and Shieh (1974), we typically use $\theta = 0.98$
j is the time step index
k is the vertical level

$$\Delta z_{k+\frac{1}{2}} = \frac{z_{k+1\frac{1}{2}} - z_{k-\frac{1}{2}}}{2}, \text{ centered at } z = k+\tfrac{1}{2} \tag{10}$$

and,

$$\Delta z_{k-\frac{1}{2}} = \frac{z_{k+\frac{1}{2}} - z_{k-1\frac{1}{2}}}{2}, \text{ centered at } z = k-\tfrac{1}{2} \tag{11}$$

Other definitions of $z_{k+\frac{1}{2}}$ and $z_{k-\frac{1}{2}}$ are possible and should be investigated for accuracy. The boundary conditions are

$$C^j_{o,\ell} = \left(1 - \frac{V_{d,\ell}}{K_o} \Delta z_1\right) C^j_{1,\ell} \tag{12}$$

where $C_{o,\ell}$ is the concentrations at $z = z_o$ and K_o is the eddy diffusivity at $z = z_o$, z_o is the surface roughness length, $\ell = 1$ and 2 are for SO_2 and SO_4 respectively, z_1 is the lowest vertical grid size, and

$$K_T \left(C^j_{k+1,\ell} - C^j_{k,\ell}\right) = 0 \tag{13}$$

where K_T is the eddy diffusivity at $z = H$, and H is the mixing height.

The efficient solution of the difference equation for many plumes require the fast inversion of a tridiagonal matrix. This is accomplished by the triangularization and back substitution sparse matrix technique of Gerald (1970). The difference equation for any level k can be represented symbolically by

$$b_k C^{j+1}_{k-1} + d_k C^{j+1}_k + a_k C^{j+1}_{k+1} = \alpha^j_k \tag{14}$$

where b_k represents coefficients below the diagonal, d_k are on diagonal elements, a_k are for elements above the diagonal, and α_k are the constant vector. The difference equation can be restated using the matrix notation

$$EF = G \tag{15}$$

where E is the tridiagonal matrix with known coefficient; F is a column vector of unknowns, C^j_k; and G is a vector of knowns involving C^j_k. The solution can be written as

$$F = E^{-1} G \tag{16}$$

or performing the triangularization of equation (14) to obtain

$$d_k^{j+1} = d_k^{j+1} - \frac{b_k^{j+1}}{d_{k-1}^{j+1}} a_{k-1}^{j+1}, \quad k = 2, 3, \ldots, n \tag{17}$$

$$\alpha_k^j = \alpha_k^j - \frac{b_k^{j+1}}{d_{k-1}^{j+1}} \alpha_{k-1}^j, \quad k = 2, 3, \ldots, n \tag{18}$$

and then back substitution to get

$$C_i^{j+1} = \frac{\alpha_i^j - a_i^{j+1} C_{i+1}^{j+1}}{d_i^{j+1}} \tag{19}$$

where i and k are vertical levels, j is the time step index, and n is the total number of levels.

B.1.2 Grid Specifications

The grid system used in the AIRSOX model is based on a polar stereographic projection, true at 60° N latitude and aligned with the 80° W meridian (Jenne, 1970). The x, y, z axes are oriented nominally east-west, north-south, and vertically, respectively. The horizontal grids, which vary with latitude, are approximately 32 km (38.1 km at 60°N latitude); this grid is the same as National Meteorological Center grid with one-tenth of the grid size. AIRSOX is a multi-layered model that can have any number of levels but which typicaly uses 12 levels above the ground, i.e., 2, 20, 100, 200, 300, 400, 500, 600, 700, 800, 900, and 1000 m (see Figure B-1). The size of the vertical grid at a specified level is a function of the vertical levels above and below the level, i.e., $\Delta z_k = f(z_{k-1}, z_{k+1})$. The lower three grid cells have varying vertical spacing; the vertical grid sizes above and centered at the 200-m level have a fixed spacing. The uppermost grid cell is limited by the mixing height (in the example shown, 1000 m).

B.1.3 Source Locations

For the purpose of matrix generation, specific emission source locations within each Air Quality Control Region are specified for each category of sources. These are based on potential inventories of actual sources. Figure B-2 shows the inventory source locations used in generating utility matrices. For the 28 Air Quality Control Regions where no actual sources were included in the inventory, an additional hypothetical source was located at the centroid of the Air Quality Control Regions (not shown in the figure). Figure B-3 shows the inventory sources used in generating industrial source matrices. Again, additional hypothetical sources were added for the 29 Air Quality Control Regions that had no source.

For area sources, a hypothetical source was located in the centroid of the country with the highest population in each Air Quality Control Region.

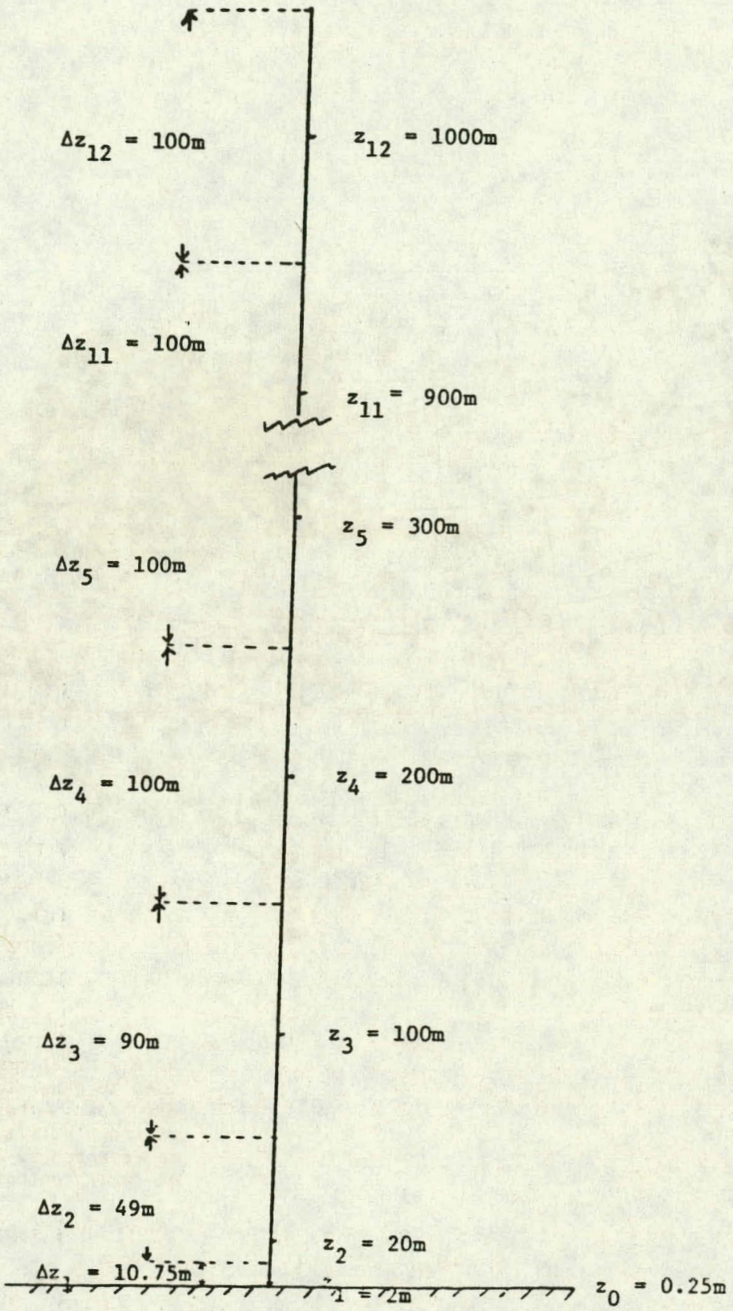

FIGURE B-1. VERTICAL LEVELS AND GRID SIZE IN THE AIRSOX MODEL

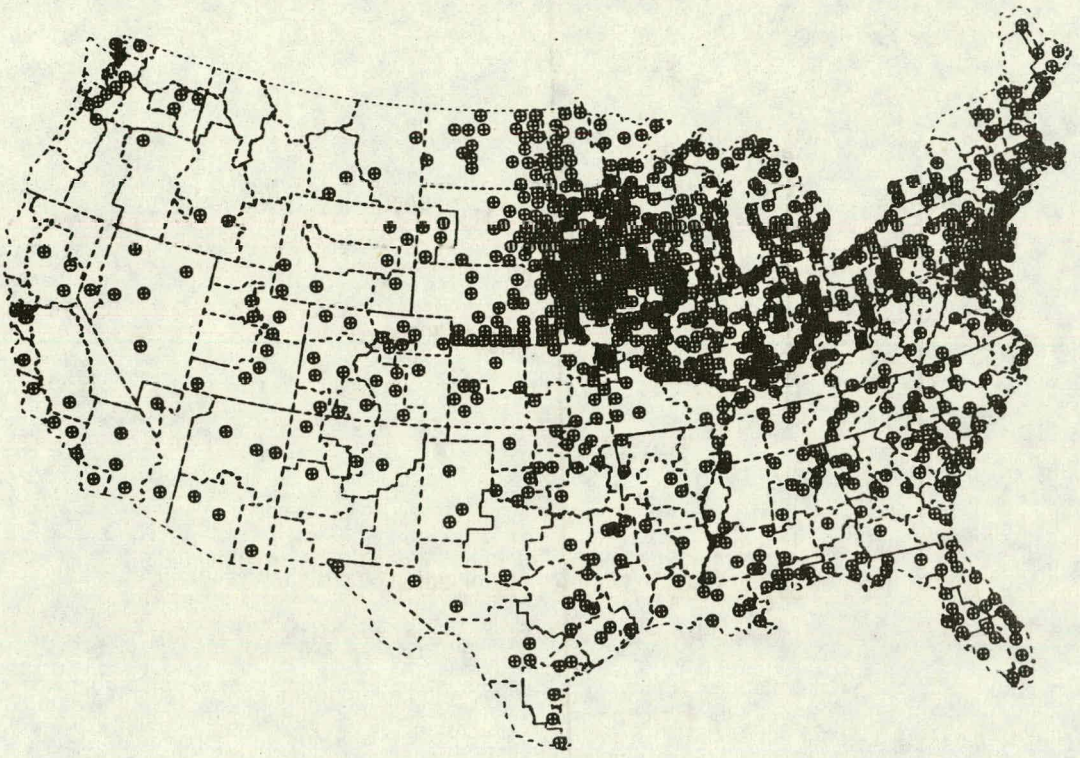

Note: Locations of utility sources used to generate the BNL matrices are shown. Those AQCRs which had no known utility sources were represented by a single source at their centroids (not shown).

FIGURE B-2. UTILITY SOURCE LOCATIONS - BNL MODEL

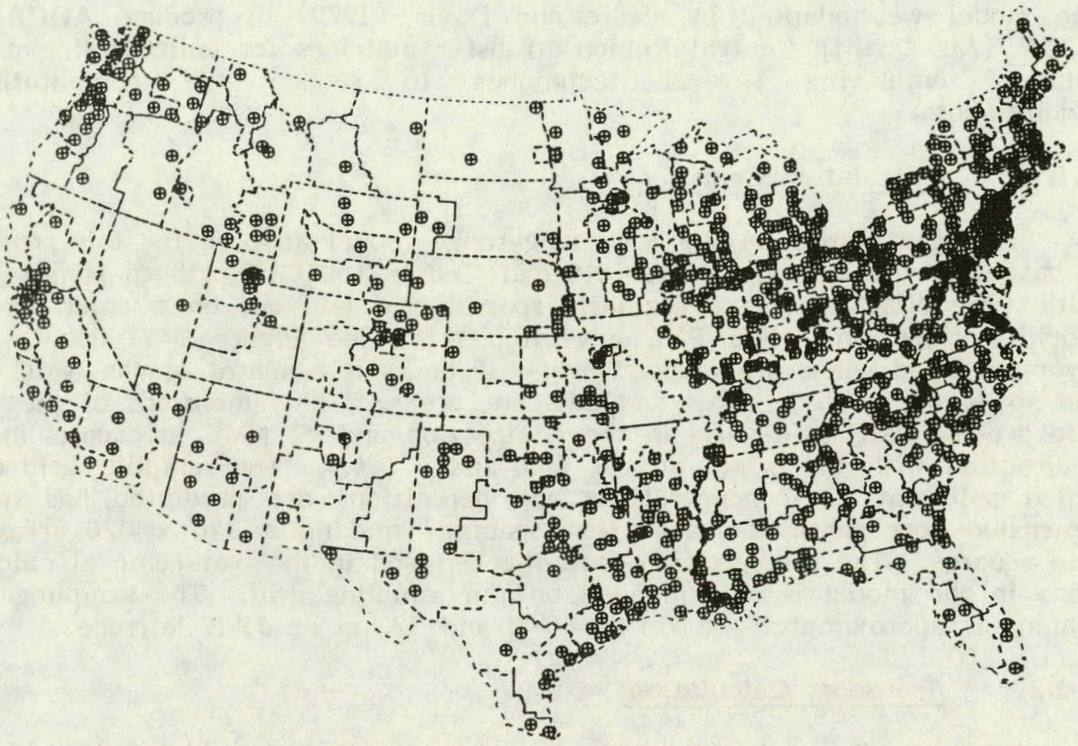

Note: Locations of utility sources used to generate the BNL matrices are shown. Those AQCRs which had no known utility sources were represented by a single source at their centroids (not shown).

FIGURE B-3. INDUSTRIAL SOURCE LOCATIONS - BNL MODEL

APPENDIX C. PACIFIC NORTHWEST NATIONAL LABORATORY LONG-RANGE TRANSPORT MODEL

C.1 MODEL DESCRIPTION

The Pacific Northwest National Laboratory (PNL) long-range transport, transformation, and removal model was developed by Wendell et al. (1976). The model was adapted by Eadie and Davis (1979) to produce AQCR-to-AQCR (Air Quality Control Region) transfer matrices for emitted fine particulates, employing several techniques to reduce the computational requirements.

C.1.1 Calculation Grids

The grid system in the PNL long-range model adopted for this program is based on the National Meteorological Center (NMC) Northern Hemisphere grid. The NMC grid is a regularly spaced grid laid out on a polar stereographic projection. The PNL advection grid (see Figure 5-7) upon which layer-averaged winds are mapped every 12 hours is a subset of the NMC grid and spans the United States and adjacent areas. The dimensions of the PNL grid are 14 NMC grid units in the x direction and 12 NMC grid units in the y direction with the origin at x = 13.0 and y = 4.0. The sampling grid upon which pollutant air concentrations and depositions are predicted has linear dimensions one-tenth the advection spacing, making a 140 x 120 array of grid squares. The precipitation data that is used in the wet-removal calculations in the model is also mapped on the sampling grid. The sampling grid spacing is approximately 38 km at 60°N and 32 km at 35°N latitude.

C.1.2 Transport Calculations

Trajectories are simulated for plume elements released hourly from an emission source location. The unit emission rate at the source position determines the initial respirable particulate mass of each plume element. Subsequent horizontal transport of these plume elements is in hourly steps using the layer-averaged winds at each advection-grid intersection point. An objective analysis scheme developed for mesoscale purposes (Wendell, 1972) interpolates wind data in space and time to provide the hourly winds at each particle position. The current transport scheme has no vertical component. It is assumed that the concentrations of respirable particulates are averaged over a time period in which the effects of vertical atmospheric processes can be adequately expressed by the parameterized vertical component of diffusion and by the mixing depth constraints. It is also assumed that the effects of vertical transport on horizontal transport can be neglected over the long assessment time period.

C.1.3 Diffusion and Diffusion Constraints

The following assumptions are made regarding atmospheric diffusion:

- Horizontal diffusion is a function of synoptic-scale wind variation only. Tennekes (1974), Bolin and Persson (1975), and Prahm and

Christensen (1977) support this assumption. All state that either horizontal turbulent diffusion around the plume center line is relatively unimportant or that it is less important than plume meandering.

- The vertical-turbulent diffusion parameterization is a function of stability in a specified diurnal cycle for all plume elements within the daytime mixed layer or the nocturnal stable layer.

- The depth of the daytime mixed layer is represented by a diurnal cycle in which a daytime layer increases from a minimum depth at sunrise to a maximum depth in the afternoon. A nocturnal layer builds to a lower depth.

- Depth of the boundary layer (mixed layer in daytime or nocturnal layer) for each hour determines which of two vertical dispersion regimes -- mixed layer or above mixed layer -- will be applied to a given plume element. Those elements released within the depth of the layer expand according to the stability of the hour. Those released above the current depth of the layer expand as if the atmosphere were extremely stable. An exception to this method occurs when releases have expanded to the maximum depth of the mixed layer during the previous day; in this case, their expansion continues according to a fixed function of travel time independent of stability or layer depth.

- Depth of the mixed layer provides a vertical constraint for releases at heights within this layer. The depth of the nocturnal boundary layer does not serve as an analogous constraint. Carson (1973) supports this assumption by depicting the mixed-layer depth as a function that increases during the daytime, then loses its definition. This picture is in relative agreement with modeling results by Venkatram and Viskanta (1976) and with experiment results by Kaimal et al. (1976) who find that about 1 hour before sunset, the convective layer disintegrates rather abruptly, although remnants of the capping inversion persist through the development of the nocturnal boundary layer.

- At the present stage of model development, terrain effects are neglected.

Diffusion equations are best explained by relating them to final concentration and deposition calculations where the average ground-level air concentrations over grid square (i,j) are given by summing time-integrated concentrations (integrated over the time interval (Δt)) and dividing by total assessment time (T). Thus,

$$\chi^{ij} = T^{-1} \sum_{m(t)} \Delta\chi^{ij}_{m}(\Delta t;t) \qquad (1)$$

where $\Delta X\,ij_m$ is the time-integrated, ground-level air concentration over (i,j) for a pollutant carried by each plume element (m) that is located over (i,j) at time (t).

At the end of each sampling interval (Δt), $\Delta X^{ij}{}_m$ is computed for the pollutant of each plume element that is on the grid by

$$\Delta X^{ij}{}_m(\Delta t;t) = \frac{Q_m\,(t)\Delta t}{A^{ij}\,Z_m} \tag{2}$$

where

Q_m (t) is the mass carried by m at t
A^{ij} is the area of (i,j)
Z_m is the vertical distribution factor for m calculated by assuming Gaussian vertical distribution modified by reflection from the ground and from the top of the mixed layer.

If the vertical constraint height is L and the effective stack height is H, $Z_m{}^{-1}$ is

$$Z_m{}^{-1} = \frac{\sqrt{2/\pi}}{(\sigma_z)m}\left\{e^{\frac{-1}{2}\left(\frac{H}{\sigma_z}\right)^2} + \sum_{k=1}^{\infty}\left[e^{\frac{-1}{2}\left(\frac{2kL\ -\ H}{\sigma_z}\right)^2} + e^{\frac{-1}{2}\left(\frac{2kL\ +\ H}{\sigma_z}\right)^2}\right]\right\} \tag{3}$$

where $(\sigma_z)_m$ is the vertical standard deviation for plume element m.

If σ_z is small compared to L, the term represented by the entire summation over k may be neglected. If σ_z is approximately equal to or larger than L, the vertical distribution is approaching uniformity. Therefore, instead of calculating Z^{-1} by a wasteful summation, Z is set equal to L:

$$Z = L \tag{4}$$

L is the height of a reflection effective for transport at height H.

In the model, the depth in meters of the daytime mixed layer (L_d) is given by

$$L_d\ (t_h) = 200 + 1300\ \sin\left[0.05\pi(t_h-6)\right] \tag{5}$$

when

$$6 \leq t_h \leq 18$$

and the depth of the nocturnal boundary layer (B_n) is given by

$$B_n\ (t_h) = 100 + 300 \sin \left[0.05\pi\ (t_h - 18)\right] \qquad (6)$$

when

$$18 < t_h < 30$$

where t_h is the hour of the day unless t_h is greater than 24, in which case t_h is specified as the hour of the day plus 24 to provide a continuous function.

These formulas were drawn up to approximate graphic results given by Carson (1973). They are advanced only for purposes of the calculations of the PNL model because the typical daytime mixed layer increases from 200 m at sunrise to 1500 m by late afternoon, and a nocturnal boundary layer develops to about 400 m.

All plume elements not spread beyond the mixed-layer depth (L) expand vertically as a function of travel distance. The increase of σ_z is calculated using

$$\sigma_z(x + \Delta x) = \sigma_z(x) + \Delta x \left.\frac{\partial \sigma_z}{\partial x}\right|_{S}^{x + 1/2\Delta x} \qquad (7)$$

where S indicates that the derivative differs according to the stability that is specified hourly in the model.

The formulas thus differentiated are those of Eimutis and Konicek (1972). If H is greater than the mixed-layer depth (L_d or B_n), whichever applies at the time, the plume elments expand at the rate of 60 percent of that for Pasquill Stability 6 (Powell et al., 1979a). This expansion rate results because mixing by mechanical turbulence is not effective above the mixed layer; therefore, the rate of vertical expansion is minimal.

All plume elements that have expanded vertically to fill the mixed layer at its maximum depth are released from the mixed-layer constraint at sunset when the boundary layer structure collapses. These puffs expand at a function of time according to:

$$\sigma_z(t+\Delta t; L_{dm}) = \sigma_z(t; L_{dm}) + \Delta t\ \sqrt{K_z/2t} \qquad (8)$$

where K_z is the vertical diffusivity.

Heffter amd Ferber (1975) recommend a value of 5 m^2/s for K_z. The plume elements not subject to the mixed-layer constraint after sunset include almost all those emitted during the previous 24 hours. Because these plumes

all have the same vertical distribution at sunset, taken to be 1800 hours, they are all assigned a common value of t, 12 hours. If L_{dm} is the maximum depth of the mixed layer at $t_h = 18$ for each of these plume elements, then

$$\sigma_z(12 \text{ hr}; L_{dm}) = \sigma_z \Big|_{t_h = 18} = \frac{L_{dm}}{\sqrt{\pi/2}} \tag{9}$$

A Gaussian plume calculation with $\sigma_z = L_{dm}\sqrt{2/\pi}$ yields the same ground concentration as calculations for evently distributed plumes over a layer of depth L_{dm}. Further plume expansion in time interval (Δt) is given by

$$\sigma_z(12 + \Delta t) = \frac{L_{dm}}{\sqrt{\pi/2}} + \Delta t\sqrt{\frac{K_z}{2\,(12 + \Delta t)}} \tag{10}$$

The daytime plume expansion is illustrated in Figure C-1. The plume at the bottom left is a low-level release, which expands at a rate corresponding to the stability of the hour to a height not greater than that of the mixed-layer depth. Farther to the right, an elevated plume, which expands very slowly so that it does not contribute to surface concentrations, is released above the mixed layer. Above both plumes, the depth of the boundary layer is shown by L_d. At a later hour when L_d rises above the stack, the second plume will also expand according to the stability of the hour. Above L_{dm}, σ_z of a plume release on a previous day is shown. This plume expands at the rate given by Equation (8), an expansion rate that reflects the effect of convection averaged over a 24-hour period at the higher levels.

The hourly stability array used for the diurnal cycle generally allows for stable conditions at night, unstable conditions in the afternoon, and neutral conditions in the transition hours. The portion of time allotted to each classifiction corresponds to an average climatology of stability over the United States based on the work of Doty et al. (1976). During unstable hours in the afternoon, all plume elements quickly become evenly distributed throughout the mixed layer.

C.1.4 Removal Mechanisms

The removal of respirable particulates from the atmosphere by dry and wet deposition are calculated by a set of ordinary linear differential equations that are solved for each plume element. These equations assume that

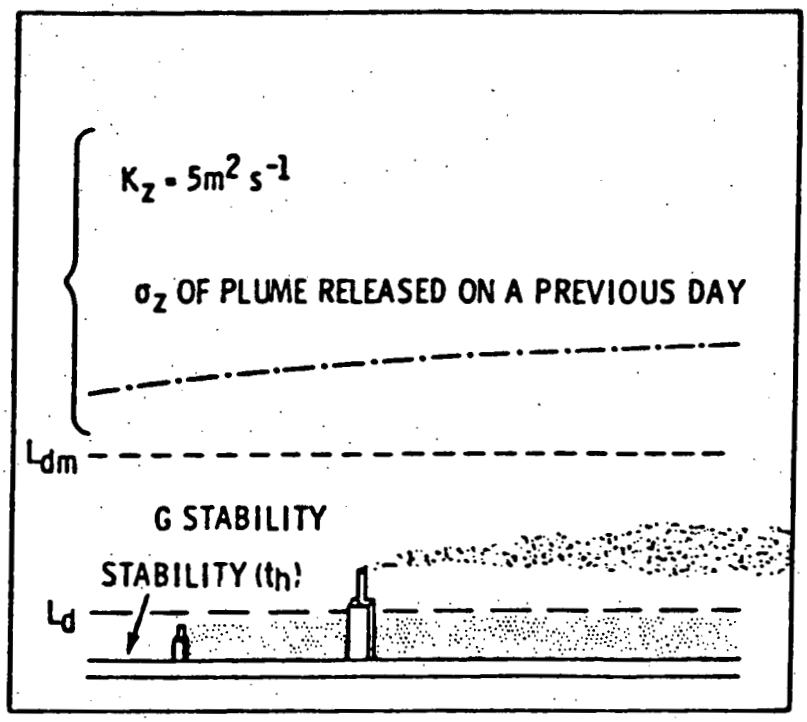

FIGURE C-1. DAYTIME PLUME EXPANSION

- Dry removal rate is obtained by multiplying the deposition velocity by the vertical distribution factor Z^{-1}.
- Wet removal rate is a function of the local precipitation rate.

The following definitions are used in the equations:

- Q(t) = Mass of respirable particulates in a plume element at time t (μg)
- D(t) = Mass deposited from a plume element up to time t (μg)
- d = Coefficient of dry deposition (hr^{-1})
- w = Coefficient of wet deposition (hr^{-1})

Given the above definitions,

$$\frac{dQ}{dt} = -(d + w)Q \tag{11}$$

$$\frac{dD}{dt} = (d + w)Q \tag{12}$$

Solutions of these equations are expressed by the change of mass for each plume element (m) over the advection time (Δt) and by the mass to be deposited over grid unit (i,j) from m over the same time interval, usually 1 hour.

The calculated deposition is expressed in terms of mass per meter^2 per month. Thus, the monthly deposition (F) applying to i,j may be written as

$$F^{ij} = Y^{-1} T^{-1} \sum_{m(t)} \Delta F^{ij}{}_m (\Delta t;t) = Y^{-1} T^{-1} \sum_{m(t)} \frac{D^{ij}{}_m(\Delta t;t)}{A^{ij}} \tag{13}$$

where Y is 1 month in units of T, and $\Delta F^{ij}{}_m$ is the deposition of pollutant, mass per unit area, over time interval (Δt) over grid squre i,j because of plume element m at time (t).

$D^{ij}{}_m$ ($\Delta t;t$) is a more complete notation for the deposited mass. The $D^{ij}{}_m$ are divided into dry and wet deposition:

$$D^{ij}{}_m = Q_m D^{ij}{}_m (\Delta t;t) \tag{14}$$

where $D^{ij}_m(\Delta t;t)$ is given by

$$D^{ij}_m(\Delta t;t) = 1 - EXP\left\{\left[-\frac{\overline{V_d}}{Z_m(t)} - \lambda P^{ij}(t)^n\right]\Delta t\right\} \quad (15)$$

where

$\overline{V_d}$ is the deposition velocity
$Z_m(t)$ is the vertical distribution factor for m
$p^{ij}(t)$ is the precipitation rate at t over grid i,j, and λ and n are precipitation scavenging parameters

The model currently assumes that $\overline{V_d}$, λ, and n are constants.

Relating Equation (12) to Equation (15) yields

$$d = \overline{V_d}/Z_m(t) \quad (16)$$

$$w = \lambda P^{ij}(t)^n \quad (17)$$

A constant value for each of these parameters was selected even though they are all known to vary in space and time with changing physical conditions.

The parameter values chosen for the model test case are

$$\overline{V_d} = 0.23 \text{ cm s}^{-1} \quad (18)$$

$$W = 0.38\ P^{ij}(t)^{.73}\ \text{hr}^{-1} \quad (19)$$

where $P^{ij}(t)$ is in mm per hour.

The dry- and wet-removal parameters were selected to approximate the removal from the atmosphere of emitted particulates in the respirable size ranges of approximately 0.1 to 3.0 μm dia. The dry deposition velocity of 0.23 cm per sec is somewhat larger than the 0.1 cm per sec often selected as a mean value for sulfate aerosols (Garland, 1978), but is well within the range of measured values for fine particulates (Droppo and Doran, 1979). The wet-removal parameterization was derived by Scott and Dana (1979) (also Scott, 1978) for sulfate aerosols, on the assumption that subcloud-sulfate aerosol acts as cloud-condensation nuclei and is removed by the

accretion process. This parameterization was applied to emitted particulates in the respirable size range on the assumption that these also serve as cloud-condensation nuclei (Pueschel 1976; Parungo et al. 1978).

C.1.5 Precipitation Averaging

In the assessments for this report, hourly precipitation is available for use. However, where a large number of sources are used or a large time period is involved, the computer cost becomes prohibitive. Therefore, a technique that allows the use of average precipitation was used. This technique uses the average precipitation rate that occurs during precipitation events. Precipitation is turned "on" for the average period of precipitation and "off" for the average period of no precipitation. For the entire assessment period for this report, a value of 3 hours of precipitation out of every 120 hours was chosen, based on a rough average of values presented by Henmi and Reiter (1978).

C.2 GRID POINT ASSESSMENTS

C.2.1 General

In general, assessments are usually carried out at source points. However, because of the large number of sources (the centroids of the 238 AQCRs) and the expense of running the long-range transport model, an alternative approach was tried using fewer source points. This alternative approach was to run the assessments for sources at grid intersects on the advection grid. Then, after weighting these grid point assessments on the basis of the inverse square of the distance from the grid point to the source point at the centroid of an AQCR, the weighted assessments were superimposed on the source and added together, forming an estimated assessment at the source point.

The assessment grid points are shown in Figure 5-7. Because there are 86 points, there is a factor of 3 fewer assessments to run. In general, the regular spacing of the NMC grid is used. There are four exceptions -- one point is used in Maine, two points in Flordia, and one point in California. Two points (Maine and California) are located at the half-grid spacing both in x and y, whereas two points in Florida are located at the half-grid only in x. The reason these additional grid points were chosen is that precipitation effects for the local region would not have shown up on the advection grid spacing. If points on the regular grid had been chosen, the points would have been over water where no precipitation would be included. Although the two points in the upper left-hand corner of Figure 5-7 are over water, these points are close enough to shore to be covered by the hourly precipitation grid area, and therefore, precipitation effects can be seen.

C.2.2 Test Cases

At the present time, the method used for testing whether more grid point assessments are needed has been through direct comparison of an assessment at a source point versus the weighted grid point assessment from the surrounding four grid points.

Two test cases for comparison have been made using meteorological data for July 1974. The first test is for a single source located in the Four Corners region. Figure C-2 shows the source location and the four surrounding NMC grid points used to interpolate the grid point assessments to the source.

The pattern of the air concentrations from an assessment run at the source point is quite similar to the air concentrations from the estimated assessment from the four NMC grid points, although there are some differences. When the centerline values were compared, ratios of these values generally ran between 0.5 to 2.0. In the single-source assessment, a large low appears in Wyoming. In the four NMC grid point estimated assessments, there are low values in Wyoming, although these values are a factor of 10 higher than the source values. In south-central Montana, factors as high as 50 occur between the two patterns. Greater differences occur in the deposition patterns; however, the overall mass balances for the Four Corners single-source and grid point comparison are essentially the same (see Table C-1).

Table C-1. Mass Balances for Single Source Four Corners Test (July 1974)

	Percent of Particulate Emissions	
Final Particulate Location	Four Corners Single Source	Four Corners Grid Estimate
Airborne--remaining over grid	8.31	7.88
Total deposited	82.79	82.91
Wet deposition only	53.92	54.10
Transported off grid	5.49	6.13
Dropped after remaining airborne for 200 hr	3.40	3.09

The second test was for multiple sources in the western United States for a Regional Issues Identification Assessment (RIIA) utility 1985 particulate analysis. The test focused on the effects of using average precipitation instead of hourly precipitation for a multisource assessment. Work performed by Davis using a single source (1979a) has shown that the mass balance is approximately the same when using the average precipitation and turning it "on" and "off" based on the average dry time and the average wet time. Because work was not performed previously using multiple sources, a run was made using the multiple sources used in the RIIA utility 1985 particulate assessment for July 1974 (Figure C-3). The results using the interpolative four-point technique for an estimated assessment for hourly precipitation and for average precipitation show patterns that are virtually the same.

The biggest differences in the assessments are in the deposition patterns for the hourly precipitation and for the average precipitation. The reason for this difference is that when precipitation is generally infrequent,

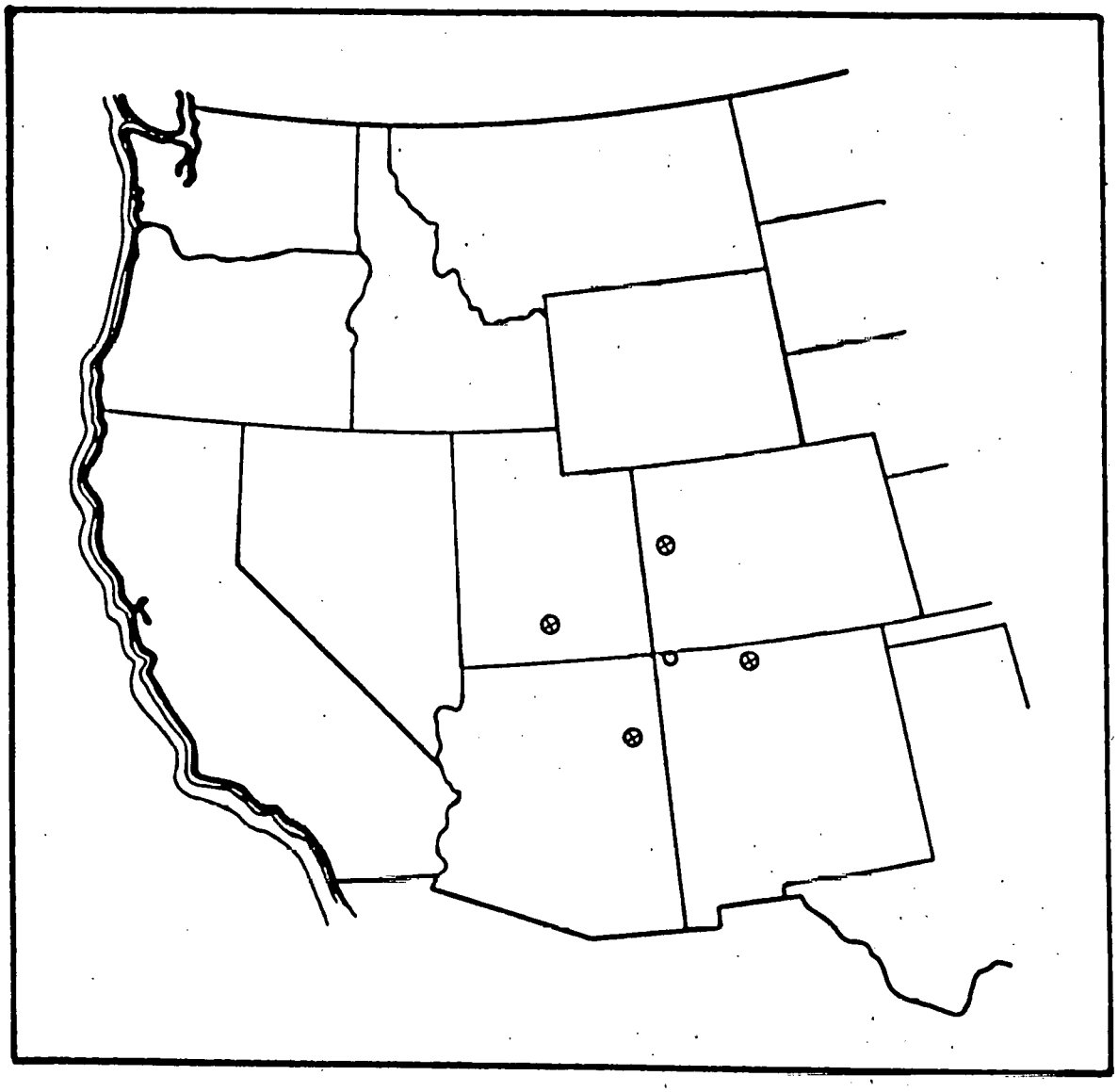

Note: Open circle is location of source in Four Corners region of Southwest. Crossed circles are the locations of the grid-point pseudo-sources used in the model.

FIGURE C-2. SOURCE LOCATION AND GRID-POINT PSEUDO-SOURCES

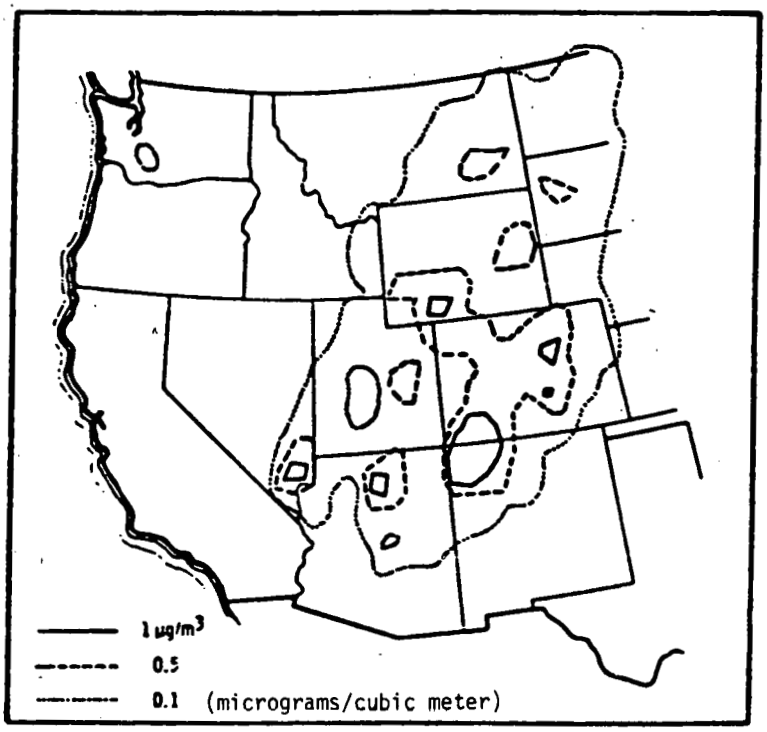

Note: Concentrations computed from RIIA Utility 1985 scenario using hourly precipitation for wet removal and July 1974 meteorology.

FIGURE C-3. AVERAGE PARTICULATE CONCENTRATIONS

six to seven events per month for this study, the deposition pattern is heavily influenced as to when and where precipitation occurs. Over longer time periods, this effect would be expected to average out.

C.3 THE AQCR ASSESSMENTS

As a result of favorable comparisons shown in the test cases, a decision was made to use the grid-point assessment technique for an assessment of monthly average respirable particulate fields emitted from all the AQCRs contained in the 48 contiguous states. The basic model parameters, as well as times over which the model was run for these assessments, is shown in Table 5-3. By using the grid-point technique, 4 months of assessments at 86 grid points were made instead of only 1 month of assessments at 238 source points, due to cost.

The 86 grid points were used to estimate assessments for a source at the centroid of each AQCR. After the assessments were made, the effect of one AQCR on another AQCR remained to be evaluated.

C.4 GENERATION OF AQCR-TO-AQCR MATRICES

C.4.1 Population-Weighted Averaging

To accomplish the population-weighted averaging over receptor AQCRs of the monthly average respirable particulate fields from emitter AQCRs, two files on the BNL computer system were integrated to produce a file containing the i and j coordinates of the grid boxes in the PNL 32-km grid system that lie wholly or partially within each AQCR. Associated with each of the grid boxes contributing to a given AQCR is a population-weighting factor equal to the population in the grid box residing within that AQCR divided by the total population residing within that AQCR.

One of the BNL fields contains for each of the grid boxes in the BNL 32-km grid system within the continental United States a list of counties by Federal Information Processing Standards (FIPS) County Code that lie wholly or partially within the grid box. For each grid box, the population residing within that box is given for the years 1970, 1975, 1980, and 1990, as well as the fractional population contribution for each county for each of those years. A second BNL file contains a list of counties within the continental United States by FIPS County Code, along with state abbreviation, county name, and AQCR number. The few counties in the United States that span two AQCRs were assigned in each case only to the one AQCR that contains the larger portion of the county.

By using the county-level information from both BNL files and taking into account the slight differences in origin and dimensions between the PNL and BNL grid systems, it was possible to develop an assignment of grid boxes in the PNL grid to the pseudo-AQCR and a population weighting factor for each grid-box assignment. The sum of the population weighting factors over the grid boxes assigned to each pseudo-AQCR equals unity. The BNL populations projections for the year 1985 form the basis for the initial population weighting for the PNL grid.

To calculate the population-weighted average over a receptor AQCR of the monthly average respirable particulate field from an emitter AQCR, the respirable particulate concentration at every grid box assigned to the receptor AQCR is multiplied by the population weighting factor. The resulting product is summed over the grid boxes assigned to the receptor AQCR to compute a population-weighted average over the receptor AQCR. This procedure is repeated for every combination of emitter and receptor AQCRs to develop an interregional, long-range transport matrix for respirable particulates.

C.4.2 Results

Four monthly average matrices were produced using meteorological data for the months January, April, July, and October 1974. There can be considerable variation in the matrix elements from one month to another as presented in Table C-2, where the monthly variations are shown for some representative AQCRs. Missing data in Table C-2 means that there was no trajectory from the source at the centroid of the emitter AQCR to any of the grid cells that contribute to the receptor AQCR during that month. Very small matrix elements, such as for receptor AQCR #14 and emitter AQCR #65 in October 1974, arise when there were not enough trajectories from the emitter AQCR to the receptor AQCR for the monthly average concentration over the receptor AQCR to be a realistic number. In these cases, as in the cases of missing data, the monthly matrix element should be considered to be zero.

It will be seen in Table C-2, although there are some month-to-month variations in the diagonal elements, these diagonal elements for the 4 months can be averaged together to produce a reasonably representative average matrix element. When the receptor AQCR is at some distance from the emitter AQCR, considerably more monthly variations are seen in the matrix elements, with differences of several orders of magnitude between monthly values sometimes the case. In these cases, 4 months of meteorological data may not be enough to obtain an average value that is reasonably representative of a climatological average.

Table C-2. Monthly Variations in Long-Range Transport AQCR-to-AQCR Matrix Elements* for Respirable Particulates as Calculated Using Meteorological Data From Four Months in 1974

Emitter AQCR	Receptor AQCR: 14** January	14** April	14** July	14** October	18** January	18** April	18** July	18** October
14**	$.634\times10^{-2}$	$.572\times10^{-2}$	$.684\times10^{-2}$	$.550\times10^{-2}$	$.315\times10^{-3}$	$.343\times10^{-4}$	$.303\times10^{-5}$	$.126\times10^{-5}$
18**	---	---	---	---	$.437\times10^{-1}$	$.149\times10^{-1}$	$.677\times10^{-1}$	$.242\times10^{-1}$
36**	$.486\times10^{-4}$	$.583\times10^{-5}$	$.167\times10^{-3}$	$.105\times10^{-3}$	$.994\times10^{-4}$	$.678\times10^{-4}$	$.191\times10^{-6}$	$.564\times10^{-5}$
65**	---	---	---	$.144\times10^{-9}$	$.801\times10^{-3}$	$.489\times10^{-3}$	$.370\times10^{-4}$	$.378\times10^{-3}$
	36**				65**			
14**	$.215\times10^{-2}$	$.190\times10^{-2}$	$.147\times10^{-2}$	$.257\times10^{-2}$	$.148\times10^{-2}$	$.136\times10^{-3}$	$.529\times10^{-6}$	$.444\times10^{-4}$
18**	---	---	---	---	---	$.947\times10^{-3}$	$.180\times10^{-4}$	$.736\times10^{-3}$
36**	$.374\times10^{-1}$	$.298\times10^{-1}$	$.527\times10^{-1}$	$.533\times10^{-1}$	$.843\times10^{-3}$	$.405\times10^{-3}$	$.300\times10^{-4}$	$.408\times10^{-4}$
65**	---	---	---	$.409\times10^{-7}$	$.381\times10^{-1}$	$.160\times10^{-1}$	$.260\times10^{-1}$	$.244\times10^{-1}$

* Monthly average over receptor AQCR of respirable particulate air concentrations in micrograms per cubic meter, resulting from 1.0 kiloton per year emission from a source at centroid of emitter AQCR.

** Counties included in AQCR:

14: AZ Apache, AZ Conconino, AZ Navajo, AZ Yavapai, CO Archuleta, CO Dolores, CO La Plata, CO Montezuma, CO San Juan, NM McKinley, NM San Juan, UT Emery, UT Garfield, UT Grand, UT Iron, UT Kane, UT San Juan, UT Washington, UT Wayne.

18: AR Crittenden, MS De Soto, TN Shelby

36: CO Adams, CO Arapahoe, CO Boulder, CO Clear Creek, CO Denver, CO Douglas, CO Gilpin, CO Jefferson

65: IL Fulton, IL Hancock, IL Hendersen, IL Knox, IL McDonough, IL Mason, IL Peoria, IL Tazewell, IL Warren, IL Woodford, IA Des Moines, IA Lee.

REFERENCES

Bass, A., 1980, "Modelling Long Range Transport and Diffusion," Second Joint Conference on Applications of Air Pollution Meteorology," American Meteorological Society, March 24-27, 1980, pp. 193-215.

Beilke, S., and G. Cravenhorst, 1978, "Heterogeneous SO_2-Oxidation in the Droplet Phase," Atmospheric Environment, No. 12, pp. 231-239.

Bhumralker, C.M., et al., 1980, "Adaptation and Application of a Long-Term Air Pollution Model ENAMAP-1 to Eastern North America," Final Report, SRI International Menlo Park, California, March 1980.

Bolin, B., and C. Persson, 1975, "Regional Dispersion and Deposition of Atmospheric Pollutants with Particular Application to Sulfur Pollution over Western Europe," Tellus XXVII, Vol. 3, pp. 281-310.

Calvert, J.G., et al., 1978, "Mechanism of the Homogeneous Oxidation of Sulfur Dioxide in the Atmosphere," Atmospheric Environment, No. 12, pp. 197-226.

Carson, D.J., 1973. "The Development of a Dry Inversion-Capped Convectively Unstable Boundary Layer," Quart. J.R. Met. Soc., Vol. 99, pp. 450-467.

Dana, M.T., et al., 1975, "Rain Scavenging of SO_2 and Sulfate From Power Plant Plumes," J. of Geo. Rsch., Vol. 80, pp. 4119-4129.

Davis, W.E., 1979a, "The Effect of Using Time Averaged Precipitation for the Estimation of Wet Deposition in a Regional Scale Model," Fourth Symposium on Turbulence, Diffusion, and Air Pollution, Reno, Nevada, January 15-18, 1979.

Davis, W.E., 1979b, "Comparison of the Results of an Eight Layer Regional Model Versus a Single Layer Regional Model for a Short Term Assessment," presented at the World Meteorological Organization Symposium on Long-Range Transport of Pollutants, Sophia, Bulgaria.

DOE, 1979a, An Assessment of National Consequences of Increased Coal Utilization: Executive Summary, TID-2945, U.S. Department of Energy, Assistant Secretary for Environment, Office of Technology Impacts, Division of Technology Assessments, February 1979.

DOE, 1979b, Regional Issue Identification and Assessment: First Annual Report, U.S. Department of Energy, Assistant Secretary for Environment, Office of Technology Impacts, Regional Assessments Division, September 1979.

DOE, to be published, "Technology Assessment of Solar Energy Systems: Environmental and Socioeconomic Implications of High and Low Solar Scenarios," U.S. Department of Energy, Assistant Secretary for Environment, Office of Environmental Assessment, Technology Assessments Division.

Doty, S.R., et al., 1976, A Climatological Analysis of Pasquill Stability Categories Based on "STAR" Summaries, Environmental Sciences Research Laboratory, U.S. Environmental Protection Agency, Research Triangle Park, North Carolina.

Draxler, R.R., 1980, "An Improved Gaussian Model for Long-Term Average Air Concentration Estimates," Atmos. Envir., Vol. 14, No. 5, pp. 597-601.

Droppo, J.G., and J.C. Doran, 1979, "Dry Deposition of Air Pollutants," in the Proceedings of the Institute of Environmental Sciences, Seattle, Washington, April 29 - May 2, 1979.

Eadie, W.J., and W.E. Davis, 1979, "The Development of a National Interregional Transport Matrix for Respirable Particulates," PNL-RAP-37, Pacific Northwest Laboratory, Richland, Washington.

Eimutis, E.C., and M.G. Konicek, 1972, "Derivations of Continuous Functions for the Lateral and Vertical Atmospheric Dispersion Coefficients," Atmos. Envir., Vol 6, pp. 859-863.

EPA, 1978, "1975 National Emissions Report," EPA-450/2-78-020, U.S. Environmental Protection Agency, May 1978.

EPA, 1979, "1976 National Emissions Report," EPA-450/4-79-019, U.S. Environmental Protection Agency, August 1979.

Garland, J.A., 1978. "Dry and Wet Removal of Sulphur from the Atmosphere," Atmos. Envir, Vol. 12, pp. 349-362.

Gerald, C.F., 1970, Applied Numerical Analysis, Addison-Wesley Publishing Company.

Heffter, J.L., 1965, "The Variation of Horizontal Diffusion Parameters with Time for Travel Periods of One Hour or Longer," J. Appl. Meteor, Vol. 4, No. 1, pp. 153-156.

Heffter, J.L., and A.D. Taylor, 1975, "A Regional-Continental Scale Transport, Diffusion, and Deposition Model, Part I: Trajectory Model," NOAA Technical Memorandum ERL ARL-50, Air Resources Laboratories, Silver Spring, Maryland.

Heffter, J.L., and G.J. Ferber, 1975, "A Regional-Continental Scale Transport, Diffusion, and Deposition Model -- Part II: Diffusion-Deposition Models," NOAA Technical Memorandum ERL ARL-50, Air Resources Laboratories, Silver Spring, Maryland.

Heffter, J.L., and G.J. Ferber, 1977, "Development and Verification of the ARL Regional-Continental Transport and Dispersion Model," Joint Conference on Applications of Air Pollution Meteorology, American Meteorological Society, Salt Lake City, Utah, Preprint Volume, November 29 - December 2, 1977, pp. 400-403.

Heffter, J.L., 1980, "Air Resources Laboratory Atmospheric Transport and Dispersion Model," NOAA Technical Memorandum ERL ARL-81, February 1980.

Henmi, T., and E.R. Reiter, 1978, "Regional Residence Time of Sulfur Dioxide Over the Eastern United States," Atmos. Envir, Vol. 12, pp. 1489-1495.

Holzworth, G.D., 1972, "Mixing Heights, Wind Species, and Potential for Urban Air Pollution throughout the Contiguous United States," AP-101, U.S. Environmental Protection Agency, Research Triangle Park, North Carolina.

Horst, T.W., 1977, "A Surface Depletion Model for Deposition from a Gaussian Plume," Atmos. Environ., No. 11, pp. 41-46.

Husar, R.B., et al., "Sulphur Budget of a Power Plant Plume," Atmos. Envir., Vol. 12, pp. 549-568.

Jenne, R.L., 1970, "The NMC Octagonal Grid," National Center for Atmospheric Research, Boulder, Colorado.

Johnson, W.B., et al., 1977, "Long-Term Regional Distribution and Transfrontier Exchanges of Airborne Sulfur Pollution in Europe," Interim Report, SRI International, Menlo Park, California.

Johnson, W.B., et al., 1978, "Long-Term Regional Patterns and Transfrontier Exchanges of Airborne Sulfur Pollution in Europe," Atmos. Environ., No. 12, pp. 511-527.

Kaimal, J.C., et al. 1976, "Turbulence Structure in Convective Boundary Layer." J. of the Atm. Sci., Vol. 33, pp. 2152-2169.

Mancuso, R.L., et al., 1978, "Evaluation and Sensitivity Analysis of the European Regional Model of Air Pollution," EUR MAP-1, Progress Report, SRI International, Menlo Park, California.

McNaughton, D.J., 1980, "Initial Comparisons of SURE/MAP3S Sulfur Oxide Observations with Long-Term Regional Model Predictions," Atmos. Environ., Vol. 14, pp. 55-63.

McNaughton, D.J., and B.J. Scott, 1980, "Modeling Evidence of Incloud Transformation of Sulfur Dioxide to Sulfate," Journal of the Air Pollution Control Association, Vol. 30, No. 3, March 1980, pp. 272-273.

Meyers, R.E., and R.T. Cederwall, 1975, "Fossil Pollutant Transport Model Development," BNL 50478, BNL RESP Annual Report, pp. 45-61, 91-106.

Meyers, R.E., et al., 1978a, "Constraints on Coal Utilization with Respect to Air Pollution Production and Transport over Long Distances, National Coal Utilization Assessment," Draft Report, Atmospheric Sciences Division, Brookhaven National Laboratory, Upton, New York.

Meyers, R.E., et al., 1978b, "Regional Issues Identification and Assessment: Atmospheric Long Range Transport," Draft Report, Atmospheric Sciences Division, Brookhaven National Laboratory, Upton, New York.

Meyers, R.E., et al., 1979a, "A Long-Range Transport Model for Calculating the Atmospheric Impacts of Residual Sulfur Oxides," Informal Report No. 26185-R1, Brookhaven National Laboratory, Upton, New York, June 1979.

Meyers, R.E., et al., 1979b, "Modeling Sulfur Dioxide Concentration in the Eastern United States: Model Sensitivity, Verification and Applications," Fourth Symposium on Turbulence, Diffusion and Air Pollution, Reno, Nevada, Preprint Volume, January 15-18, 1979, pp. 673-676.

Meyers, R.E., et al., 1979c, "Modeling Regional Atmospheric Transport and Diffusion: Some Environmental Applications," Advances in Environmental Science and Engineering, Gordon and Breach Publishers, Ziegler and Pfaffzin, Ed., pp. 118-184.

Meyers, R.E., and E.N. Ziegler, 1978, "Statistical Correlation Between Ambient Sulfate Concentration, Sulfur Dioxide Concentration, Total Suspended Particulate and Relative Humidity for Thirteen Eastern States," Environ. Sci. and Tech., Vol. 12, March 1978, pp. 302-309.

Parungo, F. et al., 1978, "Nucleation Properties of Fly Ash in a Coal-Fired Power-Plant Plume," Atmos. Envir., Vol. 12, pp. 929-935.

Powell, D.C. et al., 1979a, "A Variable Trajectory Model for Regional Assessments of Air Pollution From Sulfur Compounds," PNL-2734, Pacific Northwest Laboratory, Richland, Washington.

Powell, D.C. et al., 1979b, "MESODIFF-II: A Variable Trajectory Plume Segment Model to Assess Ground-Level Air Concentrations and Deposition of Routine Effluent Releases From Nuclear Power Facilities," PNL-2419, U.S. Nuclear Regulatory Commission.

Prahm, L.R., and O. Christensen, 1977, "Long-Range Transmission of Pollutants Simulated by the 2-D Pseudospecral Dispersion Model," J.A.M. No. 16, pp. 696-910.

Pueschell, R., 1976, "Aerosol Formation During Coal Combustion," Geophys. Res. Lett, Vol. 3, pp. 651-653.

Renne, D.S., et al., 1978, "Air Quality Impacts," The Impact of Increased Coal Consumption in the Pacific Northwest, BNWL-RAP-21, Pacific Northwest Laboratory, Richland, Washington.

Sandusky, W.F., et al., 1979, "Long-Range Transport of Sulfur in the Western United States," PNL-RAP-26, Pacific Northwest Laboratory, Richland, Washington.

Rowe, M.D., 1980, "Human Exposure to Sulfates From Coal-Fired Power Plants," Journal of the Air Pollution Control Association, Vol. 30, No. 6, June 1980, pp. 682-684.

Scott, B.C., 1978, "Parameterization of Sulfate Removal by Precipitation," J.A.M., Vol. 17, pp. 1375-1389.

Scott, B.C., and M.T. Dana, 1979, "Deviation of Wet Removal Rates in SO_2 Gas and SO_4 Aerosol," PNL-2850, PT3, Pacific Northwest Laboratory, Richland, Washington.

Shannon, J.B., 1979, "The Advanced Statistical Trajectory and Air Pollution Model," ANL/RER-79-1, Argonne National Laboratories.

Shir, C.C., and L.J. Shieh, 1974, "A Generalized Urban Air Pollution Model and Its Application to the Study of SO_2 Distribution in the St. Louis Metropolitan Area," J. Appl. Met. No. 13, pp. 185-204.

Tennekes, H., 1974, "The Atmospheric Boundary Layer," Physics Today, pp. 52-63.

Turner, D.B., 1979, "Atmospheric Dispersion Modeling: A Critical Review," Journal of the Air Pollution Control Association, Vol., 29, No. 5, May 1979, pp. 502-519.

Venkatram, A., and R. Viskanta, 1976, "Radiative Effects of Pollutants on the Planetary Boundary Layer," EPA-600/4-76-039, U.S. Environmental Protection Agency, Office of Research and Development, Research Triangle Park, North Carolina.

Wendell, L.L., 1972, "Mesoscale Wind Fields and Transport Estimates Determined From a Network of Wind Towers," Mon. Wea. Rev., Vol. 100, pp. 565-578.

Wendell, L.L., et al., 1976, "A Regional Scale Model for Computing Deposition and Ground Level Air Concentration of SO_2 and SO_4 from Elevated and Ground Soruces," Preprints from the Third Symposium on Atmospheric Turbulence, Diffusion and Air Quality, Amer. Meteor. Soc., Raleigh, North Carolina.

Wight, G.D., et al., 1978, "Formation and Transport of Ozone in the Northeast Quadrant of the U.S. Air Quality Meteorology and Atmospheric Ozone," ASTM STP 653, American Society for Testing and Materials, Philadelphia, Pennsylvania, pp. 445-457.

Wolff, G.T., et al., 1977, "Anatomy of Two Ozone Transport Episodes in the Washington, D.C. to Boston, Massachusetts Corridor," Environ. Sci. and Tech., No. 11, pp. 506-510.

☆U.S. GOVERNMENT PRINTING OFFICE: 1981—341-076:1152